

BIBLIOGRAPHIC INFORMATION

PB94-204013

Report Nos:

Title: Evaluation of Seismic Serviceability of Water Supply Networks with Application to the San Francisco Auxiliary Water Supply System.

Date: 21 Jan 94

Authors: I. Markov, M. Grigoriu, and T. O'Rourke.

Performing Organization: Cornell Univ., Ithaca, NY. School of Civil and Environmental Engineering.

Performing Organization Report Nos: NCEER-94-0001

Sponsoring Organization: *National Center for Earthquake Engineering Research, Buffalo, NY.*National Science Foundation, Arlington, VA.*New York State Science and Technology Foundation, Albany.

Contract Nos: NSF-BCS-90-25010, NYSSTF-NEC-91029

Type of Report and Period Covered: Technical rept.

NTIS Field/Group Codes: 50B (Civil Engineering), 85E (Pipeline Transportation)

Price: PC A07/MF A02

Availability: Available from the National Technical Information Service, Springfield, VA. 22161

Number of Pages: 142p

Keywords: *Water supplies, *Earthquake resistant structures, *Pipelines, Earthquake engineering, Flow equations, Seismic effects, Earthquake damage, Hydraulics, Regression analysis, Algorithms, Earthquakes, Water flow, Potable water, *Serviceability, San Francisco(California).

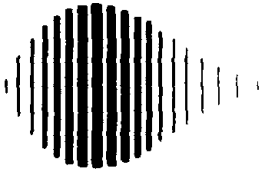
Abstract: A new method is presented for estimating the serviceability of water networks damaged during earthquakes. Several measures are developed for evaluating the serviceability. These seismic serviceability measures are random variables that depend on uncertain parameters such as seismic intensity, water supply, system damage state, and water demand. The determination of the proposed serviceability measures involves hydraulic analyses of water supply systems in various damage states. Commercially available softwares for hydraulic analysis are configured for intact networks and can not be used reliably for heavily damaged and leaking systems. A computer code is developed for the hydraulic analysis of damaged water supply systems. The code eliminates those portions of the network which have negative pressures, and predicts the available flow and pressure at the demand nodes. The hydraulic analysis also accounts for the dependence of C-factors, which represents internal pipe roughness, on the pipe diameter. This dependence is validated by fire flow tests performed in San Francisco. The code has capabilities of simulating a seismic network performance with the uncertain parameters. The serviceability measures and the proposed algorithm for

BIBLIOGRAPHIC INFORMATION

Continued...

PB94-204013

hydraulic analysis are applied to evaluate the seismic serviceability of the Auxiliary Water Supply System in San Francisco.



PB94-204013

**NATIONAL CENTER FOR EARTHQUAKE
ENGINEERING RESEARCH**

State University of New York at Buffalo

**An Evaluation of Seismic Serviceability of
Water Supply Networks with Application to the
San Francisco Auxiliary Water Supply System**

by

I. Markov

Supervised by

M. Grigoriu and T. O'Rourke

Cornell University

School of Civil and Environmental Engineering

Ithaca, New York 14853

Technical Report NCEER-94-0001

January 21, 1994

REPRODUCED BY
U.S. Department of Commerce
National Technical Information Service
Springfield, Virginia 22161

This research was conducted at Cornell University and was partially supported by the National Science Foundation under Grant No. BCS 90-25010 and the New York State Science and Technology Foundation under Grant No. NEC-91029.

NOTICE

This report was prepared by Cornell University as a result of research sponsored by the National Center for Earthquake Engineering Research (NCEER) through grants from the National Science Foundation, the New York State Science and Technology Foundation, and other sponsors. Neither NCEER, associates of NCEER, its sponsors, Cornell University, nor any person acting on their behalf:

- a. makes any warranty, express or implied, with respect to the use of any information, apparatus, method, or process disclosed in this report or that such use may not infringe upon privately owned rights; or
- b. assumes any liabilities of whatsoever kind with respect to the use of, or the damage resulting from the use of, any information, apparatus, method or process disclosed in this report.

Any opinions, findings, and conclusions or recommendations expressed in this publication are those of the author(s) and do not necessarily reflect the views of NCEER, the National Science Foundation, the New York State Science and Technology Foundation, or other sponsors.



PB94-204013

**An Evaluation of Seismic Serviceability of
Water Supply Networks with Application to the
San Francisco Auxiliary Water Supply System**

by

I. Markov¹

Supervised by

M. Grigoriu² and T. O'Rourke²

January 21, 1994

Technical Report NCEER-94-0001

NCEER Task Numbers 90-3004, 91-3322, 92-3302B and 93-3304A

NSF Master Contract Number BCS 90-25010

and

NYSSTF Grant Number NEC-91029

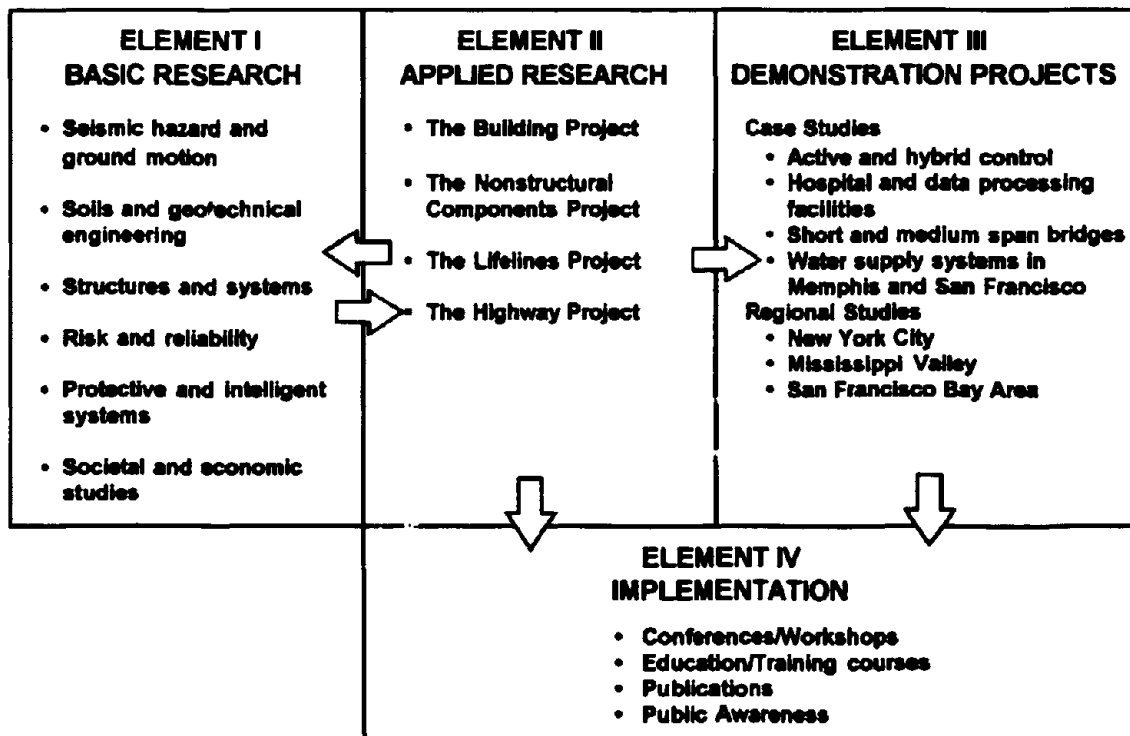
- 1 Graduate Research Assistant, School of Civil and Environmental Engineering, Cornell University
2 Professor, School of Civil and Environmental Engineering, Cornell University

NATIONAL CENTER FOR EARTHQUAKE ENGINEERING RESEARCH
State University of New York at Buffalo
Red Jacket Quadrangle, Buffalo, NY 14261

PREFACE

The National Center for Earthquake Engineering Research (NCEER) was established to expand and disseminate knowledge about earthquakes, improve earthquake-resistant design, and implement seismic hazard mitigation procedures to minimize loss of lives and property. The emphasis is on structures in the eastern and central United States and lifelines throughout the country that are found in zones of low, moderate, and high seismicity.

NCEER's research and implementation plan in years six through ten (1991-1996) comprises four interlocked elements, as shown in the figure below. Element I, Basic Research, is carried out to support projects in the Applied Research area. Element II, Applied Research, is the major focus of work for years six through ten. Element III, Demonstration Projects, have been planned to support Applied Research projects, and will be either case studies or regional studies. Element IV, Implementation, will result from activity in the four Applied Research projects, and from Demonstration Projects.



Research tasks in the Lifeline Project evaluate seismic performance of lifeline systems, and recommend and implement measures for mitigating the societal risk arising from their failures or disruption caused by earthquakes. Water delivery, crude oil transmission, gas pipelines, electric power and telecommunications systems are being studied. Regardless of the specific systems to be considered, research tasks focus on (1) seismic vulnerability and strengthening; (2) repair and restoration; (3) risk and reliability; (4) disaster planning; and (5) dissemination of research products.

The end products of the **Lifeline Project** will include technical reports, computer codes and manuals, design and retrofit guidelines, and recommended procedures for repair and restoration of seismically damaged systems.

The **risk and reliability program** constitutes one of the important areas of research in the **Lifeline Project**. The program is concerned with reducing the uncertainty in current models which characterize and predict seismically induced ground motion, and resulting structural damage and system unavailability. The goal of the program is to provide analytical and empirical procedures to bridge the gap between traditional earthquake engineering and socioeconomic considerations for the most cost-effective seismic hazard mitigation. Among others, the following tasks are being carried out:

1. Study seismic damage and develop fragility curves for existing structures.
2. Develop retrofit and strengthening strategies.
3. Develop intelligent structures using high-tech and traditional sensors for on-line and real-time diagnoses of structural integrity under seismic excitation.
4. Improve and promote damage-control design for new structures.
5. Study critical code issues and assist code groups to upgrade seismic design code.
6. Investigate the integrity of nonstructural systems under seismic conditions.

A new method is presented for estimating the serviceability of water networks damaged during earthquakes. The proposed serviceability measures account for the uncertainty in seismic ground motion, soil conditions, current system damage state, and required water demand. The analysis is based on the Monte-Carlo simulation method and involves a large number of hydraulic analyses of water supply systems in various damage states. Probabilistic models are used to generate realistic damage states. Commercially available software for hydraulic analysis are configured for ideal networks that are undamaged and do not leak. The use of these software in the analysis of actual water supply systems, that may experience damage and leaks, can result in unrealistic predictions, such as high negative hydraulic pressures at nodes.

A computer code with graphic capabilities, GISALLE, is developed for calculating the seismic serviceability of water supply systems. The code has a preprocessor for generating realizations of the damage states and the water demands, a module for hydraulic analysis, and a postprocessor for analyzing statistically the system response to the generated input. The hydraulic analysis is based on an algorithm that accounts for breaks and leaks in water supply systems.

The Auxiliary Water Supply System in San Francisco is used to validate the proposed method of analysis. The validation includes fire flow tests performed by the San Francisco fire department and observations during the 1989 Loma Prieta earthquake. Numerical results of deterministic and stochastic parametric studies show that the algorithm for calculating serviceability measures is robust and efficient.



PB94-204013

ABSTRACT

A new method is presented for estimating a serviceability of water networks damaged during earthquakes. Several measures are developed for evaluating the serviceability. These seismic serviceability measures are random variables that depend on uncertain parameters such as seismic intensity, water supply, system damage state, and water demand. The determination of the proposed serviceability measures involves hydraulic analyses of water supply systems in various damage states. Commercially available softwares for hydraulic analysis are configured for intact networks and can not be used reliably for heavily damaged and leaking systems. A computer code is developed for the hydraulic analysis of damaged water supply systems. The code eliminates those portions of the network which have negative pressures, and predicts the available flow and pressure at the demand nodes. The hydraulic analysis also accounts for the dependence of C-factors, which represents internal pipe roughness, on the pipe diameter. This dependence is validated by fire flow tests performed in San Francisco. The code has capabilities of simulating a seismic network performance with the uncertain parameters. The serviceability measures and the proposed algorithm for hydraulic analysis are applied to evaluate the seismic serviceability of the Auxiliary Water Supply System in San Francisco. Numerical results of deterministic and stochastic parametric studies show that the algorithm for calculating serviceability measures is robust and efficient.

ACKNOWLEDGMENTS

This research is supported by the National Center for Earthquake Engineering Research (NCEER) under the NCEER Contract Numbers 90-3004, 91-3322, 92-3302B, and 93-3304A.

TABLE OF CONTENTS

SECTION	TITLE	PAGE
1	INTRODUCTION	1-1
1.1	Overview	1-1
1.2	Objectives	1-2
1.3	Outline	1-2
2	HYDRAULIC NETWORK MODELS FOR UNDAM- AGED SYSTEMS	2-1
2.1	Introduction	2-1
2.2	Components of a Distribution System	2-1
2.3	Governing Equations of Flow	2-3
2.3.1	Equations of Continuity	2-4
2.3.2	Equations of Energy	2-4
2.3.3	Energy Losses	2-4
2.4	Methods of Solution	2-6
2.4.1	Hardy Cross Method	2-6
2.4.2	Newton-Raphson Method	2-7
2.5	Summary	2-8
3	HYDRAULIC NETWORK MODELS FOR DAMAGED SYSTEMS	3-1
3.1	Introduction	3-1
3.2	Formulation	3-2
3.3	Negative Pressure	3-4
3.4	Potential Damage States of a Pipeline System	3-5
3.5	System Definition and Serviceability Analysis	3-6
3.6	Summary	3-8

TABLE OF CONTENTS (Cont'd)

4	SAN FRANCISCO AUXILIARY WATER SUPPLY SYSTEM	4-1
4.1	Introduction	4-1
4.2	Geotechnical Characteristics	4-1
4.3	Water Supply System in San Francisco	4-4
4.3.1	Auxiliary Water Supply System (AWSS)	4-4
4.3.2	The Municipal Water Supply System (MWSS)	4-10
4.3.3	The Portable Water Supply Systems (PWSS)	4-10
4.3.4	Underground Cisterns	4-10
4.4	Summary	4-11
5	GISALLE	5-1
5.1	Introduction	5-1
5.2	Organization of the Computer Code	5-1
5.3	Definition Module	5-3
5.4	Modification Module	5-3
5.4.1	On-Off Module	5-5
5.4.2	Edit Module	5-5
5.5	Damage Module	5-6
5.5.1	Pipe Break Module	5-6
5.5.2	Hydrant Break Module	5-9
5.5.3	Fire Module	5-10
5.6	Hydraulic Analysis Module	5-12
5.7	Statistical Module	5-14
5.7.1	Performance Index Module	5-14
5.7.2	Fragility Curve Module	5-15
5.7.3	Regression Analysis	5-16
5.8	Results Module	5-21

TABLE OF CONTENTS (Cont'd)

5.9	Summary	5-21
6	VALIDATION OF GISALLE	6-1
6.1	Introduction	6-1
6.2	Test Problems.....	6-1
6.2.1	Elimination of Negative Pressure Nodes.....	6-2
6.2.2	Effect of Partial Flow Analysis on AWSS.....	6-10
6.3	Modeling of Pump Stations.....	6-10
6.3.1	Pump Characteristic Curves	6-10
6.3.2	Modeling of the Pump Characteristic Curves.....	6-13
6.3.3	Effect of Pump Characterization on the AWSS	6-18
6.4	Demand Simulation	6-18
6.5	Flow Tests	6-21
6.5.1	Determination of Roughness Coefficients	6-21
6.5.2	Computer Modeling	6-25
6.6	Summary	6-25
7	LOMA PRIETA EARTHQUAKE SCENARIO	7-1
7.1	Introduction	7-1
7.2	1989 Loma Prieta Earthquake	7-1
7.3	Computer Analysis of Loma Prieta Event	7-2
7.4	Summary	7-5
8	SENSITIVITY STUDIES	8-1
8.1	Introduction	8-1
8.2	Parameters Selection	8-1
8.2.1	Supply Scenarios	8-1
8.2.2	Fire Scenarios	8-3
8.2.3	Damage Scenarios	8-4

TABLE OF CONTENTS (Cont'd)

8.3	Results of Deterministic Analyses	8-5
8.3.1	Loma Prieta and Filbert St. Damage	8-5
8.3.2	Infirm Area Damage States	8-7
8.4	Results of Stochastic Analyses	8-13
8.5	Summary	8-19
9	SUMMARY AND RECOMMENDATIONS	9-1
10	REFERENCES	10-1

LIST OF ILUSTRATIONS

FIGURE	TITLE	PAGE
2.1	Modeling of a Pressure Reducing Valve	2-2
4.1	Plan View of San Francisco Showing Zones of 1906 Soil Liquefaction and Inspection After the 1989 Earthquake	4-2
4.2	The Auxiliary Water Supply System (AWSS) of San Francisco.....	4-6
4.3	A Typical Hydrant	4-7
4.4	Schematic Cross-section of the AWSS	4-8
4.5	The Locations of Ten Infirm Areas in the City of San Francisco.....	4-9
5.1	GISALLE Flow-Chart	5-2
5.2	Computer Presentation of the AWSS.....	5-4
5.3	Schematic Diagram of Hydrant Simulation	5-5
5.4	Variation of Mean Damage Repairs with Earthquake Intensity	5-8
5.5	Schematic Diagram of Pipe-Break Simulation	5-9
5.6	Variation of Fire Ignitions with Seismic Intensity	5-11
5.7	Computer Displays of Fragility Curve and 95% Confidence Level for Damage Indices S_d	5-17
5.8	Computer Displays for Damage Indices S_d with Selected Damage Scenario	5-18
5.9	Graphical Presentation of the Flow Distribution.....	5-22
5.10	Graphical Presentation of the Pressure Distribution	5-23
6.1	Test Problem 1: No Elimination of Nodes	6-2
6.2	Test Problem 2: Elimination of No-Flow Node	6-4
6.3	Test Problem 3: Elimination of Initialy Prtial Flow Node.....	6-7
6.4	Locations of Broken Pipes	6-12
6.5	Pump Characteristic Curve	6-14
6.6	Regression Curve.....	6-15
6.7	Three Point Characteristic Curve	6-16
6.8	One Point Pump Characterization	6-18

LIST OF ILLUSTRATIONS (Cont'd)

6.9	Locations of Fire Hydrants	6-20
6.10	Available Flows for Alternate Water Paths	6-22
6.11	Available Flows for a Single Water Path	6-22
6.12	Monitored Locations for 9 Field Tests	6-23
6.13	Variation of Roughness Coefficient C with Pipe Diameter.....	6-25
7.1	Breaks and Leaks in AWSS Caused by Loma Prieta Earthquake	7-3
8.1	Locations of Damage States, Fires and Water supplies	8-2
8.2	Available Flows at the Marina, the Folsom and Alabama St. for Various Damage States and Supply Scenarios	8-6
8.3	Flow Path with Damaged Infirm Area 1	8-8
8.4	Flow Path with Damaged Infirm Area 2	8-8
8.5	Flow Path with Damaged Infirm Area 3	8-9
8.6	Flow Path with Damaged Infirm Area 4	8-9
8.7	Flow Path with Damaged Infirm Area 5	8-10
8.8	Flow Path with Damaged Infirm Area 6	8-10
8.9	Flow Path with Damaged Infirm Area 7	8-11
8.10	Flow Path with Damaged Infirm Area 8	8-11
8.11	Flow Path with Damaged Infirm Area 9	8-12
8.12	Flow Path with Damaged Infirm Area 10	8-12
8.13	JST Water Loss vs. Break Location.....	8-13
8.14	Performance indices S_d and S_s for Loma Prieta Damage (LP) and Loma Prieta and Filbert St. Damage (LP+F)	8-14
8.15	Fragility Curve for the Damage Indices	8-16
8.16	Fragility Curve for the Serviceability Indices	8-17
8.17	Flow Path in the AWSS with Damage at Filbert St. and Infirm Area 1	8-18

LIST OF TABLES

TABLE	TITLE	PAGE
6.I	Test 1 - Flow and Preassure Distribution	6-3
6.II	Case 2 - GISALLE Results After Step 1	6-5
6.III	Case 2 - GISALLE Results After Step 2	6-6
6.IV	Case 3 - GISALLE Results After Step 1	6-8
6.V	Case 3 - GISALLE Results After Step 2	6-9
6.VI	Effect of Implementation of Partial Flow and Interactive Analysis ..	6-11
6.VII	Sensitivity Study for the Selection of a Middle Point	6-17
6.VIII	Sensitivity Study of Pump Curve Characterization	6-19
6.IX	Results of Field Tests and Computer Analyses	6-26
7.I	Results of the Earthquake Simulation	7-4

NOTATION

The following list of notation is used in this report.

a = constant (=1.852) for Hazen-Williams equation

a_p = constant for pump flow

b_k = constant for pipe k

c = constant for pipe k

d_k = diameter of pipe k

e_1 = objective function

e_2 = objective function

f = dimensionless friction factor

g = ground acceleration

h = hydrant number

h_{fk} = head loss due to friction in pipe k

h_{mk} = minor loss in pipe k

i, j = node numbers

k = pipe numbers

l = loop number

m = iteration number

n = number of observations

n_f = number of field tests

n_h = number of hydrants

n_n = number of nodes

n_p = number of pipes

n_{pi} = number of pipes merging node i

n_{pl} = number of pipes in loop l

p_i = available pressure at node i

p_h = available pressure at hydrant h

p_i^* = required pressure at node i

p_h^* = required pressure at hydrant h

$p_{t,i}$ = calculated pressure at monitored location i in test t
 $p_{t,i}^*$ = measured pressure at monitored location i in test t
 r = number of monitored locations per each test
 s = unit step function
 t = test number
 u = random number
 v = dynamic viscosity
 v_p = pipe amplification factor
 v_h = hydrant amplification factor
 v_f = fire amplification factor
 κ = number of estimated parameters in regression model
 A_k = cross sectional area of pipe k
 A_p = pump constant
 B = dimensional constant
 B_p = pump constant
 C = coefficient of friction
 C_p = pump constant
 C_k = coefficient of friction of pipe k
 E_i = elevation at node i
 G = parameter for iteration
 G_i = function of heads
 H_i = head at node i
 H_p = pump head
 K_h = constant dependent on h_{fk} , h_{mk} , units, C_k , and D_k , for pipe k
 K_{fk} = constant dependent on h_{mk} , units, C_k , and D_k , for pipe k
 K_{mk} = constant dependent on h_{fk} units, C_k , and D_k , for pipe k
 L = pipe length
 L_k = length of pipe k
 P_p = probability of pipe failure
 P_h = probability of hydrant failure

P_f = probability of fire ignition
 Re = Reynolds number
 R_l = residual head loss in loop l
 S_d = damage index
 S_s = serviceability index
 Q_k = flow in the pipe k
 Q_i^* = required flow at node i
 \tilde{Q}_h = external flow at hydrant h
 \tilde{Q}_i = external flow at node i
 \tilde{Q}_h^* = required flow at hydrant h
 Q_p = pump flow
 Q_T = total available flow in a damaged system
 Q_T^* = total required flow
 Q_{TO} = total available flow in a undamaged system
 Q_{ik} = flow through pipe k at node i
 U = random variable
 V = flow velocity
 HP = pump horsepower
 ΔH = change of head loss
 γ = specific weight of water
 ϵ = roughness of the pipe
 ϵ = error term
 β_i = regression coefficients
 $\lambda(I)$ = mean break rate for Mercaly Intensity I
 $[b]$ = partition of matrix A
 $[d]$ = partition of matrix A
 $\{r\}$ = vector r
 $\{r_1\}$ = partition vector of r
 $\{r_2\}$ = partition vector of r

$\{x\}$ = vector x

$\{x_1\}$ = partition of vector X

$\{x_2\}$ = partition of vector X

$[A]$ = matrix A

$[D]$ = matrix D

$[\tilde{Q}]$ = matrix \tilde{Q}

H = vector H

$[I]$ = identity matrix I

$\{X\}$ = vector of unknowns

SECTION 1

INTRODUCTION

1.1 Overview

Water supply systems can be significantly damaged during seismic ground shaking. Damage of a system may cut off water supply in certain areas or leave a whole city without water. The city of San Francisco has two water supply systems: the Municipal Water Supply System (MWSS) and the Auxiliary Water Supply System (AWSS). The MWSS provides drinking and serviceability water as well as fire protection for the city. The fire protection capability is limited as it was observed after the 1906 earthquake when a large portion of the city was burned. The AWSS, designed after the earthquake, serve solely for City's fire protection. The maintains of the AWSS seismic serviceability during earthquakes is essential to prevent a major City's fire destruction.

The seismic serviceability of a water supply system depends on several factors such as: the vulnerability of system components, system topology, earthquake intensity, soil conditions, fire scenarios and operation strategies. The assessment of the effect of these parts on the seismic serviceability of a water supply system is a complex task.

One way of providing a measure of the seismic serviceability of a water supply systems is to quantify the fire fighting capability of the system following an earthquake. The evaluation of the seismic serviceability of a water supply system involves a relatively large number of hydraulic analyses of the system in various damaged states.

The existing methods for hydraulic analysis are based on the assumption that the pipelines of a water system are full of water, even when water pressures falls below the atmospheric pressure. However, a distribution system can not sustain significant negative pressures because leaks at joints, valves and damaged components tend to vent and subdue negative pressure. Therefore, some pipelines may not have flow or may exhibit a partial flow, in contradiction to the assumption of full flow. These flow conditions can not be modeled by the existing methods for hydraulic analysis. A new method has been developed that can analyze actual water supply of damaged systems.

It is possible in principle to evaluate the seismic performance of water supply system by cal-

culating the stress level in every component during an earthquake and evaluating the seismic performance of these components. However, the approach is impractical because of the system complexity and uncertainty in earthquake characteristics. The analysis in this report is based on correlations between component damage and earthquake intensity developed from repair records. Resultant correlations can be applied to generate likely damage states and fire demands in water supply systems exposed to earthquakes. The method is particularly useful in seismic regions with limited seismic records and/or insufficient information on the state of the water system under consideration.

The determination of the seismic serviceability of a water supply system has several phases. First, damage states of the water supply system and fire scenarios are generated consistent with site seismicity, soil conditions, and pipeline characteristics. Second, hydraulic analyses are performed to determine available flow and pressure at hydrants close to simulated fires. Third, statistics are obtained on flows and pressures, and indices are developed for quantifying the system serviceability.

A simulation code was developed at Cornell University for evaluating the seismic serviceability of water distribution networks. The code, entitled GISALLE (Graphical Interactive Serviceability Analysis of Life-Lines subjected to Earthquakes), has been applied to evaluate the seismic performance of the Auxiliary Water Supply System (AWSS) in San Francisco.

1.2 Objectives

The overall purpose of this report is to (1) present a new method for estimating seismic serviceability of damaged water supply systems and (2) validate the GISALLE code. The report describes the features and capabilities of the code. It also includes the results of deterministic and stochastic parametric studies of the San Francisco AWSS.

1.3 Outline

The report consists of ten Sections. After the introduction Section 2 review hydraulic network models for undamaged systems. It provides governing equations for flow and pressure distribution, and presents two existing methods of solution. Section 3 presents a new formulation of hydraulic analysis for damaged systems that can account for negative pressures

and ruptured pipelines. Section 4 describes the AWSS and geotechnical characteristics of the soil in the region. Section 5 outlines available modules in the GISALLE code. Section 6 validates the GISALLE code by test problems and flow tests. It also examines mathematical models of pump stations and fire demands, and evaluates values of the roughness coefficients in the pipes for the AWSS. Section 7 explores the serviceability of the AWSS after the Loma Prieta earthquake. Section 8 presents the results of deterministic and stochastic parametric studies for the AWSS performed with GISALLE. Section 9 summarizes the results of the analysis in the report. Numerical results show that the algorithm can predict the seismic performance of the AWSS accurately and efficiently. Section 10 is the references section.

SECTION 2

HYDRAULIC NETWORK MODELS FOR UNDAMAGED SYSTEMS

2.1 Introduction

Available hydraulic heads at joints and flows in pipes are crucial for predicting the performance of a water supply system. These parameters satisfy a system of nonlinear algebraic equations that have to be solved numerically.

Hardy Cross [7,31] first introduced an iterative method to calculate flows and heads for water supply systems. This method can be used to evaluate the flow characteristics of simple systems or to check selected portions of more complex system. The convergence rate, however, is slow and depends strongly on the initial solution used to begin the iteration. In the last decade, alternative numerical solutions which are linked with computer applications, have been developed for finding flows and heads.

Currently available methods for hydraulic analysis are based on the assumption that pipelines are always full of water even when the water pressure falls below the atmospheric pressure. The assumption is unrealistic because water distribution systems are not perfectly tight to the atmosphere. Water leaks that commonly occur at pipe joints, behave like air-inlet valves. Therefore, negative water pressures can not occur in water supply systems. The consideration of leaks increases drastically the nonlinearity of the flow and head equations because some pipelines may have no flow or free surface flow.

In this section, a brief description of the major components of a water distribution system is included. The governing equations of flow are presented. The characteristics of the available analysis methods are discussed together with their advantages and drawbacks.

2.2 Components of a Distribution System

The components of a water distribution system control flows and/or pressures. These components need to be included in the mathematical model of the network. Typical components

of water supply systems are:

1. *Junction or node.* It is a point where two or more pipes meet or where a special component needs to be placed.
2. *Pipe.* A pipe is a closed conduit that carries water between two junctions.
3. *Fixed Grade Nodes.* Junctions where water pressures are known are normally called fixed grade nodes, e.g., connections to storage tanks, reservoirs or a discharge point where pressure is prescribed. The pressures at fixed grade nodes are treated as boundary conditions in the hydraulic analysis.
4. *Orifice.* This type of component is common in fire protection installations, e.g., sprinklers and hydrants. It is an outlet of a distribution system through which water is delivered at a certain minimum pressure. An orifice can be modeled as a pipe of specified diameter.
5. *Check Valve.* It allows water to flow in a single direction only. The pipe with a check valve is eliminated during analysis if the flow is against the operating direction of the valve.
6. *Pressure Reducing Valve (PRV).* It maintains a specified pressure downstream from it. If the upstream pressure is higher, it creates enough head loss to reduce the downstream pressure to a specified level. The PRV can not maintain the specified pressure if bypasses occur or if the pressure at upstream node drops below the specified pressure.

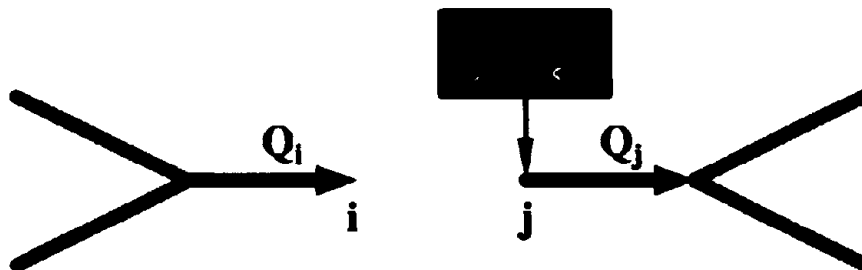


Figure 2.1: Modeling of a Pressure Reducing Valve

The modeling of a pressure reducing valve involves several steps:

- a. At the location of the pressure reducing valve, two disconnected nodes, i and j , are introduced as shown in Figure 2.1. Let i be the upstream node.

- b. The downstream node j is modeled as a fixed grade node. This may be done by connecting the node with a reservoir. At the upstream node, i , a flow demand Q_i is estimated.
 - c. The supply system is then solved to obtain the inflow, Q_j , through node j and compared with Q_i . If the difference is within the required accuracy, the solution is accepted, else an updated outflow at node i is estimated and the iteration is continued.
7. *Pumps*. It produces a local increment in pressure within a pipeline by feeding additional water into the network. The characteristics of pumps will be discussed in Section 6.
8. *Broken Pipes and Hydrants*. Breaks and leaks of pipelines can occur even during normal operating conditions. Seismic events may cause a large number of breaks and leaks in water supply systems. The particular damage state of a water supply system following an earthquake depends on the characteristics of the seismic waves, the extent of permanent ground deformations, and the strength of the system components.

The random spatial distribution of broken pipes and hydrants leads to complex flow conditions that cannot be characterized deterministically. Moreover, flowless pipeline and pipeline with partial flow can be present in the system. A broken pipe is modeled by replacing it with two pipes that are opened to atmosphere. The model provides an upper bound on damage because breaks are usually partial and because even a fully broken pipe can sustain pressure due to surrounding soil. A broken hydrant is modeled by additional pipe open to atmospheric pressure.
9. *Air Inlet Valve*. It admits air into a node when the corresponding pressure drops below the atmospheric or some other prescribed negative pressure.

2.3 Governing Equations of Flow

Two basic equations are used to analyze water distribution systems. They are known as the equations of continuity and energy.

2.3.1 Equations of Continuity

The law of conservation of mass states that the sum of the flows coming into and going out of a junction is zero, [7,31], e.g., at node i ,

$$\sum_k^{n_{pi}} Q_{ik} - \bar{Q}_i = 0 \quad (2.1)$$

where Q_{ik} is flow in pipe k connected at node i , \bar{Q}_i is discharge at node i . The summation takes place over all the pipes merging at node i . This condition must be satisfied at all nodes i .

2.3.2 Equations of Energy

The hydraulic head at node i is

$$H_i = E_i + p_i/\gamma \quad (2.2)$$

where E_i and p_i are the elevation and pressure at node i , and γ denotes the specific weight of water. The energy equation for a pipe k connecting nodes i and j is [7]

$$H_i - H_j = h_{f_k} + h_{m_k} \quad (2.3)$$

where h_{f_k} is head loss due to friction and h_{m_k} is minor head loss due to bends and joints between pipe segments.

An alternative to the energy equation is the loop equation, which states that the sum of the losses in each closed loop l of a water distribution network must vanish, i.e.,

$$\sum_k h_k = 0 \quad (2.4)$$

where $h_k = h_{f_k} + h_{m_k}$ is the total head loss in pipe k forming loop l and the summation takes place over all the pipes in the loop.

2.3.3 Energy Losses

As previously indicated, there are two types of losses that contribute to the decrease of head along a pipeline: *friction losses* and *minor losses*

Friction Losses

Friction loss, h_{fk} , relates to the flow, Q_k , in a pipe, k , by

$$h_{fk} = K_{fk} Q_k^a \quad (2.5)$$

where K_{fk} and a are constants that can be calculated in several ways. According to the Darcy-Weisbach equation [7,31], for $a = 2$,

$$K_{fk} = \frac{8fl_k}{gD_k^5\pi^2}, \quad (2.6)$$

where g is acceleration due to gravity, f is friction factor dependent on flow and pipe characteristics, l_k is length and d_k is diameter of pipe k . A method of computing f is described in [9].

The Hazen-William equation for $a = 1.852$ gives

$$K_{fk} = \frac{Bl_k}{C^{1.852}d_k^{4.87}} \quad (2.7)$$

where B is a dimensional constant, e.g., if l_k and d_k are in feet, $B = 4.73$. The values of C for different materials are available in [7,31,9].

The Manning equation for $a = 2$ gives

$$K_{fk} = \frac{4.637l_k\epsilon^2}{d_k^{5.333}} \quad (2.8)$$

where ϵ is a roughness factor. Its values for different materials can be found in [7,31,9].

Minor Losses

Minor head losses due to bends, valves, etc. are generally defined as [7,31],

$$h_{mk} = \frac{K_{mk}}{2gA_k^2} Q_k^2 \quad (2.9)$$

where K_{mk} is a coefficient depending on the type of pipe fitting that causes the head loss. Values of K_{mk} for various fittings are available in [7]. A_k is the cross section area of pipe k .

2.4 Methods of Solution

Flows in pipes and hydraulic heads at nodes are the unknowns for a water supply system. Flows and heads are related by the energy loss Eqs. (2.5) and (2.9). The flow continuity Eqs. (2.1) for nodes can be expressed as a set of nonlinear algebraic equations in terms of heads. These equations can be solved by iteration. Flows can then be obtained from the heads using Eqs. (2.3), (2.5), and (2.9). Similarly the loop Eq. (2.4) can be expressed in terms of flows. They can be solved by iteration. Two iterative methods for solving these nonlinear equations are discussed: the Hardy Cross and the Newton Raphson methods.

2.4.1 Hardy Cross Method

A common form of Hardy Cross method takes flows Q_k as unknowns and involves the following steps [7,31]:

1. Flows Q_k in all pipes are initially estimated with the constraint that at each junction the total flow is zero Eq. (2.1).
2. Consider a loop l of the system with n_{pl} pipes and the friction loss only. The friction loss in pipe k of loop l is $h_{fk} = K_{fk} Q_k^a$ (Eq. 2.5) where K_{fk} and a depend on the head loss equation (Eqs. 2.6, 2.7, 2.8). Due to error in the estimation of flows, the total head loss around the loop l , say in clockwise direction, will not vanish. The residual loss, R_l , is

$$R_l = \sum_{k=1}^{n_{pl}} K_{fk} Q_k^a \quad (2.1)$$

where $K_{fk} Q_k^a$ is positive if the direction of Q_k is in the clockwise direction of the loop.

3. Let dQ_l be the change of flow in the loop l . Then

$$\frac{dR_l}{dQ_l} = \sum_{k=1}^{n_{pl}} a K_{fk} Q_k^{a-1} \quad (2.2)$$

The derivative dR_l/dQ_l can be used to obtain a linearize correction,

$$\Delta Q_l = -\frac{R_l}{dR_l/dQ_l} \quad (2.3)$$

for Q_k . ΔQ_l is added to Q_k to obtain an improved flow estimate.

4. Steps 1 to 3 are repeated for all the loops of the network.
5. Steps 1 to 4 are repeated as long as the flow corrections ΔQ_i in all of the loops are not within a desired accuracy. Hydraulic heads at nodes can be obtained from the computed flows using Eqs. (2.3), (2.5), and (2.9).

In Hardy Cross method the loop equations are considered to determine the hydraulic state of the system. Generally, the number of equations is not very large because there are fewer loops than nodes or pipes. The solution procedure is simple because the loops are considered one at a time. This makes the method suitable for solving small systems by hand calculations. However, the method is difficult to code for computer use because it involves cumbersome record keeping of the loops and pipes. Thus, the use of the method for analyzing large systems is not attractive. Moreover, the convergence rate of the method is poor and depends strongly on the initial estimate of the flows in the pipes to start the iteration [31]. The method also does not allow modeling components where pressure is defined, e.g., broken pipes, because it is only possible to specify flow through the pipes. In spite of these, the method is widely used in the practice, e.g., Wood's computer code developed at University of Kentucky is based on this method [63].

2.4.2 Newton-Raphson Method

A common form of the Newton-Raphson method, in which heads are the basic unknowns, involves the following steps [9]:

1. Express the continuity Eq. (2.1) at each node i in terms of hydraulic heads. This results in

$$G_i(H_i, H_j) = 0, \quad j = 1, \dots, n_{pi} \quad (2.4)$$

where G_i is function $\sum_k Q_{ik} - \bar{Q}_i$ of Eq. (2.1) expressed in terms of the hydraulic heads, H_i and all heads H_j at nodes connected with n_{pi} pipes merging to node i . Q_{ik} and H_i are related nonlinearly by Eqs. (2.3), (2.5), and (2.9). Thus, G_i can be expressed as functions of heads only and are nonlinear functions of variables.

2. Form a system of nonlinear equations with Eqs. (2.4) applied at all of the nodes

$$\underline{G}(\underline{H}) = 0 \quad (2.5)$$

where \underline{G} is the vector of continuity equations for nodes $i = 1, \dots, n_n$ and $\underline{H}^T = \{H_1, \dots, H_{n_n}\}$ is vector of hydraulic heads.

3. Solve Eqs (2.5) by iteration using the Newton-Raphson method. The iterative formula for this method is

$$H^{(m+1)} = H^{(m)} - D^{-1}(H^{(m)})\bar{Q}(H^{(m)}) \quad (2.6)$$

where $H^{(m)}$ is the estimate at the m -th iteration for the heads, and $D^{-1}(H^{(m)})$ is the inverse of

$$D = \begin{bmatrix} \frac{\partial G_1}{\partial H_1} & \frac{\partial G_1}{\partial H_2} & \cdots & \frac{\partial G_1}{\partial H_{nn}} \\ \frac{\partial G_2}{\partial H_1} & \frac{\partial G_2}{\partial H_2} & \cdots & \frac{\partial G_2}{\partial H_{nn}} \\ \vdots & \vdots & \ddots & \vdots \\ \frac{\partial G_{nn}}{\partial H_1} & \frac{\partial G_{nn}}{\partial H_2} & \cdots & \frac{\partial G_{nn}}{\partial H_{nn}} \end{bmatrix} \text{ at } H^{(m)} \quad (2.7)$$

Iteration is started with an estimate of heads, $H^{(0)}$, at all the nodes of the system. This estimate can be based on experience. D and G are computed at $H^{(0)}$. Then Eq. (2.6) is used to obtain an improved estimate of heads, $H^{(1)}$. Iteration is repeated until the differences between the $(m+1)$ th and the (m) th heads are within a desired accuracy. Flows are obtained from the computed heads using Eqs. (2.3), (2.5), and (2.9).

The advantage of the Newton-Raphson method is its quadratic convergence rate, i.e., the error of the result of the $(m+1)$ th iteration is proportional to the square of the result of the (m) th iteration and is independent of the initial choice of $H^{(0)}$. However, it is impossible to model components where the discharge is specified, because in this method it is only possible to specify pressures at nodes.

2.5 Summary

This section provides information on the components and hydraulic analysis of water supply systems. Two methods are commonly used for the analysis of flow and pressure distribution in undamaged systems: The Hardy-Cross method and the Newton-Rapson method. However, these methods are not suitable for the analysis of damaged water distribution systems because they can predict high negative pressures that cannot occur in actual system.

SECTION 3

HYDRAULIC NETWORK MODELS FOR DAMAGED SYSTEMS

3.1 Introduction

Water distribution networks are designed to deliver water to each junction of the system in sufficient quantities and at adequate positive pressure satisfying design demands. The output of the system can be altered drastically if the system is damaged, e.g. following a seismic event. Current methods of hydraulic analysis may predict large negative pressures at many junctions of the damaged network because of the assumption of continuity of flow. Negative pressure can develop only if the system is perfectly air tight. However, physical systems have leaks so that negative pressures cannot be maintained.

This Section presents a new method for the analysis of damaged water distribution networks. The method is based on the assumption that air is admitted into pipelines when one or more nodal pressures are significantly below the atmospheric pressure. The unknown parameters are flows and hydraulic heads. They satisfy a set of nonlinear algebraic equations which can be solved by iteration. The number of equations in this new method is equal to the total number of nodes and pipes of the system. In contrast, the total number of equations involved in the Newton-Raphson method or the Hardy-Cross method is smaller than total number of nodes and pipes.

An important factors for estimating system performance are serviceability and degree of damage. The serviceability can be defined, e.g., as the ratio of total available flow, at a set of prescribed hydrants of a system in a particular damaged state, to a specified demand. The degree of the system damage can be defined, e.g., as the ratio of total available flow for the damage state to the total available flow for the undamaged system. A simulation method is developed to estimate the performance of water supply systems based upon the above formulation. It involves (1) generation of fire scenarios consistent with site fire risk; (2) hydraulic analyses for undamage state; (3) generation of sample damage states for water supply systems consistent with site seismicity; (4) hydraulic analyses of damaged systems; and (5) development of post-earthquake performance measures from statistics of the analyses performed in the second and fourth step.

3.2 Formulation

The continuity and energy requirements in Eqs. (2.1) and (2.3) are used simultaneously to form a set of nonlinear algebraic equations in terms of unknown pressures and flows characterizing a supply system. The unknowns are solved by iteration. Minor losses due to system components in Eq. (2.9) are assumed to be small compared to friction losses in long straight piping and hence are ignored in this formulation.

The flows in the the friction loss Eq. (2.5) can be either positive or negative depending of direction of the flows. To account for the sign Eq. (2.5) is modified to

$$h_{fk} = K_{fk}|Q_k|^{a-1}Q_k \quad (3.1)$$

From Eqs. (2.2), (2.3) and (3.1)

$$p_i - p_j = \gamma K_k |Q_k|^{a-1} Q_k - \gamma E_i + \gamma E_j \quad (3.2)$$

where E_i and p_i are elevation and pressure at node i , γ is the specific weight of water, K_k and a are constants dependent on head loss Eqs. (2.6), (2.7), or (2.8).

The flows Q_{ik} in pipelines merging at a node i and the discharge flow \bar{Q}_i at node i satisfy the continuity condition given by Eq. (2.1)

$$\sum_k^{n_{pi}} Q_{ik} = \bar{Q}_i \quad (3.3)$$

where the summation extends over all the pipes converging to node i .

Eqs. (3.2) and (3.3) form a set of n_p nonlinear and n_n linear algebraic equations,

$$Q_k - b_k p_i + b_k p_j = \gamma b_k (E_i - E_j), \quad k = 1, 2, \dots, n_p \quad (3.4)$$

and

$$\sum_k^{n_{pi}} Q_{ik} = \bar{Q}_i, \quad i = 1, \dots, n_n \quad (3.5)$$

where

$$b_k = \frac{1}{\gamma K_k |Q_k|^{a-1}} \quad (3.6)$$

In Eqs. (3.4) and (3.5), Q_k and p_i are the unknowns, E_i and \bar{Q}_i are known quantities. Thus the total number of unknowns in this method is $n_p + n_n$. The number of unknowns in

the Hardy Cross and the Newton Raphson methods, described in Section 2 are n_p and n_n respectively. Eqs. (3.4) and (3.5) can be written as,

$$[A]\{X\} = \{r\} \quad (3.7)$$

where

$$\{X\}^T = \{Q_1, Q_2, \dots, Q_{n_p}, p_1, p_2, \dots, p_{n_n}\} \quad (3.8)$$

$$\{r\}^T = \{c_1, c_2, \dots, c_{n_p}, \tilde{Q}_1, \tilde{Q}_2, \dots, \tilde{Q}_{n_n}\} \quad (3.9)$$

and $c_i = \gamma b_k(E_i - E_j)$. The matrix $[A]$ is of the form

$$[A] = \begin{bmatrix} [I] & [b] \\ [d] & [0] \end{bmatrix} \quad (3.10)$$

In Eq. (3.10), the unit matrix $[I]$ is of size $(n_p \times n_p)$, the matrix $[d]$, consisting of 1, -1 and 0's, is of size $(n_n \times n_p)$, and the lower right block $[0]$ has only zeros. The upper right block $[b]$ of size $(n_p \times n_n)$, contains functions of Q_k defined by Eq. (3.6). Both the lower left and upper right corner blocks are sparse matrices. Eq. (3.7) can be rewritten as

$$\begin{bmatrix} [I] & [b] \\ [d] & [0] \end{bmatrix} \begin{Bmatrix} x_1 \\ x_2 \end{Bmatrix} = \begin{Bmatrix} r_1 \\ r_2 \end{Bmatrix} \quad (3.11)$$

where $\{x_1\}^T = \{Q_1, Q_2, \dots, Q_{n_p}\}$, $\{x_2\}^T = \{p_1, p_2, \dots, p_{n_n}\}$, $\{r_1\}^T = \{c_1, c_2, \dots, c_{n_p}\}$ and $\{r_2\}^T = \{\tilde{Q}_1, \tilde{Q}_2, \dots, \tilde{Q}_{n_n}\}$. From Eq. (3.11) we obtain

$$[d][b]\{x_2\} = [d]\{r_1\} - \{r_2\} \quad (3.12)$$

$$\{x_1\} = \{r_1\} - [b]\{x_2\} \quad (3.13)$$

which can be used to determine $\{x_1\}$ and $\{x_2\}$ by iteration. The matrix $[d][b]$ in Eq. (3.12) is symmetric of size $(n_n \times n_n)$ and is in general sparse. A sparse matrix equation solver is used to compute $\{x_2\}$ from Eq. (3.12).

Consider a seismic event causing a fire scenario consisting of n_h fires with required flows \tilde{Q}_i^* at minimum positive pressures p_i^* , $i = 1, \dots, n_h$. Let \tilde{Q}_i , $i = 1, \dots, n_h$ be estimated discharges at the hydrants nodes i closest to these fires. Let p_i , $i = 1, \dots, n_h$ be the pressures at hydrant nodes i obtained by hydraulic analysis of the system. Some of these pressures may be less than p_i^* . Let $n_h = 1$, in which case the pressure p_1 decreases monotonically with increase

of \tilde{Q}_1 . In order to supply water with a pressure $p_1 = p_1^*$, analyses are performed iteratively with \tilde{Q}_1 as iterate. When $n_h > 1$, the analyses are still performed iteratively, but instead of solving for $p_i = p_i^*, i = 1, \dots, n_h$, an objective function such as

$$e = \sum_{i=1}^{n_h} |\tilde{Q}_i - \tilde{Q}_i^*| s(p_i - p_i^*) \quad (3.14)$$

can be minimized. Here

$$\begin{aligned} s(x) &= 0, \text{ for } x < 0 \\ &= 1, \text{ for } x \geq 0 \end{aligned} \quad (3.15)$$

The minimization is performed by proportionately varying all the \tilde{Q}_i s such that a single parameter $\tilde{Q}_i/\tilde{Q}_i^*$ is used in the iteration.

The proposed method of solution follows five steps:

1. Flows, $Q_k, k = 1, \dots, n_p$, through all the pipes and discharge, $\tilde{Q}_i, i = 1, \dots, n_h$, at fire hydrants of the network are estimated. The matrix $[b]$ is formed from the flows through the pipes.
2. Pressures at nodes are obtained by solving Eq. (3.4) and Eq. (3.5) simultaneously using a symmetric, sparse matrix equation solver.
3. The flows Q_k are updated according to Eq. (3.4)
4. Steps 1 through 3 are repeated until the absolute values of all the differences between the current and the previous values of flows are less than a specified tolerance.
5. Steps 1 through 4 are repeated to minimize the objective function in Eq. (3.14), by proportionately varying \tilde{Q}_i .

3.3 Negative Pressure

Hydraulic analysis of damaged supply systems, using equations of continuity and energy, can predict large negative pressures at nodes. To address this problem, the present analysis is based on the assumption that the system admits air at node i when the pressure, p_i , at this node falls below atmospheric pressure. This assumption is consistent with the performance of pipeline systems because they are not air tight.

Consider a node i with $p_i < 0$ and hydraulic head $H_i = E_i + p_i/\gamma$, where zero stands for the atmospheric pressure. Since the physical systems are not air tight, air enters the system through node i causing the pressure at node i to become equal to atmospheric so that $p_i = 0$. Then, the head at node i is $H_i = E_i + p_i/\gamma = E_i$. Let Q_k be the flow through pipe k connecting nodes i and j . Flows Q_k are zero if $E_i = H_i > H_j$ for all nodes j . In this case, node i is called a *no-flow* node. Flows Q_k are not zero when the above condition is not satisfied for all nodes j . In this case, the condition for an open channel flow or, partial flow, is met for pipelines k with $H_j > E_i$. The corresponding node is reported to as *partial-flow* node.

The solution of a damaged pipeline system involves several phases. First, nodes with negative pressure are identified and divided into two categories: no-flow nodes and partial flow nodes. The no-flow nodes and the pipes converging to these nodes are eliminated sequentially, starting with the node of highest negative pressure. Flows and pressures are recalculated after each elimination. The no-flow nodes may isolate a part of the network, in which case that part is simply taken out from the system. Second, partial flow nodes are considered. Let i be a partial flow node and j be a node connected to i so that $H_j > E_i$. Then, the pipe connecting nodes i and j has partial flow. The effect of partial flow in the pipe is approximated by decreasing the roughness coefficient of the full flow pipes until $p_i = 0$. This is a heuristic approach. Thus, the explicit calculation for an open channel profile is avoided. While adjusting any no-flow or partial flow node, the previously adjusted nodes are checked to ensure that they continue to meet the criteria for no-flow and partial flow nodes. The algorithm involves lengthy computations because of repeated flow analyses of the entire network.

3.4 Potential Damage States of a Pipeline System

In this report the characterization of seismic performance of network components is based on records relative to seismic waves and permanent ground deformations from previous earthquakes. These observations can be used to develop approximate relationships between the mean break rates of pipelines $\lambda(I)$ and modified Mercalli Intensity, I . The probability of at least one break in a pipeline of length L caused by an earthquake of intensity I can be approximated by

$$P_p(L, I) = 1 - \exp(-\lambda(I)L) \quad (3.1)$$

if it is assumed that the breaks occur according to a homogeneous Poisson process of intensity $\lambda(I)$. Local soil conditions can be accounted for by letting $\lambda(I)$ be a function of location. In this case the pipe break follows an inhomogeneous Poisson process. According to this model, pipelines can be either fully operational (0% damage) or disconnected (100% damage).

Estimates of the mean break rate $\lambda(I)$ obtained from field observations usually include disconnected and partially damaged pipelines. Since, the partially damaged pipelines still provide some flow, the analysis based on these estimates tends to be conservative. The model could be refined by considering additional damage states, such as leaks, which do not involve a complete loss of continuity. However, information currently available from post-earthquake studies is insufficient to calibrate such a model.

In addition to pipe breaks a system can be damaged by hydrant breaks. The occurrence of hydrant breaks can be modeled by a Bernoulli random variable. According to this model only two outcomes are possible: hydrant breaks or hydrant survives.

The Bernoulli model also can be used to generate fire ignition. Fire ignition results in water demand at the closest hydrant. Thus, the hydrant can be either open in case of fire or closed in case of no fire. The size of the fire determines the water demand at the hydrant. The water demand is modeled by a random quantity with a lognormal distribution. A detailed presentation of Bernoulli modeling procedure will be in Section 5.

3.5 System Definition and Serviceability Analysis

A network includes pipes, pumps, reservoirs, hydrants, valves, and other components, that may be turned on or off selectively. The system components must be specified before any analysis is performed.

Following the system definition and the selection of earthquake intensity I , damage states containing pipe and hydrant breaks can be generated, from the water supply system. Damage state can be obtained by generating a number, u , from a uniformly distributed random variable U in the range (0, 1) for each pipe and each hydrant and comparing these numbers with probabilities $P_p(L, I)$ in Eq. (3.1) for pipe breaks and with the failure probabilities, P_h , of a hydrant. If $u < P_p(L, I)$ at least one pipe break occurs along the pipe so that the nodes at the pipe ends are opened to the atmosphere. Otherwise, connectivity between these nodes is retained. Hydrants can be modeled only at nodes. If $u < P_h$ the hydrant breaks. A pipe

open to atmospheric pressure is added to the node to model the hydrant break. A sample of the damage state of a system can be generated by applying this procedure to all pipes and nodes of the system.

Fire ignitions can be obtained in similar fashion as hydrant breaks by replacing the failure probability P_h by the probability P_f of having a fire in the vicinity of a hydrant. Fires can be modeled only at nodes. A pipe open to 20psi pressure is added to the node to enable a water demand. The water demand at the node can be generated from lognormal distribution assuming the second moment characterization of the demand is known.

Consider a fire scenario consisting of n_h fires demanding flows \bar{Q}_i^* at minimum hydrant pressures p_i^* near hydrant nodes $i = 1, 2, \dots, n_h$. Consider the objective function in Eq. (3.14) corresponding to \bar{Q}_i^* and p_i^* . The damaged system can be analyzed, using this objective function and the method for hydraulic analysis in this report. Let \bar{Q}_i and p_i be the discharges and pressures at hydrant nodes i . The total available flow, Q_T , is defined as the sum of discharges from the hydrants with pressures $p_i \geq p_i^*$. Thus,

$$Q_T = \sum_{i=1}^{n_h} \bar{Q}_i s(p_i - p_i^*) \quad (3.1)$$

is a sample of a random variable depending on earthquake intensity, damage state, and fire scenario in the system. The function $s(p_i - p_i^*)$ has been defined in Eq. (3.15).

The available flow Q_T can be used to develop the post-earthquake performance measures: the serviceability index S_s

$$S_s = \frac{Q_T}{\sum_{i=1}^{n_h} \bar{Q}_i^*} = \frac{Q_T}{Q_T^*} \quad (3.2)$$

and the damage index S_d

$$S_d = \frac{Q_T}{Q_{T0}} \quad (3.3)$$

where Q_T^* is the total required and Q_{T0} is the total available flow for the undamaged system.

Values of S_s and S_d corresponding to simulated damage states and a specified fire scenario can be regressed against earthquake intensity I to develop global serviceability measures for a water supply systems. These regressions constitute fragility curves of the system. Fragility curves can also be developed for modified version of the original system, e.g., by replacing some of its components with stronger components. The approach can be used to identify the most critical components of a system.

3.6 Summary

A new method is presented for the analysis of damaged water supply systems . The method can account for the negative pressure that usually develops in systems that are damaged by seismic excitation. The method provides estimates for the system serviceability in damaged state and the degree of damage.

SECTION 4

SAN FRANCISCO AUXILIARY WATER SUPPLY SYSTEM

4.1 Introduction

The Auxiliary Water Supply System (AWSS) supplies water exclusively for fire protection of the San Francisco. The system was constructed after the 1906 earthquake when became evident that the Municipal Water Supply System (MWSS) alone could not provide sufficient fire protection for the city. The AWSS is a high pressure system that covers approximately 20sq. miles of the city area. Within this area, historical evidence distinguish locations with potentials for soil liquefaction and large ground deformation [35,40]. Several areas are particularly identified for which has been shown a clear evidence between ground deformation caused by soil liquefaction and damage to underground pipeline system. Detail soil investigation of these areas are helping to estimate the amplification of permanent ground motion attributed to soil liquefaction.

This section has two major parts. The first part of this section describes the geotechnical characteristics of the areas with soil liquefaction potentials. The second part fully describes the AWSS. In addition, it briefly describes the MWSS and Portable Water Supply Systems (PWSS) as contributing water systems for the City's fire protection.

4.2 Geotechnical Characteristics

Four well defined areas are particularly vulnerable to earthquake hazards in the city of San Francisco. Figure 4.1 shows those areas of severe ground shaking, soil liquefaction and large ground deformations observed during the 1906 and 1989 earthquakes. The areas, which are bounded by dashed lines, include the Marina district, South of Market, Mission Creek, and Foot of Market. In this areas fill had been placed along the waterfront, inlets, coves, marshes, and ravines. A brief geotechnical description of these filled zones is presented to indicate their vulnerability during earthquakes.

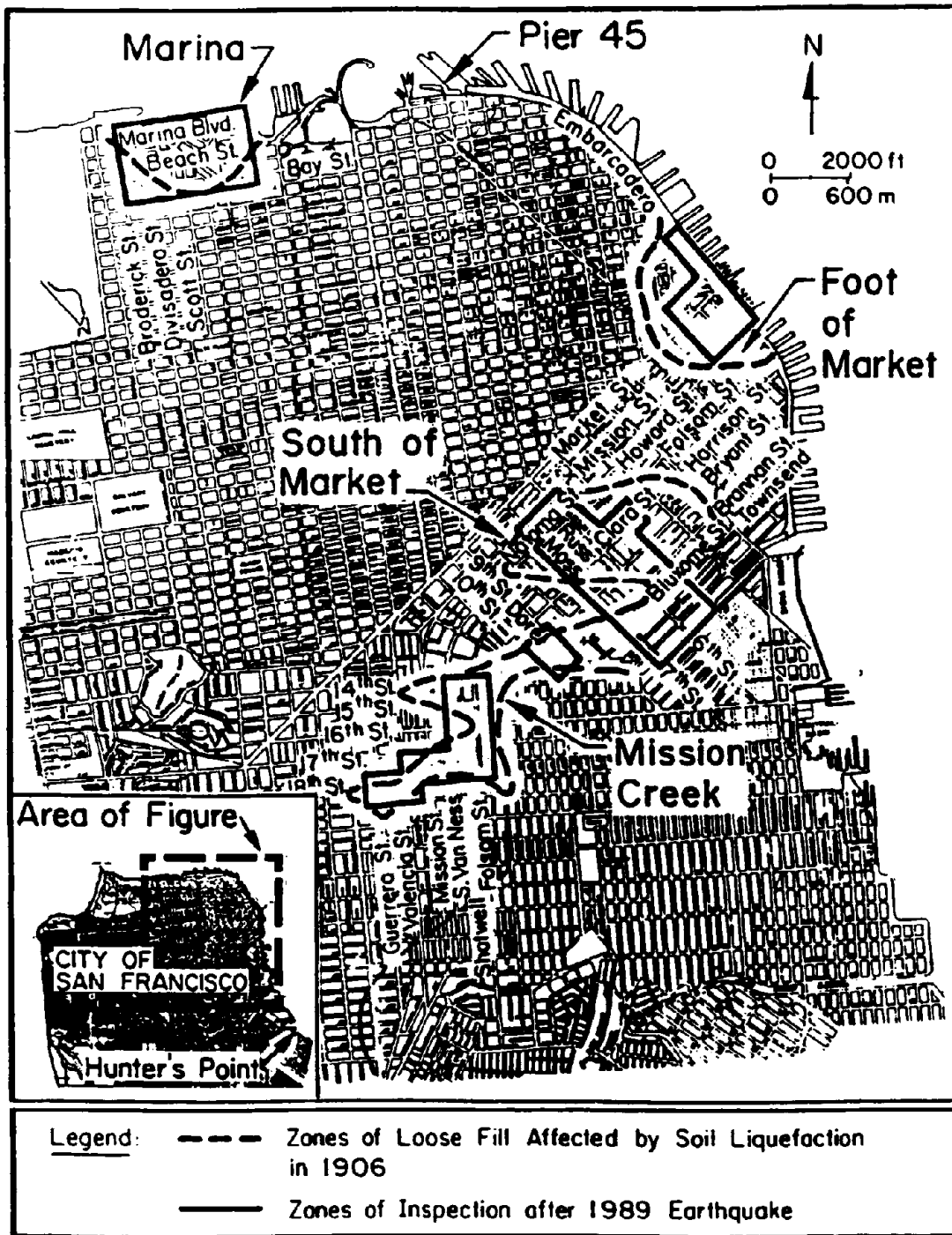


Figure 4.1: Plan View of San Francisco Showing Zones of 1906 Soil Liquefaction and Inspection After the 1989 Earthquake

The Marina site was developed in two stages by placing sandy fills on soft clays and silts. The first stage is mostly related to land-tipped fills prior to 1900. The second stage occurred in 1912 when sandy sediments were dragged and pumped into the lagoon bounded by an old seawall. The maximum depth of fill is about 20-ft. The depth of water table is about 8-ft. Fills and deposits are placed on top of Holocene bay mud. It has been shown [39] that these fills have a relatively high susceptibility to liquefaction.

The South of Market site is the area of old Sullivan Marsh, a tidal marsh which was contiguous with two small tidal streams. The original shore line of Mission Bay was at this site. The area was filled in 1850's with material excavated from the nearby sand dunes [32]. The fill varies in the depth with average thickness of about 20-ft. The depth of water table is approximately 6-12-ft. The fill is underlined by a peat deposit, about 3-6-ft thick. Liquefaction potential analyses were performed for the fill indicating that the area is highly susceptible to soil liquefaction for events comparable in magnitude and intensity to those experienced during the Loma Prieta earthquake [39].

The Mission Creek site is the area of former tidal creek and neighboring salt marsh. Fill is generally a very loose fine sand, about 20-ft thick. A water table is approximately 3-9-ft below ground surface. The fill is underlined by about 20-ft of Holocene bay mud, with approximately 120-ft of dune sands and stiff clays, to weathered serpentine bedrock at a depth of roughly 60-ft from the ground surface. The liquefaction potential analyses of the site also indicate highly susceptible to soil liquefaction for events comparable in magnitude and intensity to those experienced during the Loma Prieta earthquake [39].

The Foot of Market site is the downtown area of San Francisco. Development of this area begun in the 1850's when the original shore line was displaced. The artificial fill is primarily composed of loose fine sand or silty sand with rubble. Depth of the fill varies approximately from 20-40-ft. A deep deposit of silty clay and dense clayey fine sand underlines the fill. The ground water table is at depth of about 6-15-ft. This site experienced a high intensity of liquefaction and permanent ground displacement during 1906 and 1989 earthquakes.

Geotechnical characteristics and historical evidence of these four areas indicate a high potential for widespread liquefaction ground failure. Amplification of bedrock motion through the deposits of soft clay and silt contributed to strong shaking and damage at the surface. Such amplification also was responsible for triggering soil liquefaction by which would not have been attained without the presence of soft bay sediments.

Pipelines tend to follow ground deformation since they are placed in ground. It has been

shown a remarkable correlation between the locations of pipeline breaks and surface topography [36]. A large number of breaks had been observed along the boundary between solid and artificially made ground. Breaks in pipelines were primary result of permanent ground motions in the areas vulnerable to soil liquefaction. The GISALLE allows modeling of this phenomena by introducing an amplification factor for pipes crossing the zones of high potentials for liquefaction.

4.3 Water Supply System in San Francisco

There are two main water supply systems in the city of San Francisco: the Auxiliary Water Supply System (AWSS) and the Municipal Water Supply System (MWSS). The systems are totally independent since the AWSS is used only for fire protection while the MWSS provides the main source of domestic and commercial water. However, the MWSS can be used as an additional support for fire fighting purposes as well. In addition to these two systems the city of San Francisco has also a Portable Water Supply System (PWSS). In the past, the PWSS has provided an important contribution to the City's fire protection.

4.3.1 Auxiliary Water Supply System (AWSS)

Nearly 85% of the total damage to the City of San Francisco caused by the 1906 earthquake was due to fire destruction. The existing water supply system, MWSS, failed to provide sufficient amount of water because of the large number of breaks in the trunk and distribution lines. The need for construction of the AWSS emerged after this earthquake. The system was designed to provide a supplementary network that would work independently of, and in parallel with, the MWSS. The major portion of the system was built in the decade following the 1906 earthquake. It covered the Central Business District on the North-East part of the City. Throughout the years the system was gradually extended into other parts of the City, although the original portion still constitutes the majority of the network.

The AWSS operates at a pressure of about 150psi. The system is the backbone of the fire protection of the San Francisco. It is owned and operated by the San Francisco Fire Department (SFFD). The AWSS has no domestic and commercial connections and is used only to provide water for fire demands. Figure 4.2 shows a plan view of the AWSS, with contour lines of equal elevation. The network is separated into two zones: the Lower Zone,

shown with solid lines and the Upper Zone, drawn with dashed lines. Two zones can be connected to increase the pressure in the Lower Zone.

The AWSS is composed of approximately 125 miles of buried pipes with nominal diameter ranging from 10-20 inches. Nearly 100 miles of the system is cast iron, of which about 25 miles of ductile iron pipe have been added during the past several years. Pipes are connected by sleeved joints and restrained against pullout by longitudinal bolts. However the joints can rotate to allow pipelines to accommodate for differential ground settlement. Flow in the pipes and different regions of the network is controlled by standard gate valves and check valves. The valves are operated from a control center located at the Jones Street Tank house. The control center provides readings from a limited number of pressure gauges distributed throughout the system. A number of gate valves can be remotely operated from the center via land lines. However, many gate valves in the system must be operated manually. The outflow from the system is provided through the fire hydrants.

The Hydrants are typically constructed of 8-in diameter cast iron elbow supported by a concrete thrust block at approximately 5-ft below the surface level as shown in Figure 4.3. Because of the high pressure in the mains, fire trucks are not required to feed individual nozzles. Using a special pressure regulating device known as a "Gleeson" valve, the pressure to several fire hoses can be controlled directly at the hydrant, making the AWSS usable even in the case that access to a fire by fire trucks is impossible. A shut-off valve is located between the hydrant and the network and is used to control water supply, and to maintain and replace hydrants.

The Water Supply of the AWSS is provided from three major sources: reservoirs, pump stations and fire boats.

Three reservoirs are available: Twin Peak Reservoir, Ashbury Tank, and Jones Street Tank as shown in Figure 4.4. The Twin Peak Reservoir is located on the highest point of San Francisco. The reservoir supplies the Upper Zone as well as the Lower Zone. This is the largest reservoir with a capacity of 10 million gallons. The capacity may not be adequate under emergency conditions which can result after an earthquake. The Ashbury Tank supplies water and controls pressure in the Upper Zone. It has a capacity of 0.5 million of gallons. The Jones Street Tank supplies water and controls pressure in the Lower Zone. It has a capacity of 0.75 million gallons. The Lower Zone pressure can be increased by opening the valve at the JST house. The pressure in the Upper Zone is controlled by the Twin Peak and the Ashbury Tank.

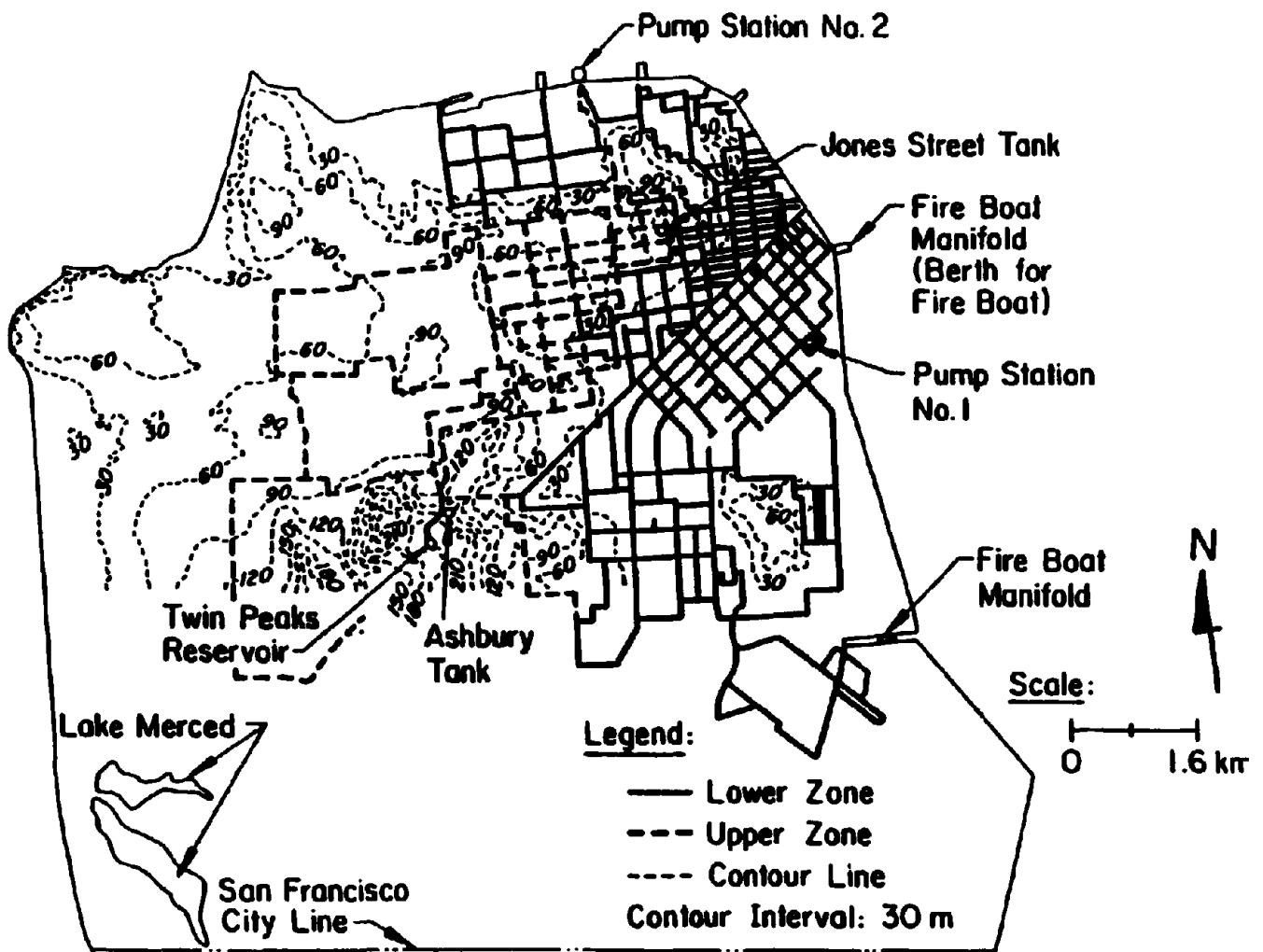


Figure 4.2: The Auxiliary Water Supply System (AWSS) of San Francisco

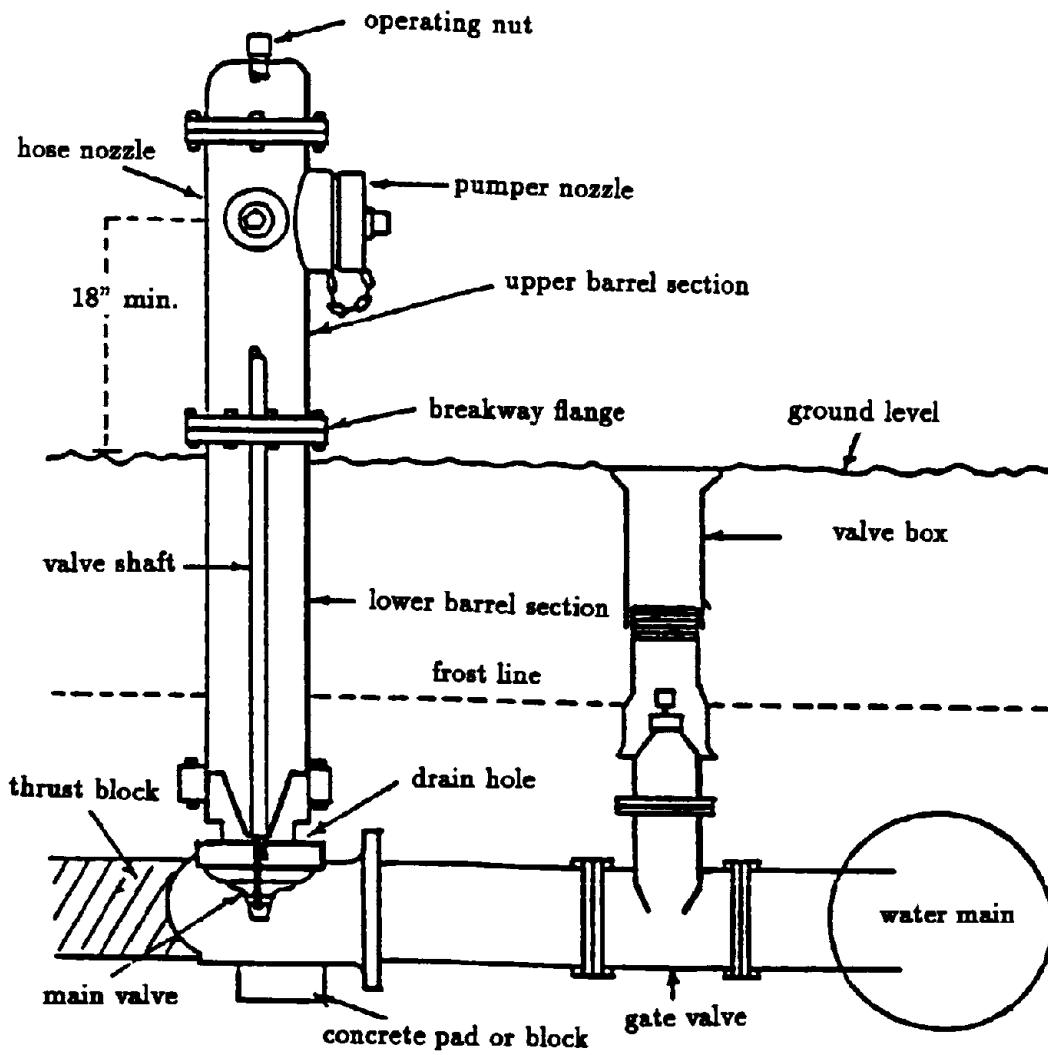


Figure 4.3: A Typical Hydrant

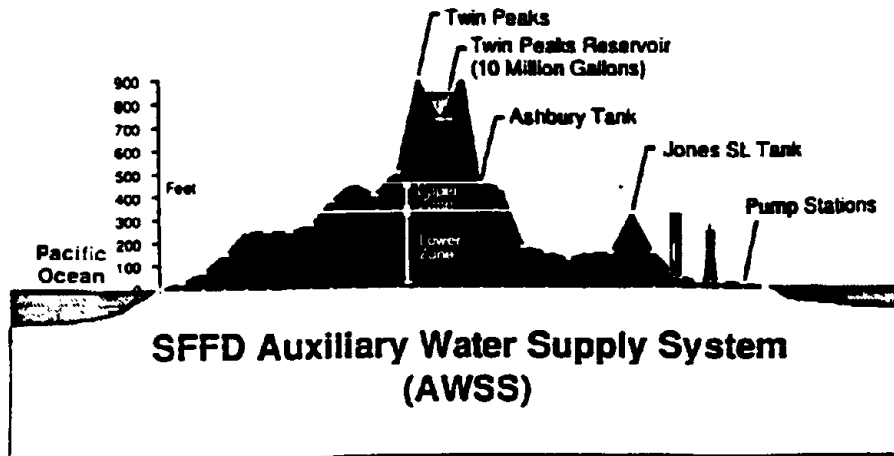


Figure 4.4: Schematic Cross-section of the AWSS

Two pump stations can contribute to the reservoirs supply by pumping water from San Francisco Bay into the system. Originally, both pump stations were steam powered and were converted to diesel power in the 1970's. The pump stations have four engines, each of which has capacity of 2,500 gpm at 300 psi. Pump station No.1 located at the corner of 2nd and Townsend Sts. and supplies only the Lower Zone. However, Pump station No.2 located at Aquatic Park can supply both Zones.

The AWSS has five manifold connections along the City's waterfront, that permit the City fireboat *Phoenix* to act as an additional "pump station", supplying the AWSS with San Francisco Bay water. The *Phoenix* pump capacity is 9,600 gpm at 150 psi.

The damage of the San Francisco MWSS in the 1906 earthquake was related to ground failures and concentrated in zones corresponding to filled-in land. It is very likely that similar ground failures can occur in future earthquakes. Therefore, the AWSS was designed to accommodate for the critical zones. The system has ten zones, referred as "infirm areas" as shown schematically in Figure 4.5. The areas coincide to the zones of expected ground failure. In the infirm areas the pipe network is specially valved to minimize the water loss in case of failure. All of the gate valves isolating the infirm areas are closed. Thus, water main breaks occurring in the infirm areas can be quickly isolated. On the other hand, should major fire demand be required in these areas the water supply can be increased significantly by opening these valves.

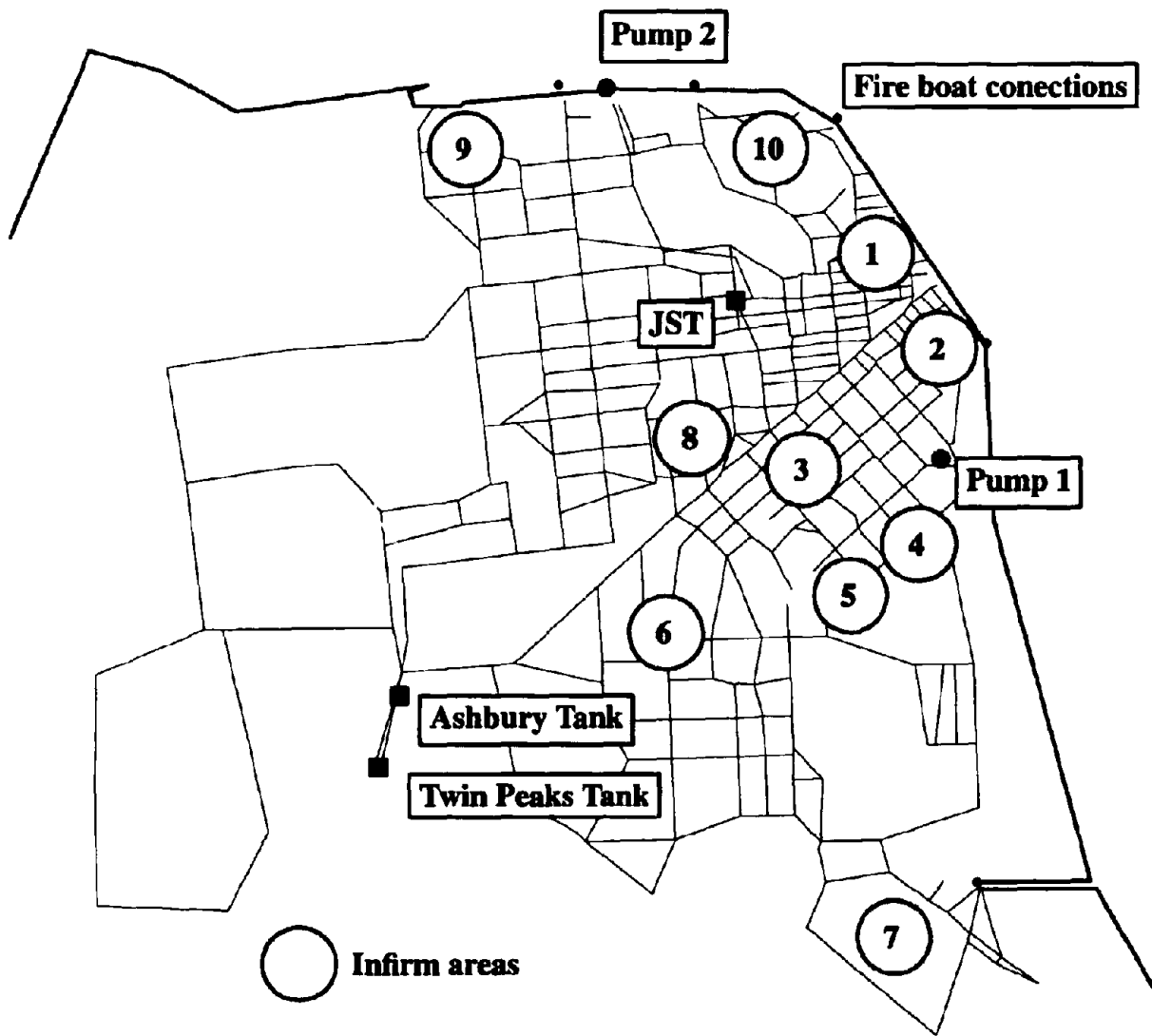


Figure 4.5: The Locations of Ten Infirm Areas in the City of San Francisco

4.3.2 The Municipal Water Supply System (MWSS)

This system can be used as a supplement to the AWSS for fire fighting via hydrants and sprinklers. The MWSS provides water from 18 different reservoirs and a number of smaller storage tanks. The water is stored at different levels creating zones, or districts, where water is distributed within a certain range of pressure. There are 23 different pressure districts, of which the Sunset and University Mound Reservoir System are the largest. The pipelines in these systems range in diameter from 8 to 60 inches, and vary in composition from riveted and welded steel to cast iron.

4.3.3 The Portable Water Supply Systems (PWSS)

This system can increase the reliability of fire fighting water supply in North-East quadrant of San Francisco because major fires can and do occur [51] at large distances from the AWSS pipe network. The basic components of the PWSS are: (1) Hose Tenders, trucks capable of carrying 5000-ft. of large diameter e.g., 5-in hose, and a high pressure monitor for master stream, (2) Hose Ramps, which allow vehicle to cross the hose when it is charged, (3) Gated Inlet Way, allowing water supply into large diameter from standard fire hose, (4) Gleeson valve, a pressure reducing valve, and (5) Portable Hydrants, that allow water to be distributed from large diameter hose.

The large diameter hose is carried on hose tenders, together with portable hydrants, pressure reducing Gleeson valves and other fittings. Each hose tender carries almost one mile of hose, and is capable of laying the hose in about twenty minutes. Hoses are intermittently fitted with portable hydrants, providing points of water supply at many locations along the hose.

4.3.4 Underground Cisterns

The city of San Francisco has also 151 cisterns mainly in the northeast region of the City. These cisterns are typically of concrete construction. Only few are brick that were constructed prior to the 1906 Earthquake. Cisterns have capacity of approximately 75,000 gallons. They are located at street intersections, accessible by a manhole. They are highly reliable and have an extremely low maintenance. The cisterns are completely independent of all piping and are filled from pumpers by the San Francisco fire department. In the event of a water main failure, water may be drafted from these cisterns via manholes. A bond

issue was passed in 1986 for constructing an additional 95 cisterns outside of the northeast quadrant of the City.

4.4 Summary

The geotechnical description of the area covered by the AWSS indicate existence of several zones with high potentials for soil liquefaction. The components of the AWSS in these zones are likely to be exposed to large ground deformation. Degree of the permanent ground movement can be estimated from the specific soil characteristics of these areas. This zonal vulnerability of the system is implemented in the GISALLE code.

The description of the AWSS demonstrates the complexity of this system. It is not possible to predict accurately neither the potential spatial distribution and intensity of the system damage nor the potential fire demand caused by seismic events. Therefore, system damage state and fire demand scenario need to be modeled as random quantities. A computer simulation algorithm is the only convenient way to analyze and predict the seismic performance of AWSS. A computer code, GISALLE, provides such a tool for analyzing the seismic performance of water systems.

SECTION 5

GISALLE

5.1 Introduction

An interactive computer code with graphical capabilities, GISALLE, was developed at Cornell University for evaluating the seismic performance of water distribution networks. The code is applied to determine the seismic serviceability of the Auxiliary Water Supply System (AWSS) in San Francisco. Several performance indices can be determined.

The code involves modules for system definition, system modification, seismic damage modeling, hydraulic analysis, statistical analysis and presentation of results. The modules for seismic damage representation and statistical analysis involve probabilistic, simulation, and statistical concepts.

The GISALLE code includes a pre- and post-processor with graphic interface to facilitate the system definition and display probabilistic measures of system serviceability. The code demonstrates how computer simulation of complex lifeline networks can be used for rapid system analysis in case of emergency and for management within the context of practical, day-to-day operational demands.

5.2 Organization of the Computer Code

Figure 5.1 shows the major components of GISALLE. The code has preprocessing, analysis, and postprocessing capabilities. The *Preprocessor* can be used to generate damage states of the water supply system consistent with the site seismicity, soil conditions, conflagration risk and network characteristics. The *Analysis* determines available flows and pressures at critical hydrant locations that correspond to generated damage state and fire scenario. The output consist of pipe flows and node pressures, serviceability indices, and fragility curves. The *Postprocessor* provides display of flows, pressures, and serviceability measures.

The principal modules of GISALLE are the definition, modification, damage, hydraulic analysis, statistical, and results modules.

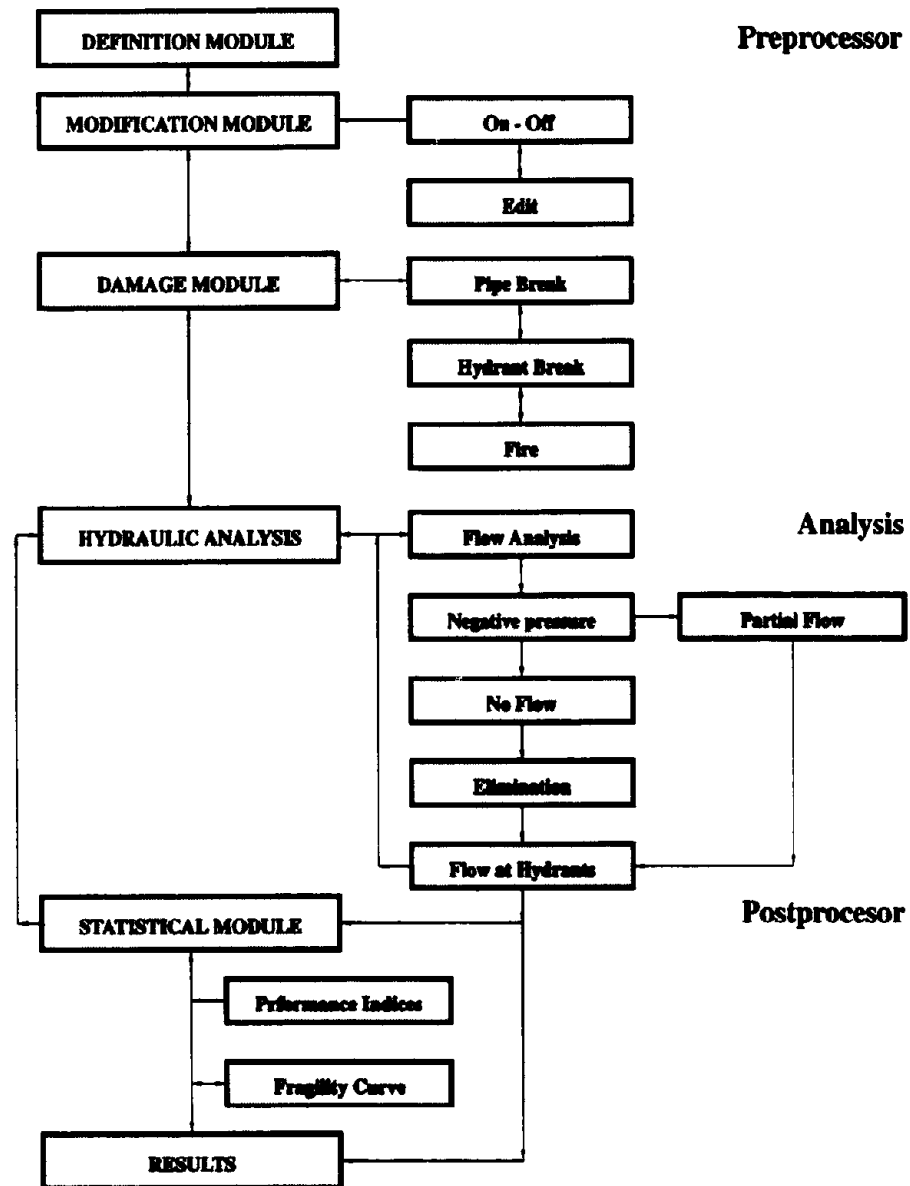


Figure 5.1: GISALLE Flow-Chart

5.3 Definition Module

The GISALLE code has a library of undamaged water supply systems in the form of data files. Figure 5.2 shows the graphical representation of the AWSS on the computer screen as provided by GISALLE. This is a 2-D approximation of the as-built system because pipeline of diameter smaller than 10-in are not shown and not all junctions are presented. However, demands for the pipes or regions not shown can be specified at corresponding nodes. Pipelines of different diameters are represented by lines of different thicknesses increasing with the pipe diameter. Three water supply sources are also shown in the figure: the Twin Peak Reservoir, the Ashbury Tank, and the Jones St. Tank. The figure shows five fire boat manifolds along the bay line. Fire boats may be connected to one or more manifolds. The figure shows also Pump Stations 1 and 2. These stations are modeled as single pumps or combinations of pumps with characteristics described in Section 6.

The data file provides a full description of a water supply system. It contains information on pipes, valves, and nodes. The pipes are characterized by size, length, roughness coefficient, soil condition, and nodal connectivity. The valves are modeled as 10-ft-long pipes inserted between two nodes. Valves are described either as closed or check valves. Closed valves prevent the flow in the corresponding pipes. Check valves are modeled as closed pipes only if water flow is against the operating direction. The nodes are specified by coordinates, elevation, specified demand, soil condition, fire risk, and connectivity to pipes. Description of nodes include additional information if nodes are connected to fixed or variable grade components. Fixed grade nodes are nodes connected to reservoirs, storage tanks or a discharge point where pressure is specified. Variable grade nodes are nodes, connected to pumps and fire boats. The GISALLE code can be applied to analyze very large networks transporting water or other fluids. The program accepts British and SI units.

5.4 Modification Module

The initial data file stored in the GISALLE library can be modified to correspond to a particular supply-demand scenario by means of the modification module containing interactive computer graphics code. The module has two parts: *The On-Off Module* and *The Edit Module*. The modification module can be skipped to call the analysis module directly.

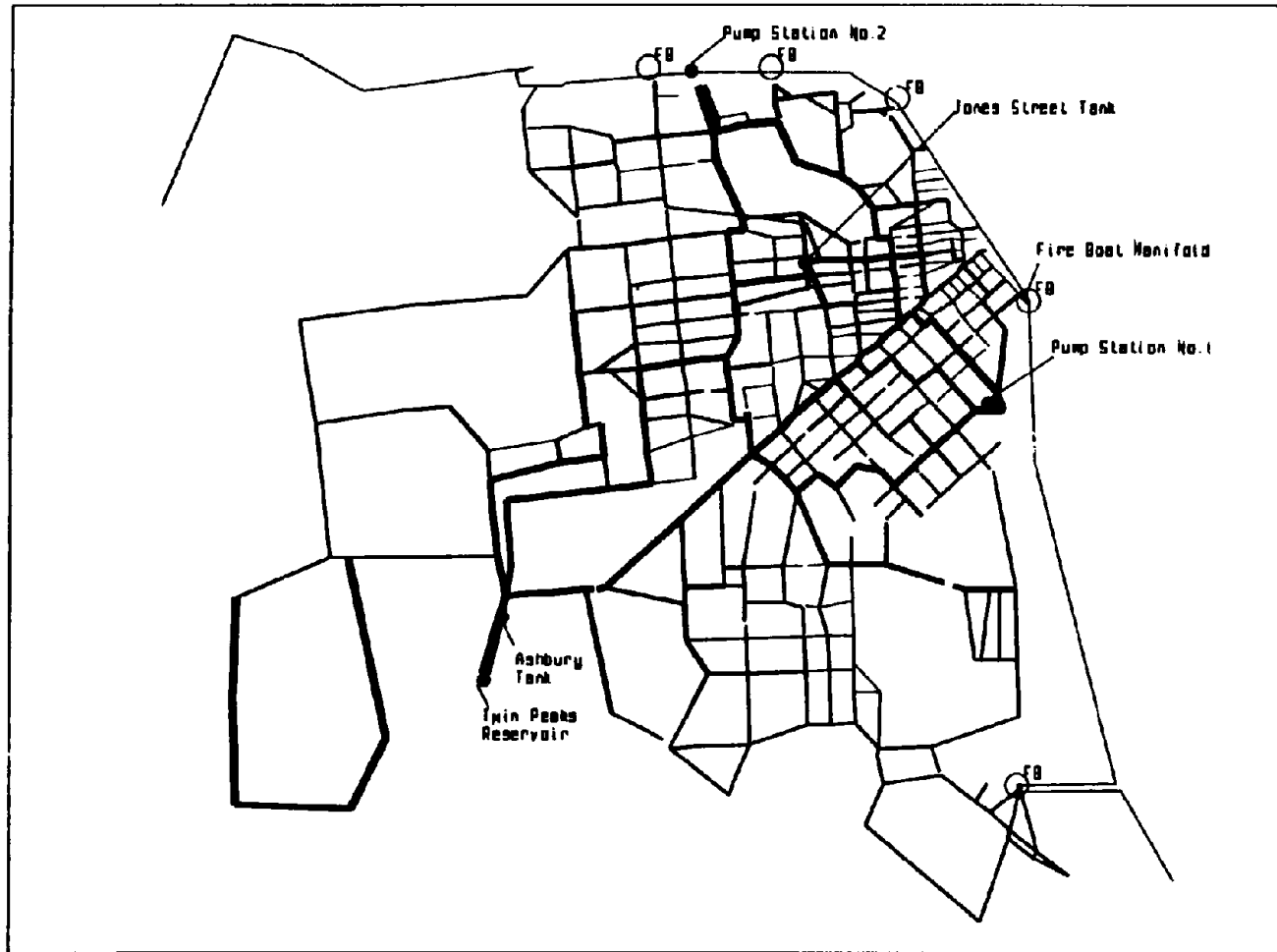


Figure 5.2: Computer Presentation of the AWSS

5.4.1 On-Off Module

The On-Off Module represent an efficient way of activating or deactivating components of the system, such as tanks, pumps, fire boats and hydrants, specified in the initial data file.

Open hydrants are modeled as shown in Figure 5.3 and can be introduced at any node of the system. An open hydrant at a node can be represented by 10-ft-long, 8-in.-diameter pipe placed at this node and with a pressure of at least 20psi at the free end. This pressure is commonly required by fire insurance underwriters as the minimum acceptable pressure. The pressure provides an adequate margin of safety against excessive demand by a fire truck, which can, in turn, cause negative water pressure and collapse of flexible hoses. However, the code allows any specification of pressure, at the discretion of the program operator, to explore emergency conditions in which required pressures can be lower or higher than those consistent with the underwriting standards.

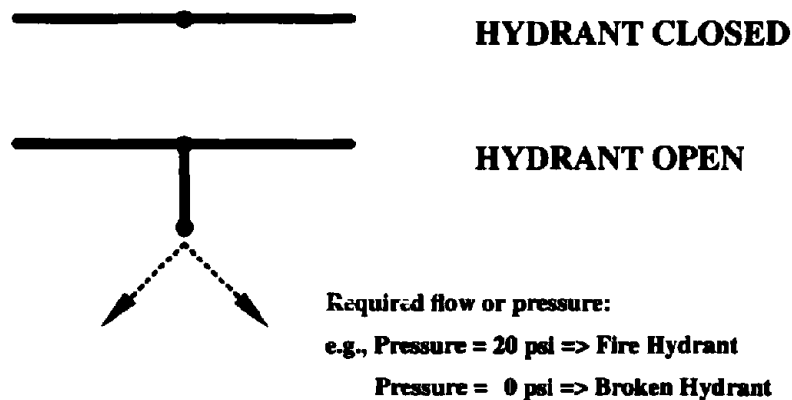


Figure 5.3: Schematic Diagram of Hydrant Simulation

5.4.2 Edit Module

The Edit Module can be used to add/delete system components and to specify their seismic vulnerability. System components e.g. pipes, nodes, and valves can be added or deleted from the system. This allows the user to study potential extension of the system and to optimize the valving strategy. The seismic vulnerability of the components is characterized by different

amplification factors, assigned to the pipes, hydrants, and valves. The components with different amplification factors are distinguished by its color. Reliability of tanks and pumps can be estimated by amplification factor assigned to corresponding connection pipes. This allows to study the effect of potential regional soil liquefaction. Particular pipes can be upgraded from their strength to earthquake resistant pipes that sustain no damage during seismic events. This feature can be used to detect the most critical system components from the sensitivity of the system performance with respect to this component. A particular component is critical if its upgrade to a seismic resistance component results in a significant increase of the system performance. An optimal upgrading strategy can be developed based on sensitivity studies and economical consideration.

5.5 Damage Module

The damage state following an earthquake depends on (1) the reliability of individual system components e.g., pipelines, valves, hydrants, tanks and pump stations, (2) vulnerability to the fire initiation (3) the soil conditions, and (4) the characteristics of the seismic event. Damage of a system can be caused by permanent ground displacements and/or traveling ground waves. Permanent ground displacement can disconnect major portions of a water supply system from reservoirs and other water sources. On the other hand, breaks, leaks and fire demands caused by seismic waves tend to be distributed over the entire system. Distribution of pipe breaks, hydrant breaks and fire demands is accomplished by *the Pipe Break Module*, *the Hydrant Break Module* and *the Fire Module*.

5.5.1 Pipe Break Module

Two options are available for characterizing the pipe breaks distribution following an earthquake. They are based on two models: deterministic and probabilistic. The deterministic option enables the user to input breaks at specified locations by means of computer graphics. This option is useful to analyze the effects of particular pipe breaks on the system performance.

A Poisson model is used to generate randomly distributed pipe breaks in the system. Let $\lambda(I)$ be the mean break rate of a pipe subject to an earthquake of intensity I . Then, the pipe fails with probability

$$P_{pk}(L, I) = 1 - \exp(-L_k v_{pk} \lambda(I)) \quad (5.1)$$

if its length is L_k . The vulnerability of the pipes in the areas where amplification of ground motion is expected can be accommodated with amplification factor, v_{pk} , assigned to each pipe k . The GISALLE code generates a uniformly distributed random number u in (0,1) for every pipe and compare this number with the calculated failure probability P_{pk} in Eq. (5.1) for this pipe. A break occurs in the pipe if u exceeds $1 - P_{pk}$.

The amplification factor v_{pk} can be estimated from the soil condition in the vicinity of each pipe k . This factor can also account for the different mechanical characteristics of the pipe.

The mean break rate can be estimated from repair records following major earthquakes [35]. Figure 5.4 shows mean repair rates for cast iron pipes as a function of the Modified Mercally Intensity (MMI) observed following several U.S. earthquakes including the 1989 Loma Prieta earthquake. A linear trend between repair rates and earthquake intensity is also shown. The data for earthquake intensities in the MVI to MVII range involve damage caused by traveling ground waves, whereas data for the MVIII and MIX intensities involve both traveling and permanent ground movement effects.

Figure 5.5 shows the mechanical model for pipe breaks. Consider a pipe segment of length L connecting the two nodes. To simulate a break a closed valve is introduced on the pipe to prevent flow between the nodes. Two new pipes of length $L/2$ and same diameter as the original one are added to each node with atmospheric pressure fixed at the open end of these pipes. The procedure simulates a complete rupture at the center of the original pipe. It is possible to simulate partially broken pipes. However, such a refinement may not be justified because of the limited data on pipeline performance. Moreover, the proposed model is conservative because it overestimates the amount of lost water through leaks as explained in Section 2.

The mechanical model for pipe breaks in Figure 5.5 can cause a discontinuity in the system and result in instability of the solution of the flow equations. A subroutine checks for this condition and, if necessary, replaces closed valves by 1-in.-diameter pipes. This small diameter effectively eliminates flow, while maintaining hydraulic connectivity and computational stability. A slight increase in solution time results for each replacement of a closed valve by a small diameter pipe.

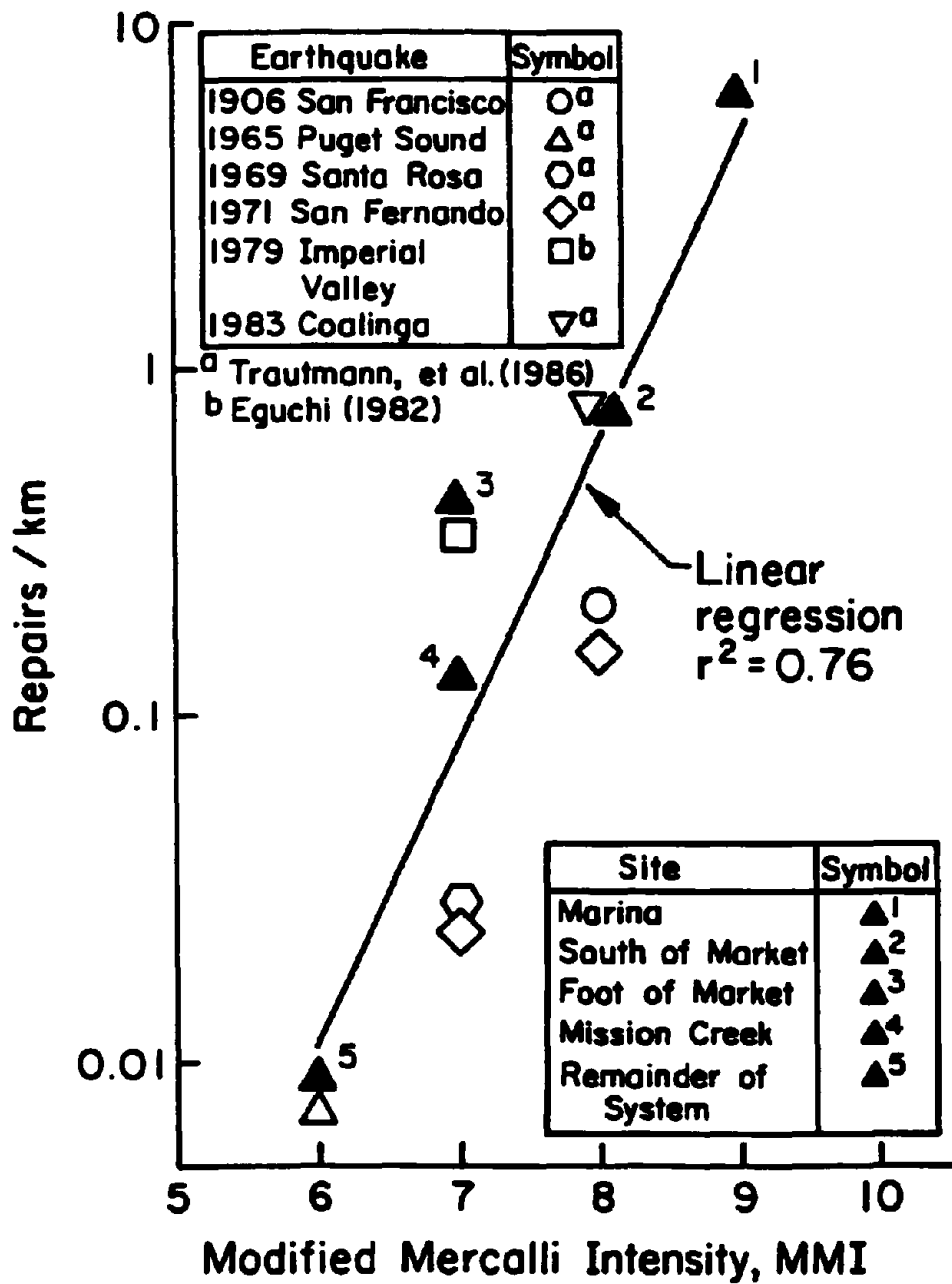


Figure 5.4: Variation of Mean Damage Repairs with Earthquake Intensity

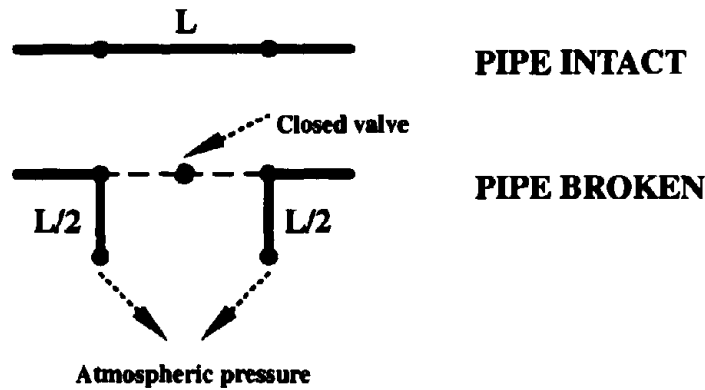


Figure 5.5: Schematic Diagram of Pipe-Break Simulation

5.5.2 Hydrant Break Module

This module provides deterministic and random options for hydrant breaks distribution. The deterministic option specifies location of hydrant breaks. The hydrant break location does not necessarily refer to a particular hydrant, but rather to a general area which may involve approximately one city block with several hydrants. This modeling procedure is verified in Section 6.

A broken hydrant at a node is modeled as shown in Figure 5.3 by a 5-ft-long and 8-in.-diameter pipe. The pipe is connected to the node at one end and open to atmospheric pressure at the other end. The model is based on the assumption that a typical 10-ft-long hydrant breaks in the middle of its length. The deterministic option allows to specify a hydrant break at any node. The selection of these locations may relate to areas of great potential for permanent ground displacement, potential of fallen brick buildings that may break a hydrant, and other vulnerable areas known from past experience. The module allows the user to study the significance of particular hydrant breaks on overall network performance.

The random option generates hydrant breaks throughout the system. Hydrants breaks occur according to a Bernoulli model of parameters $v_{h_i} P_{h_i}$, where P_{h_i} is probability of hydrant failure and v_{h_i} is seismic amplification factor at node i . The seismic amplification factor may vary with location. The module generates a uniformly distributed random number u in

(0,1) for each hydrant and compares it with the assigned and modified probability of failure $v_{h_i} P_{h_i}$. A hydrant break at node i occurs if u_i exceeds $1 - v_{h_i} P_{h_i}$.

5.5.3 Fire Module

This module allows the user two options for fire modeling: deterministic and random. In the deterministic option fires are specified by its location and intensity. The deterministic approach is used when locations of fires and fire intensities are either estimated or a priori known. Performance of a system is analyzed for a given fire scenario.

The random approach is used to generate fire ignition and intensity consistent with the site fire vulnerability, conflagration risk, earthquake intensity, and soil condition.

The fire ignition corresponds to the location of the closest hydrant at which a water demand is required. The fire ignition can be modeled as a Bernoulli distribution with parameter $v_{f_i} P_{f_i}$ where P_{f_i} is probability of having open hydrant at node i , specified in the input file. The model allows modification of this probability for the locations with different fire vulnerability. The modification is controlled by a fire amplification factor v_{f_i} assigned at each node i . It is possible to localize the fire initiation to only several locations by setting the fire amplification factor to zero for the rest of area. The model generates a sequence of n_n trials where n_n is the total number of nodes with fire potentials. The trials are identical, mutually independent, and each trial can result in either open or closed hydrant. For example, the model generates a set of uniformly distributed random numbers u in (0,1) and compares it with the value of $v_{f_i} P_{f_i}$ at each node i . The fire ignites if u_i exceeds $1 - v_{f_i} P_{f_i}$. The hydrant is open in case of fire or closed in case of no fire.

The fire intensity typically depends on earthquake intensity, degree of structural damage and character of building content and can be related to building floor area [49]. Figure 5.6 shows such relation developed for 20-th century fire ignitions. Building floor area is expressed in units of Single Family Equivalent Dwellings (SFED) and seismic activity is expressed in terms of Modified Mercalli Intensity. There is a clear trend in increase of fire ignitions with increase of earthquake intensity.

The fire intensity in the fire module is characterized by a water demand \tilde{Q}_h^* required for fire fighting. The demand \tilde{Q}_h^* is modeled as a random variable with a lognormal probability density function (PDF)

FIRE IGNITION PER EQUIV DWELLING

20th C. U.S. Data

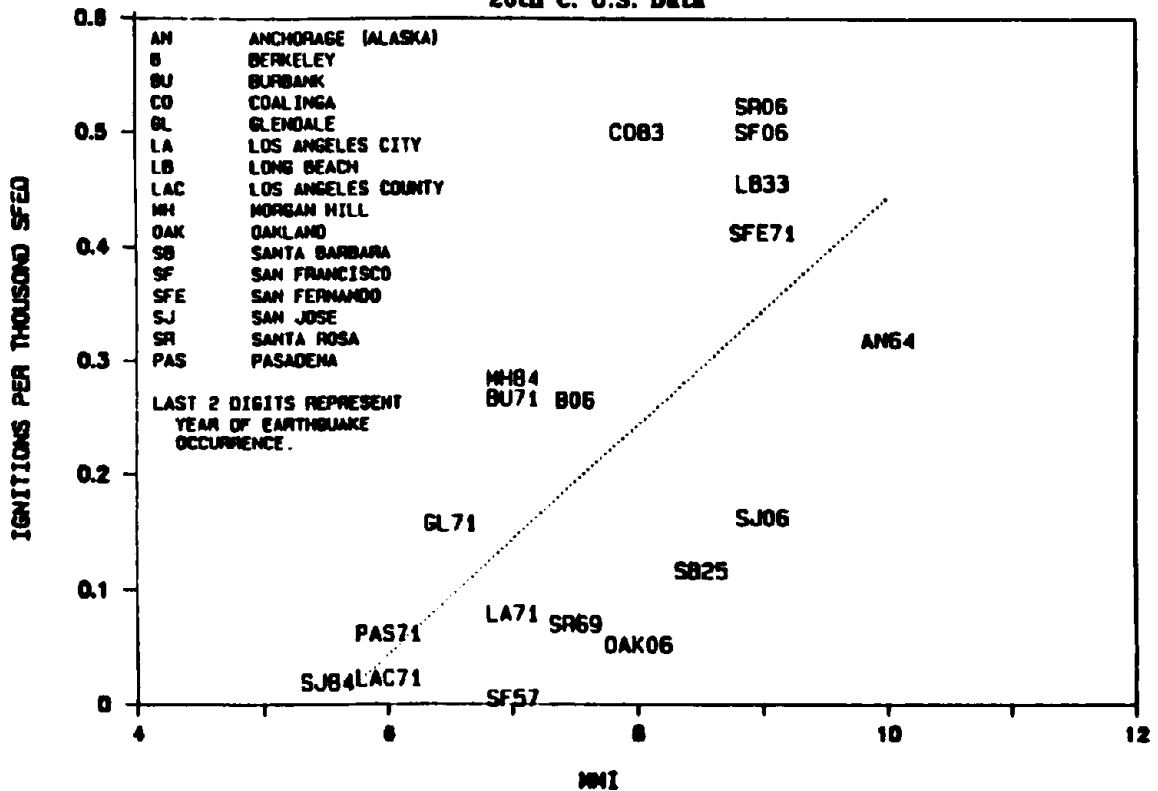


Figure 5.6: Variation of Fire Ignitions with Seismic Intensity

$$f_{\bar{Q}_k^*}(\bar{q}_k^*) = \frac{1}{\sqrt{2\pi\sigma\bar{q}_k^*}} e^{-[\ln(\bar{q}_k^*) - \mu]^2 / (2\sigma^2)} \quad (5.2)$$

The lognormal distribution has mean $E(\bar{q}_k^*) = e^{\mu + \sigma^2/2}$ and standard deviation $V(\bar{q}_k^*) = e^{2\mu + \sigma^2}(e^{\sigma^2} - 1)$. The lognormal PDF is used to prevent negative demands in case of small demand and large standard deviation. Variable $\ln(\bar{q}_k^*)$ is a normally distributed with mean μ and standard deviation σ that are assigned by the user.

5.6 Hydraulic Analysis Module

Currently available computer codes for the hydraulic analysis of water supply systems, such as the Wood program mentioned in Section 2, are based on the assumption that the pressure remains positive at all nodes. The assumption is invalid when dealing with realistic systems that are not air tight because of breaks and leaks. These codes when applied to analysis of damaged systems can predict unrealistically negative pressures at some nodes. Moreover, pressures at hydrants and nodes can not be specified when these codes are used. Therefore, alternative computer codes are needed for estimating the seismic serviceability of water supply systems. This module can determine flows and pressures in a damaged water supply system. The solution is based on the Hazen-Williams formula and involves an iterative procedure.

Consider a network with n_n nodes and n_p pipes. The flows Q_k in pipe $k = 1, \dots, n_p$ connecting nodes i and j , and the pressures p_i and p_j , at these nodes, are the unknowns. There are $n_p + n_n$ unknowns satisfying the same number of nonlinear equations. The first set of equations represent the conservation of energy (Eq. 3.4):

$$Q_k - b_k p_i + b_k p_j = \gamma b_k (E_i - E_j), \quad k = 1, 2, \dots, n_p \quad (5.1)$$

in which Eq. (3.6)

$$b_k = \frac{1}{\gamma K_k |Q_k|^{a-1}} \quad (5.2)$$

E_i = the elevation of node i ; K_k = a constant dependent on units, roughness coefficient and diameter of the k^{th} pipe; $a = 1.852$ is the constant independent of units used in the Hazen-William equation; and γ = the specific weight of water. The second set of equations

represents flow continuity (Eq. 3.5)

$$\sum_{k=1}^{n_{pi}} Q_{ik} = \tilde{Q}_i, \quad i = 1, 2, \dots, n_n \quad (5.3)$$

in which Q_{ik} is the flow in pipe k connecting node i to another node, \tilde{Q}_i is the discharge flow at node i , and n_{pi} is number of pipes k merging at node i . The hydraulic analysis accounts for the fact that air can be admitted in the pipeline system when the pressure at a node is smaller than atmospheric pressure.

The system of Eqs. (5.1) and (5.3) can be solved by iteration. First, initial values are assumed for the flows Q_k . The pressures p_i can be obtained by solving Eqs. (5.1) and (5.3) simultaneously. Then, these pressures can be used in Eq. (5.1) to obtain new values of the flows Q_k . The iteration is continued until the difference between flows Q_k in consecutive iterations is smaller than a specified tolerance. The convergence is fast because a loop-balancing scheme uses an efficient, sparse matrix equation solver. The sparse matrix solver uses a real array for nonzero elements and two integer arrays to define the position of the nonzero elements. In addition, a Gaussian elimination is performed with partial pivoting to increase the stability of the solution.

The computer code identifies the nodes with negative pressures at every step of the iteration procedure. A node i with pressure $p_i < 0$ and the pipes connecting it to nodes j are eliminated from the system if $E_i > E_j + p_j/\gamma$ for all j because there is no flow in this set of pipes. The zero pressure stands for the atmospheric pressure. The node i is classified as no-flow node. A node i is classified as a partial-flow node if $p_i < 0$ and the inequalities $E_i > E_j + p_j/\gamma$ are satisfied for some nodes j .

The partial flow or open channel flow is characterized by the existence of a free water surface. The surface represents a boundary subject to the atmospheric pressure. The analysis of the partial flow is more complex than for the full pipe flow. The hydraulic analysis module performs an approximate partial flow analysis. The approximation assures flow under the atmospheric pressure. It replaces partial flow with full flow by increasing the roughness coefficient such that the pressure at the partial flow node is equal to the atmospheric pressure. The effect of this approximation is examined at Section 6.

The hydraulic module have two options for elimination of the negative pressure nodes: automatic and interactive. The automatic option eliminates all nodes with negative pressure below a specified treshold. The treshold is specified as a percentage level of the highest negative pressure in the system at every iteration step. The interactive subroutine allows the

user to specify a different threshold for the negative pressure at each iteration. The interactive option is useful for verification of the results obtained by the automatic option.

5.7 Statistical Module

This module develops probabilistic measures for the seismic serviceability of a damaged water supply system. It determines *performance indices* and *fragility curves*. The performance index module provides estimates of the post earthquake system serviceability and of the degree of system damage. The fragility curve module gives a global serviceability measure of the network for earthquake of intensities over a specified range. These two modules enable the user to determine: 1) the effect of the pipe and hydrant break rate, conflagration risk and earthquake intensity on the capability of the network to supply water at fire hydrants 2) the water loss from the system, and 3) the effect of retrofitting or replacing selected pipelines with earthquake resistant lines on the overall performance of a water supply system.

5.7.1 Performance Index Module

Two performance indices are calculated, as indicated in Section 3: the serviceability index and the damage index. The serviceability index is equal to the ratio of the total available flow of the system Q_T for a specified damage state to the total required flow Q_T^* .

$$S_s = \frac{Q_T}{Q_T^*} \quad (5.1)$$

This index depends on the current demand and the system capacity. The damage index can be obtained from the ratio of Q_T to the total available flow corresponding the undamaged system Q_{T0} ,

$$S_d = \frac{Q_T}{Q_{T0}} \quad (5.2)$$

Both indices correspond to a specified set of hydrants used to withdraw water from the system. Let n_h be the number of hydrants in the set. The total available flow Q_T represents the sum of the available flow at these hydrants. The performance indices can be time dependent because of changes in the supply-demand scenario following an earthquake. The analysis can be repeated for new scenarios to account for these changes.

The total available flow is a random variable depending on the system damage state (Eq. 3.1)

$$Q_T = \sum_{h=1}^{n_h} \tilde{Q}_h s(p_h - p_h^*) \quad (5.3)$$

in which, \tilde{Q}_h and p_h are the available flow and pressure at hydrant h , p_h^* is deterministic value for the required pressure at this hydrant, and s is the unit step function which is one for $p_h - p_h^* \geq 0$ and zero otherwise.

The determination of the flows \tilde{Q}_h in Eq. (5.3) is not unique when the number of operating hydrants n_h is greater than one as explained in Section 3. An optimization algorithm can be used to find the flows \tilde{Q}_h from the condition that an objective function Eq. (3.14)

$$e_1 = \sum_{h=1}^{n_h} |\tilde{Q}_h - \tilde{Q}_h^*| \quad (5.4)$$

be minimized, with the constraints $p_h \geq p_h^*$, $h = 1, \dots, n_h$, where \tilde{Q}_h^* is a random variable for the required flow at hydrant h as explained previously.

5.7.2 Fragility Curve Module

This module evaluates the overall seismic performance of a water supply system via fragility curves. The module involves hydraulic analyses of the system in simulated damage states consistent with site seismicity and statistical analysis of available flows in these states. It provides measures of seismic serviceability and their variation with site seismic intensity and is based on the performance indices in Eqs. (5.1) and (5.2).

A Monte-Carlo simulation method and statistical methods are used to characterize the serviceability of a water supply system by the performance indices in Eqs. (5.1) and (5.2). The method involves several phases. First, hydraulic analyses are performed for undamaged states and generated fire scenarios. Second, damage states are generated for the water supply system consistent with the range of expected seismic events at the site. Third, indices S_s and S_d are calculated for these damage states. The seeds of the random numbers used to generate damage states are recorded. Fourth, regression lines are constructed based on S_s and S_d values corresponding to the damage states generated in the second phase. Exponential and up to fourth order polynomial regression lines are available and selected confidence level can be obtained for each of the lines as will be explained in Section 5.7.3

These regression lines estimate damage and serviceability of a water supply system given earthquake intensity. These lines can also be referred as fragility lines because they represent overall reliability assessment of system seismic performance.

Figure 5.7 shows a regression line corresponding to 10 values of the mean break rate λ ranging from 0.01 to 0.1 breaks/km. Three Monte-Carlo runs were performed for each value of λ . The total of 30 corresponding values of the damage index S_d are graphically shown in the figure. A third degree polynomial regression was fitted to these values. The figure also shows 95% confidence interval which indicates that the mean value of damage index will fall within this interval with probability of 0.95. The coefficient of determination R^2 , and confidence level or mathematical expression of the regression curve can be shown in the upper right window of the screen. The coefficient of determination indicates that 43% of variation of the damage index is explained by this third degree polynomial regression. Similar representation is available for the serviceability index S_s .

The module also allows the user to see the fire scenario and damage state of the system associated with a particular value of λ and S_d or S_s . The damage state corresponding to ($\lambda = 0.03br/km$, $S_d = 0.623$), the enlarged dot in the upper left window, is shown in Figure 5.8. The upper right window shows the numerical value of the damage index S_d , the mean pipe break rate λ , probability of hydrant break, probability of fire ignition, and seeds used to generate the corresponding damage and fire scenario. The seeds can be used to recall the particular hydraulic analyses and to obtain flow and pressure distributions.

5.7.3 Regression Analysis

Regression analysis is used to estimate the relation between the performance indices and earthquake intensity. Polynomial regression and exponential regression are available in the GISALLE code.

A polynomial regression model of order k is

$$y = \beta_0 + \beta_1 x + \beta_2 x^2 + \dots + \beta_k x^k + \epsilon \quad (5.5)$$

where x is the independent variable, y is the expected response, $\beta_0, \beta_1, \dots, \beta_k$ are unknown regression coefficients, and ϵ is an error term. The GISALLE provides models for $k = 1 \dots 4$ where x is earthquake intensity and y is the performance index. These models are linear regression models since they are linear in the unknowns $\beta_0, \beta_1, \dots, \beta_k$.

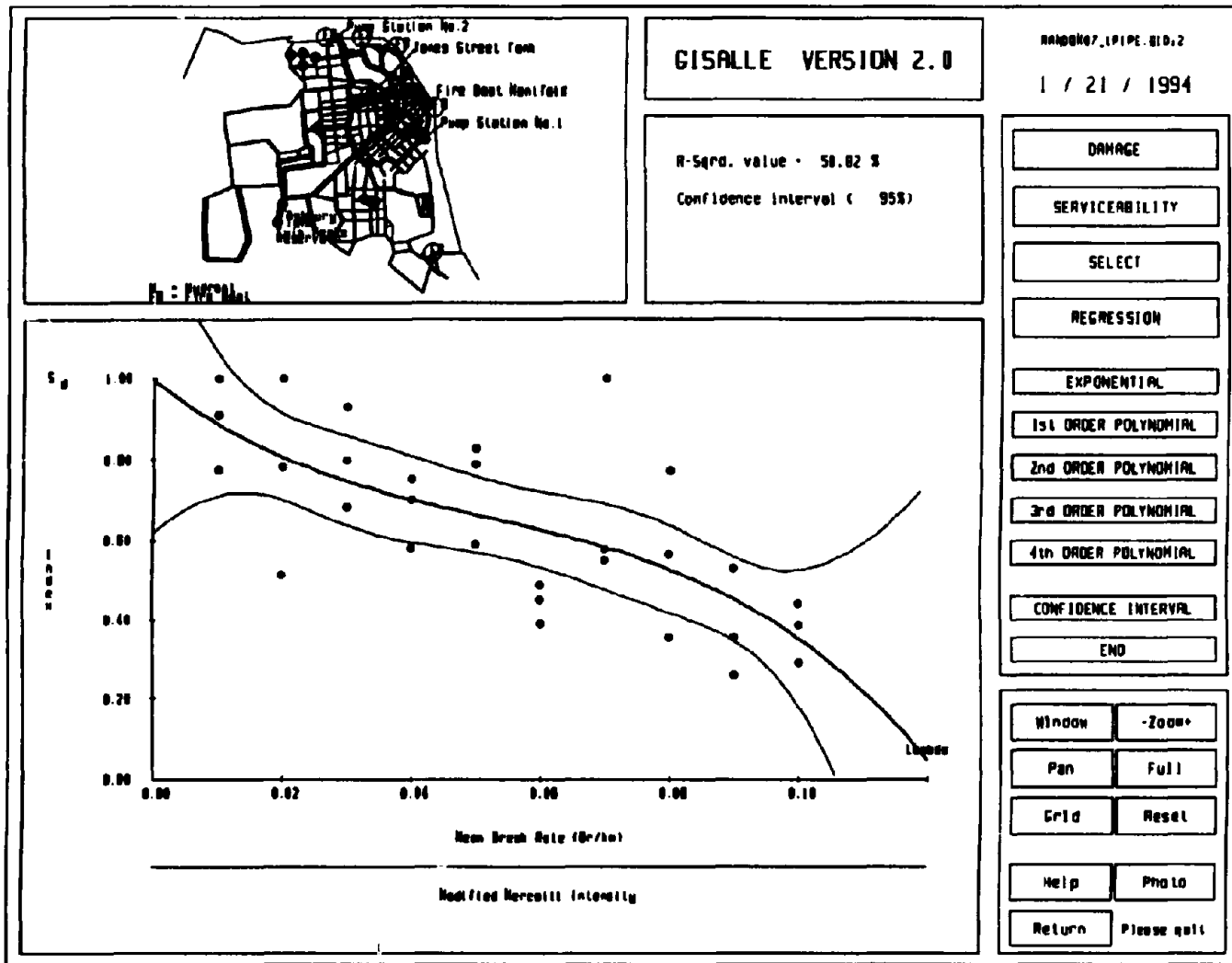


Figure 5.7: Computer Displays of Fragility Curve and 95% Confidence Level for Damage Indices S_d

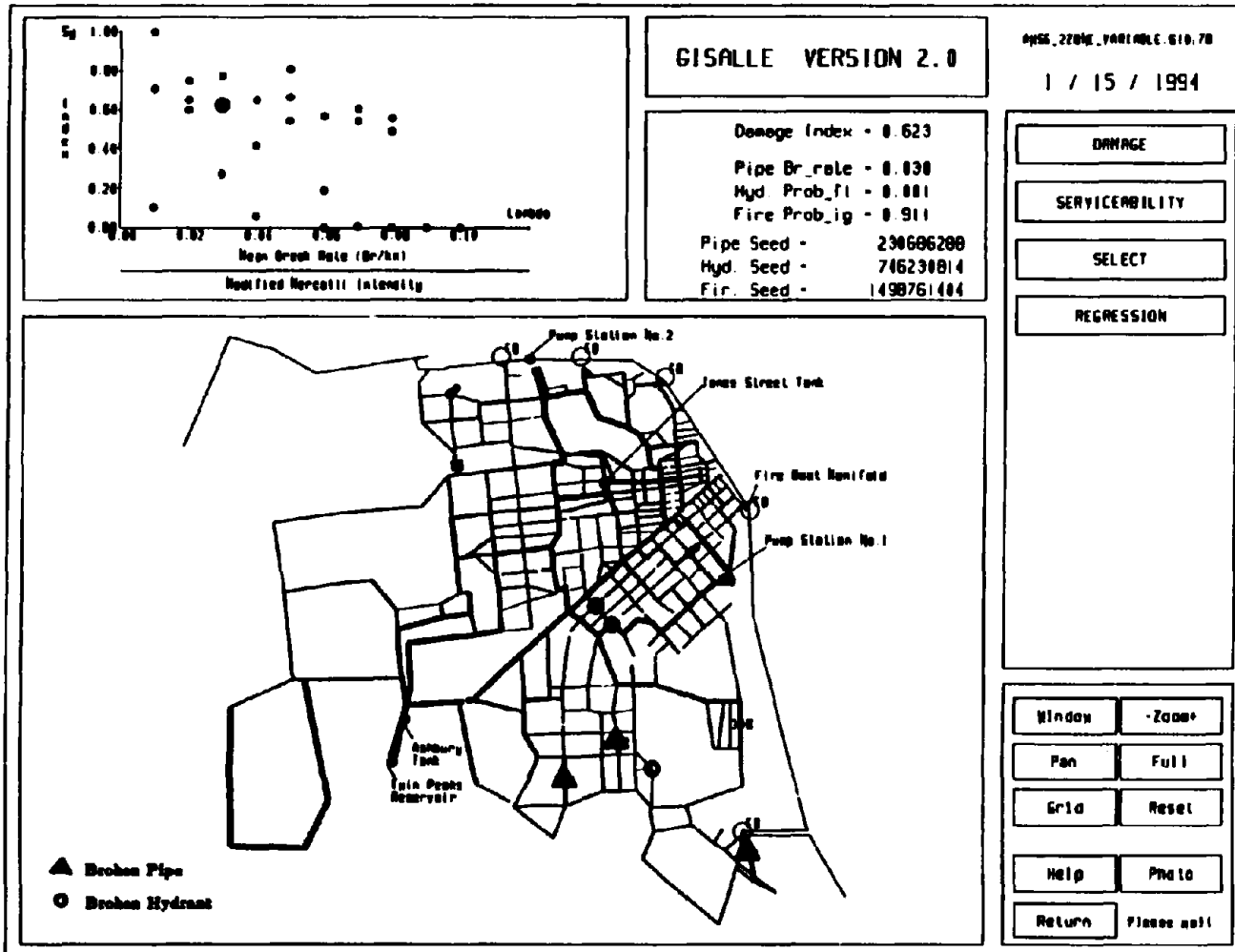


Figure 5.8: Computer Displays for Damage Indices S_d with Selected Damage Scenario

The error term result from the inability of the model to fit the data exactly. The error ε is a random variable with mean $\mu = 0$ and unknown variance σ^2 . The errors are assumed to be uncorrelated for different values of x . The response y is a random variable with mean μ_y and $Var(y) = \sigma^2$.

The polynomial model is analyzed by a multiple linear regression technique. The Eq.(5.5) can be written using the transformation of variables $x_1 = x, x_2 = x^2, \dots, x_k = x^k$ as

$$y = \beta_0 + \beta_1 x_1 + \beta_2 x_2 + \dots + \beta_k x_k + \varepsilon \quad (5.6)$$

which is a multiple linear regression model involving k variables.

The method of least squares is used to estimate the regression coefficients in this model. The Gaus-Markov theorem states that under given assumptions for the error term the least square estimators are unbiased and have minimum variance. Thus, the curve given by Eq. (5.5) provides the best fit to observed response. Let n be the number of available observations, y_i be the i -th observed response, and x_{ij} be the i -th observation of variable x_j . The model gives

$$y_i = \beta_0 + \beta_1 x_{i1} + \beta_2 x_{i2} + \dots + \beta_k x_{ik} + \varepsilon_i \quad (5.7)$$

$$= \beta_0 + \sum_{j=1}^k \beta_j x_{ij} + \varepsilon_i, \quad i = 1, 2, \dots, n \quad (5.8)$$

which may be written in matrix form

$$y = X\beta + \varepsilon \quad (5.9)$$

A vector of least square estimators $\hat{\beta}$ is obtained from

$$\hat{\beta} = (X'X)^{-1}X'y \quad (5.10)$$

minimising

$$S(\beta) = (y - X\beta)'(y - X\beta) \quad (5.11)$$

$$= y'y - 2\beta'X'y + \beta X'X\beta \quad (5.12)$$

and satisfying

$$\frac{\partial S}{\partial \beta} \Big|_{\hat{\beta}} = -2X'y + 2X'X\hat{\beta} = 0 \quad (5.13)$$

The least square estimator $\hat{\beta}$ is unbiased estimator of β since $E(\hat{\beta}) = \beta$. The covariance matrix of $\hat{\beta}$ is $Cov(\hat{\beta}) = \sigma^2(X'X)^{-1}$. A fitted curve $\hat{y} = X\hat{\beta}$ provides the mean response.

A exponential regression model available in the GISALLE code is nonlinear with form

$$y = \beta_0 e^{\beta_1 x} \varepsilon \quad (5.14)$$

However, the function y can be transformed to linear function using an appropriate transformation. For example, using a logarithmic transformation

$$\ln y = \ln \beta_0 + \beta_1 x + \ln \varepsilon \quad (5.15)$$

and substituting $y' = \ln y$, $\beta'_0 = \ln \beta_0$, and $\varepsilon' = \ln \varepsilon$ the linear form is obtained

$$y' = \beta'_0 + \beta_1 x + \varepsilon' \quad (5.16)$$

The error term ε' is assumed independent normally distributed variable with mean zero and variance σ^2 .

An estimate $\hat{\sigma}$ of σ is obtained from

$$\hat{\sigma} = \frac{SS_e}{n - \kappa} \quad (5.17)$$

where $SS_e = (y - X\hat{\beta})'(y - X\hat{\beta}) = y'y - \hat{\beta}'X'y$ is a residual sum of squares, n is a number of observations, and κ is number of parameters estimated in the regression model. The residual is the difference between the observed value y_i and corresponding fitted value \hat{y}_i .

An interval estimation of the mean response is used to predict how close the mean response is likely to be to the true response. For example, a 95 percent confidence interval implies the true value of the mean response will fall within this interval with probability 0.95. In general the higher the confidence level the wider the confidence interval.

Let $x'_0 = \{x_{01}, x_{02}, \dots, x_{0k}\}$ be particular values of the variables for which the mean response is estimated. The fitted value at this point is $\hat{y}_0 = x'_0 \hat{\beta}$. Then, e.g., $100[1 - \alpha] = 95$, percent confidence interval at this point is

$$\hat{y}_0 - t_{\alpha/2, n-\kappa} \sqrt{\hat{\sigma}^2 x_0 (X'X)^{-1} x_0} \leq y_0 \leq \hat{y}_0 + t_{\alpha/2, n-\kappa} \sqrt{\hat{\sigma}^2 x_0 (X'X)^{-1} x_0} \quad (5.18)$$

where $t_{\alpha/2, n-\kappa}$ is probability $P(-t_{\alpha/2} \leq T \leq t_{\alpha/2})$ with T as random variable with t -distribution, $\hat{\sigma}$ given by Eq.(5.17). The t -distribution approaches the normal distribution provided that number of observation is large enough so that the Central Limit Theorem can apply. Confidence interval can be obtained for selected range of x_0 values.

A coefficient of determination is used to measure the proportion of observed variation that can be explained by a regression model. The coefficient of determination is defined as

$$R^2 = 1 - \frac{SS_r}{SS_t} \quad (5.19)$$

where SS_r is sum of squared deviations about the regression curve and SS_t is sum of squared deviations about the horizontal line at the mean of observed values. The coefficient takes the values between 0 and 1. Usually, the higher the value of R^2 the better regression model is in explaining the observations. However, the error due to repeated points for performance indices at a particular value of λ can not be explained by R^2 value.

5.8 Results Module

This module allows graphical presentation of the results of a hydraulic analysis as shown in Figures 5.9 and 5.10. The pipes eliminated from the system because of negative pressure or no flow condition are shown with dotted lines. The remaining pipelines, shown with full lines, are those which have survived the earthquake and are capable of providing a reliable stream of water for fire fighting. The module includes presentation of flows and pressures distribution throughout the system. The flow distribution is shown in Figure 5.9 where pipes with different flow rates are colored differently on the computer screen. This presentation allows an efficient way of identifying potentially critical pipes for a particular damage scenario. Pressure distribution is shown in Figure 5.10 where nodes with different pressure are shown on the computer screen with different color and marker size. Larger the marker smaller the node pressure. The module also allows the user to recall the full information for each pipe and node. The pipe information includes flow in the pipe, pipe number, pipe diameter, roughness coefficient and seismic amplification factor. Similarly, the node information includes node pressure, elevation, demand, seismic amplification factor for hydrant breaks and amplification factor for fire ignition.

5.9 Summary

GISALLE code is developed to provide a tool for analyzing seismic serviceability of water supply systems. The code is based on a new method for hydraulic analysis which can account for large negative pressures usually developed in damaged systems. The code provides deterministic and probabilistic analyses. The deterministic analyses correspond to a specified fire scenario and damage state. The probabilistic analyses account for the uncertainty in the system damage and fire scenario. Serviceability measures are obtained by simulation and regression analyses. The code has a graphic interface to facilitate interaction with the user.

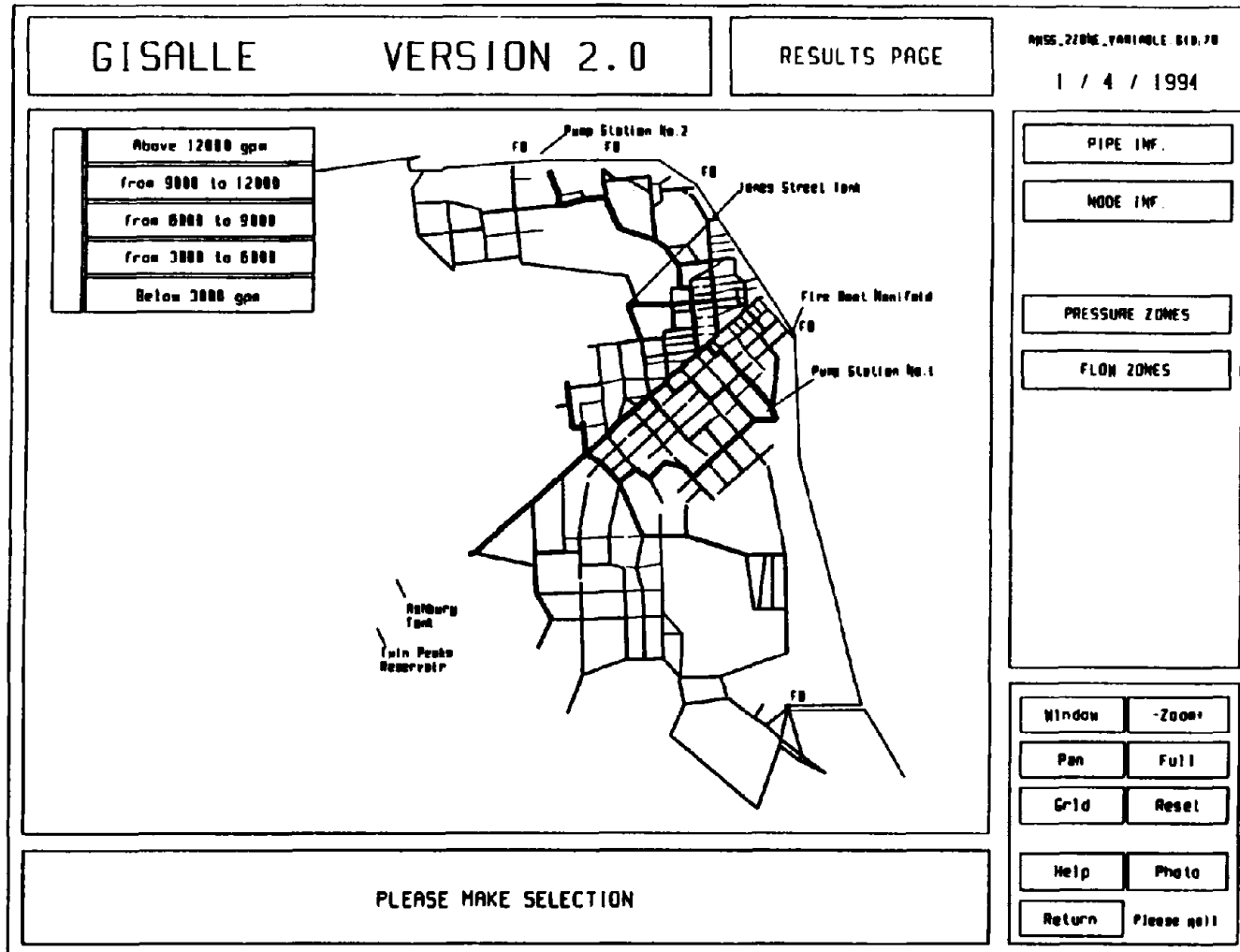


Figure 5.9: Graphical Presentation of the Flow Distribution

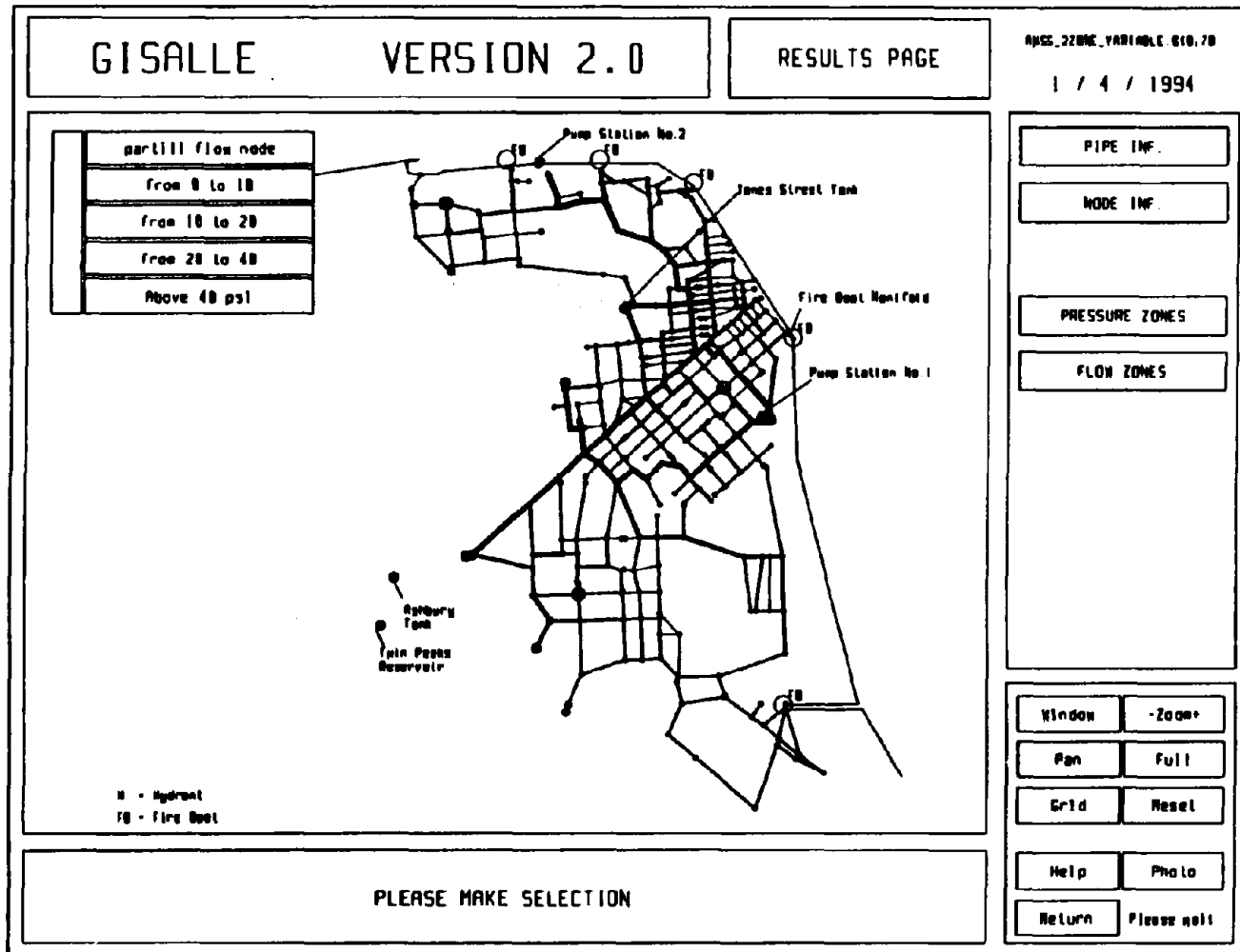


Figure 5.10: Graphical Presentation of the Pressure Distribution

SECTION 6

VALIDATION OF GISALLE

6.1 Introduction

The computer code GISALLE was validated by several means to confirm that the code is capable of reproducing the actual flows and pressures distribution in a network. The validation was accomplished by analytical and experimental tests in Sections 6.2-6.4 and Section 6.5, and 7, respectively.

The analytical tests include a verification of (1) the solution algorithm, (2) the pump model, and (3) the fire demand model. The GISALLE code was verified by several test problems that allow an independent hand calculation. Several pump models were examined such as the regression, three point, and one point models. Conditions were examined under which a fire demand can be modeled with only one open hydrant.

Experimental tests include the San Francisco Fire Department (SFFD) tests on AWSS and observations from the Loma Prieta earthquake scenario. The tests provide information on flows and pressures distribution throughout the system, for a particular demand and system configuration. The SFFD tests were used to estimate roughness coefficient in pipes. These estimates have been used in GISALLE code to predict the performance of the AWSS following the Loma Prieta earthquake. Numerical results show that GISALLE code is robust and efficient.

6.2 Test Problems

Several test problems were used to verify the procedure for eliminating nodes with negative pressures and detecting nodes with partial flow.

6.2.1 Elimination of Negative Pressure Nodes

Figure 6.1a. shows the network configuration used in the analytical tests. The network consists of 9 pipes connecting 6 nodes. The network receives water from pipe 1 at a rate of $Q=2000\text{gpm}$ and is discharged through an open hydrant at node 3. The open hydrant is modeled by 5-ft long and 8-in. diameter pipe as explained in Section 5. This pipe is connected at one end to node 3 and is open to the atmospheric zero pressure at the other end. The node elevations, pipe lengths, and pipe diameters are given in Table 6.I.

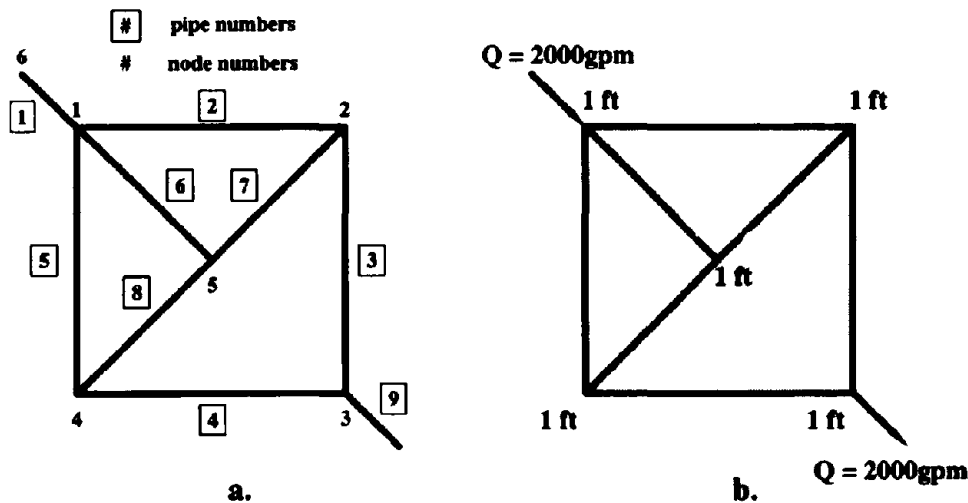


Figure 6.1: Test Problem 1: No Elimination of Nodes

According to the procedure presented in Section 3, the equation of energy balance is written for each pipe and the equation of continuity of flow is established for each node. Thus, the solution of this problem involves a set of 9 energy balance equations and 6 flow continuity equations with flows and pressures as unknowns. The equations were solved by iteration. The roughness coefficient of $C=75$ is assumed for the pipes. Three cases are considered. The node elevation varied from case to case.

Figure 6.1b illustrates Case 1. All nodes have the same elevation in this case. Result of GISALLE analysis showed that all nodes have positive pressures. Results of independent calculation and GISALLE analysis are shown in Table 6.I. An excellent agreement is obtained between the results of two analyses. The hydraulic head at a node i is given as $E_i + p_i/\gamma$, where E_i is node elevation, p_i is pressure at node i , and γ is specific weight of water. The

Table 6.I: Test 1 - Flow and Pressure Distribution

Pipe No.	Length (ft)	Dia (in)	GISALLE Flow (gpm)	Calculated Flow (gpm)
1	14.1	10	2000	2000
2	100	10	653	653
3	100	10	999	1000
4	100	10	-1001	-1000
5	100	10	653	653
6	70.5	10	694	693
7	70.5	10	-346	-347
8	70.5	10	-348	-347
9	5	8	2000	2000

Node No.	Elevation (ft)	Head (ft)	Preassure (psi)	Preassure (psi)
1	1	4.85	1.67	1.65
2	1	3.97	1.29	1.28
3	1	2.04	0.45	0.45
4	1	3.98	1.29	1.28
5	1	4.16	1.37	1.36
6	1	5.84	2.10	2.08

hydraulic head has its largest value at node 6 and gradually decreases towards the hydrant at node 3. The flow is from larger to lower head as expected.

In Case 2 procedure is examined for eliminating nodes with negative pressure. The only difference from Case 1 is the elevation of node 5 that is 20-ft in this case. The analysis is performed in two steps. First, the distribution of flows and hydraulic heads is obtained throughout the system and results are shown in Table 6.II. The flow is distributed as in Case 1. However, the pressure at node 5 became negative and equal to $p = -6.86\text{psi}$ because of the high elevation of this node. The system can not sustain negative pressure because it is not air tight so that the pressure at this node must be zero. The new hydraulic head i.e., for which $p = 0$ at node 5 is 20-ft. This hydraulic head is larger than the heads at all nodes connected with node 5. Thus, the no flow condition is met at node 5 and the node is eliminated together with all pipes merging to the node. The eliminated pipes are shown with dashed lines in Figure 6.2a. Second, a new hydraulic analysis is performed for the modified system in Figure 6.2b. The final flows and pressures are given in Table 6.III. The substantial difference in flow distribution between Case 1 and 2 is caused by the elimination of the node 5 with negative pressure. The Wood's program provides only the results of the first step which are significantly different.

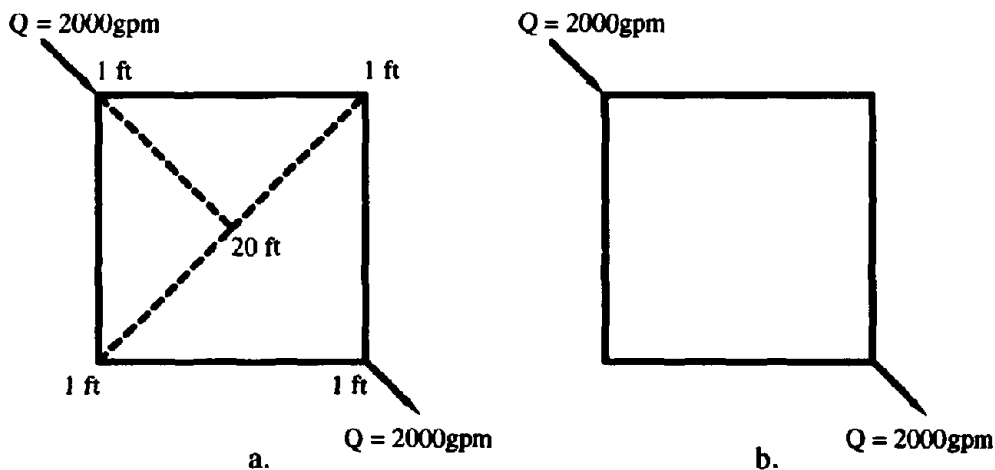


Figure 6.2: Test Problem 2: Elimination of No-Flow Node

Case 3 is designed to highlight the partial flow condition. Node 2 is elevated at 25-ft and node 5 is elevated at 10.5-ft and all the other nodes are kept at their initial elevation. Results

Table 6.II: Case 2 - GISALLE Results After Step 1

Pipe No.	Length (ft)	Dia (in)	Flow (gpm)
1	14.1	10	2000
2	100	10	653
3	100	10	999
4	100	10	-1001
5	100	10	653
6	70.5	10	694
7	70.5	10	-346
8	70.5	10	-348
9	5	8	2000

Node No.	Elevation (ft)	Head (ft)	Preassure (psi)
1	1	4.85	1.67
2	1	3.97	1.29
3	1	2.04	0.45
4	1	3.98	1.29
5	20	4.16	-6.86
6	1	5.84	2.10

Table 6.III: Case 2 - GISALLE Results After Step 2

Pipe No.	Length (ft)	Dia (in)	Flow (gpm)
1	14.1	10	2000
2	100	10	1000
3	100	10	1000
4	100	10	-1000
5	100	10	1000
6			eliminated
7			eliminated
8			eliminated
9	5	8	2000

Node No.	Elevation (ft)	Head (ft)	Preassure (psi)
1	1	5.92	2.13
2	1	3.98	1.29
3	1	2.04	0.45
4	1	3.98	1.29
5			eliminated
6	1	6.90	2.56

of the first step of analysis, based on the assumption that the system is air tight, are shown in Table 6.IV. Node 2 has the largest negative pressure of $p = -9.11$ psi. It is a no-flow node and is eliminated together with the corresponding pipes, as shown in Figure 6.3a. Results after the second step of the analysis are shown in Table 6.V. The pressure at node 5 is equal to $p = -0.14$ psi. This pressure is set to zero. The new head at the node is equal to 10.5ft that is smaller than the head at node 1 (11.32-ft.). An open channel flow condition is met because flow occurs under the atmospheric pressure. Thus, node 5 is the partial flow node. The active portion of the system is shown in Figure 6.3b. The Wood's program provides the results shown in Table 6.II and Table 6.IV. The GISALLE code provides the results shown in Table 6.III and Table 6.V. The flows and pressures distribution as well as the flow pattern are substantially different.

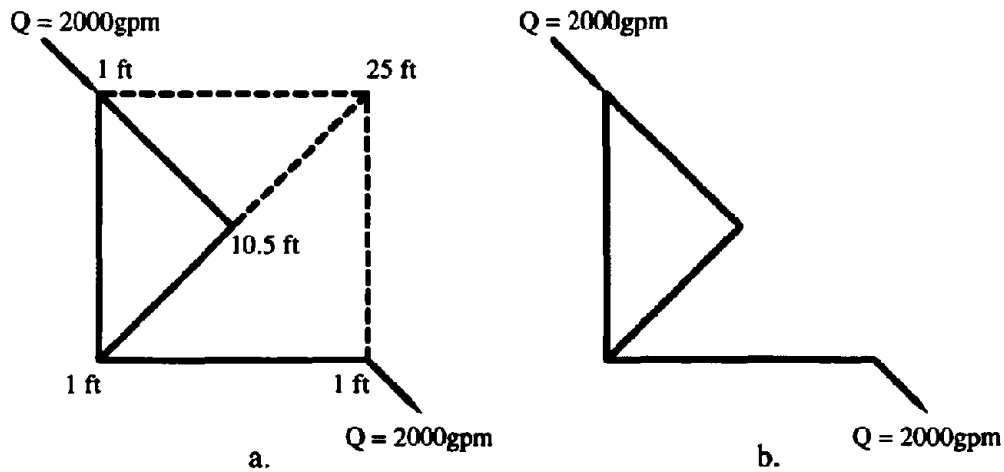


Figure 6.3: Test Problem 3: Elimination of Initially Partial Flow Node

These three test cases demonstrate that GISALLE can accurately perform hydraulic analysis of a system of diverse configuration. In contrast, results of hydraulic analysis by current commercial codes such as the Wood's program, can be unsatisfactory.

Table 6.IV: Case 3 - GISALLE Results After Step 1

Pipe No.	Length (ft)	Dia (in)	Flow (gpm)
1	14.1	10	2000
2	100	10	653
3	100	10	999
4	100	10	-1001
5	100	10	653
6	70.5	10	694
7	70.5	10	-346
8	70.5	10	-348
9	5	8	2000

Node No.	Elevation (ft)	Head (ft)	Preassure (psi)
1	1	4.85	1.67
2	25	3.97	-9.11
3	1	2.04	0.45
4	1	3.98	1.29
5	10.5	4.16	-2.75
6	1	5.84	2.10

Table 6.V: Case 3 - GISALLE Results After Step 2

Pipe No.	Length (ft)	Dia (in)	Flow (gpm)
1	14.1	10	2000
2			eliminated
3			eliminated
4	100	10	-2000
5	100	10	1092
6	70.5	10	907
7			eliminated
8	70.5	10	-907
9	5	8	2000

Node No.	Elevation (ft)	Head (ft)	Preassure (psi)
1	1	11.32	4.47
2			eliminated
3	1	2.04	0.45
4	1	9.04	3.48
5	10.5	10.18	-0.14
6	1	12.31	4.90

6.2.2 Effect of Partial Flow Analysis on AWSS

As explained in Section 5 an approximate partial flow analysis is performed in the GISALLE code. The effect of this analysis was examined. Table 6.VI presents the results of three sets of analysis corresponding to seismic events with mean pipe break rates $\lambda = 0.02, 0.04,$ and 0.06 respectively. Damage states were generated and analyses were performed for the each pipe break rate as follows: (1) the approximate partial flow analyses were ignored, (2) the approximate partial flow analyses were performed and all nodes with negative pressure were eliminated after each iteration, and (3) the approximate partial analyses were performed but only the nodes with the highest negative pressure were eliminated after each iteration. Water loss from the system and JST was monitored at locations shown in Figure 6.4.

The results indicate that for the low seismic intensity, e.g., $\lambda = 0.02$ approximate partial flow analyses and the procedure for elimination of nodes with negative pressure may not have a significant effect on the results. However, the approximate partial flow analyses may effect results significantly for higher earthquake intensities, e.g., $\lambda = 0.06$ especially on the local basis. The table shows e.g., that outflow from the broken pipe No. 5 is drastically effected. The table also shows that sequence of for elimination of nodes with negative pressure may not alter the results significantly, however, the correct result is not known.

6.3 Modeling of Pump Stations

6.3.1 Pump Characteristic Curves

Pump characteristic curves describe the operating condition of a pump. Typical pump characteristic curves are shown in the Figure. 6.5a. The total pump head flow (TPHF) curve shows the relation between head and flow provided by a pump. This relation is nonlinear due to frictional and leakage loses in the pump. The break horsepower (BHP) curve provides the pump horsepower required to satisfy the pump flow or head demand. The required pump horsepower can be accomplished by changing the operating speed of the pump. The efficiency (E) curve shows the ratio between the power required to operate the pump and the power delivered by the pump. The power delivered by the pump is given in a form of a system energy increase at the pump connection. A normal operating range of a well designed pump usually coincide with the region of the highest efficiency of the pump. The net positive suction head (NPSH) curve shows the pressure at the inlet of the pump

Table 6. VI: Effect of Implementation of Partial Flow and Interactive Analysis

LOCATIONS OF WATER FLOW (pipe No.)	PARTIAL FLOW IGNORED (1) (gpm)	ELIMINATION OF ALL NODES (2)/(1)	INTERACTIVE ELIMINATION (3)/(2)
$\lambda = 0.02$			
Jones St. Tank	5984	1	1
1	5984	1	1
$\lambda = 0.04$			
Jones St. Tank	16432	0.964	1.002
1	1041	0.840	1.339
2	5759	0.878	1.004
3	4583	1.047	0.942
4	5093	1.004	0.999
$\lambda = 0.06$			
Jones St. Tank	23866	0.533	0.985
1	272	0.886	0.888
2	2970	0.992	1.015
3	2374	0.849	0.799
4	0	0	0
5	11635	0.246	0.991
6	6606	0.777	1.042

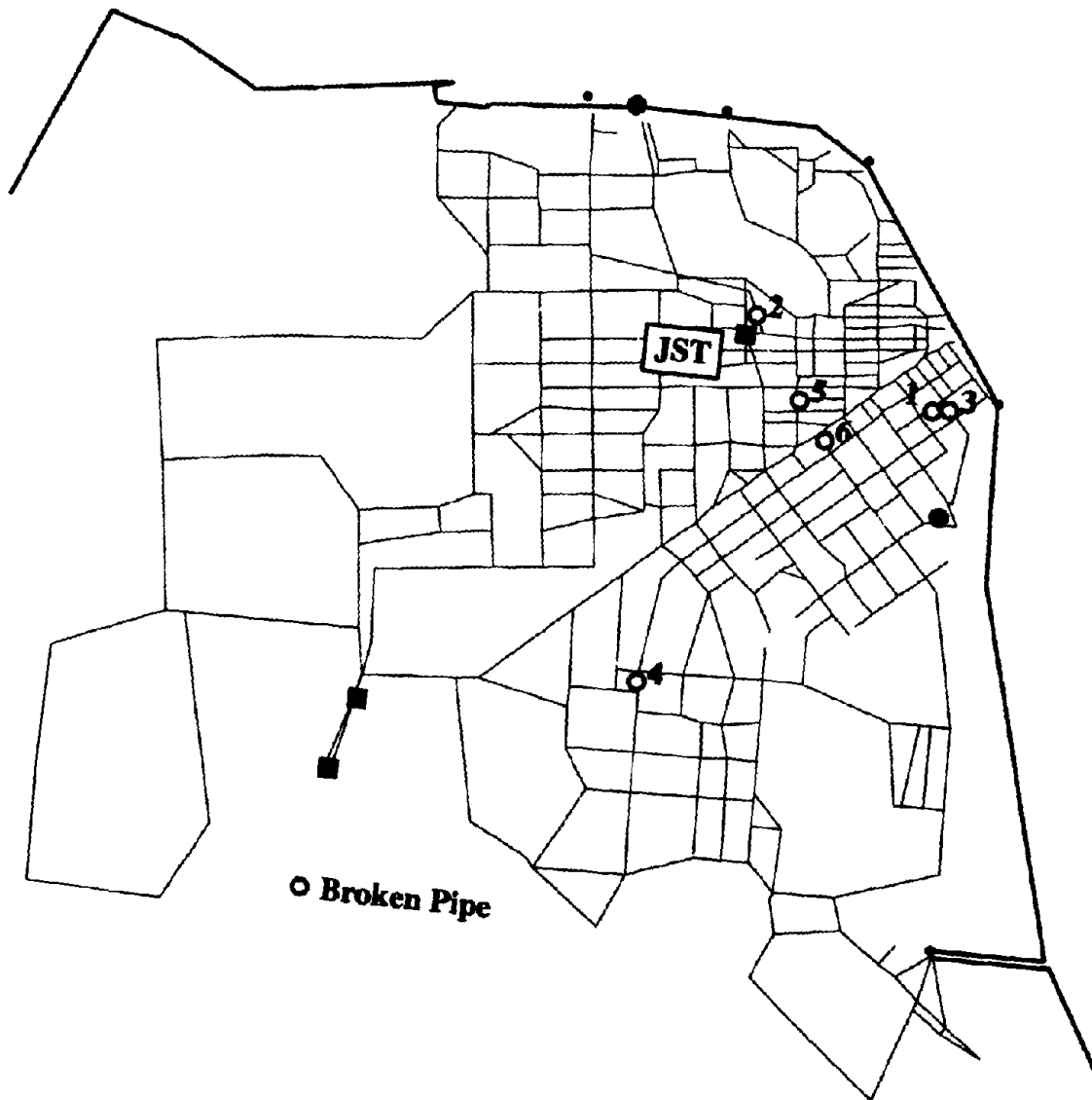


Figure 6.4: Locations of Broken Pipes

which need to be maintained for normal pump operation.

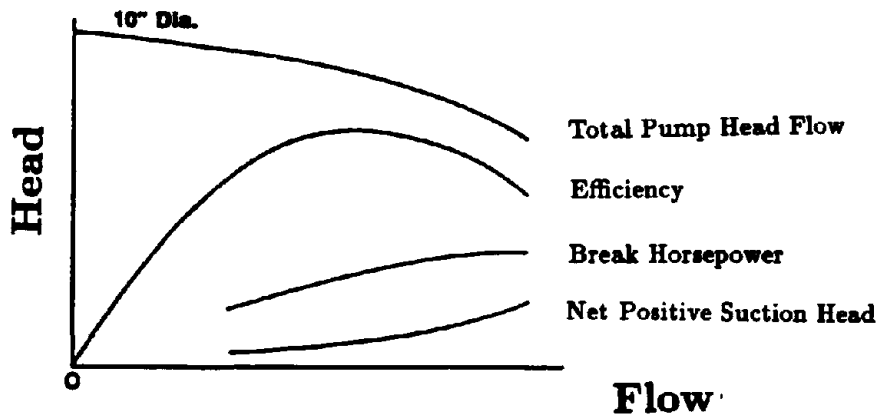
A total system head flow (TSHF) curve describes a system requirements. The curve combines existing static head, design working head and friction head curves as shown in Figure 6.5b. The static head curve gives the difference in elevation between pump location and the point of discharge. The design working head curve shows a required head that must be maintained throughout the system. The AWSS design working head is 20psi, as required by San Francisco Fire Department (SFFD) for proper operation of the fire fighting equipment. The friction head curve shows the nonlinear relation between head and flow in a system. The nonlinearity results from frictional losses in the pipes, valves, fittings and mechanical equipment.

A water supply specified by TPHF curve needs to overcome demand given by the TSHF curve for successful performance of the system. The supply can vary in the AWSS because two pumps can operate with different number of engines. As a result, the TPHF curve can approach upper bound curve which includes points B and D or the lower bound curve which includes points A and C as shown in Figure 6.5c. The system demand can also vary. For example, the higher earthquake intensity can result in the higher fire demand accommodated with the TSHF curve including points C and D. Fire demand at no earthquake situation can be accommodated with the curve including points A and B as shown on the same figure. Thus, the system head curve also can have a band. Any pump operation out of the region bounded with this four points may result in poor system performance because the system demand could be higher than available pump supply or the available head could exceed demand. The GISALLE code provides a tool to predict such situations and to enable taking appropriate measures ahead of the time.

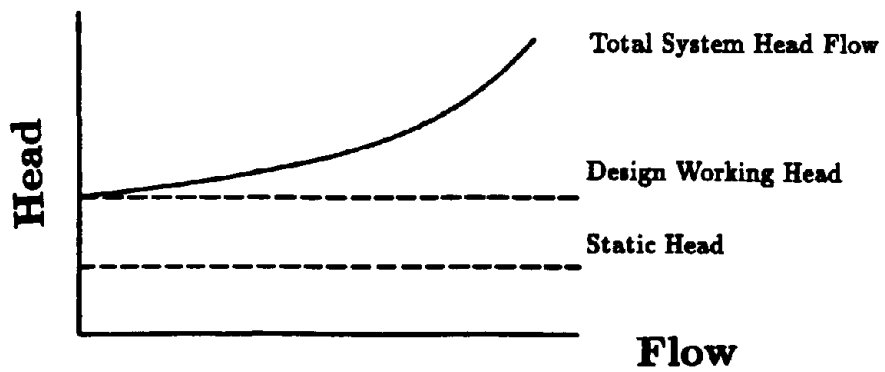
6.3.2 Modeling of the Pump Characteristic Curves

Results from pump performance test were used to model TPHF characteristic curve for AWSS pumps. Tests on the pumps were performed by SFFD. A typical result for a pump with a single engine running are shown in Figure 6.6. Eight points $(Q_n, H_n), n = 1, \dots, 8$ obtained from experimental data describe head-flow relation in a normal operating range of the pump. The normal operating range of the pump in this test covered the flow interval from 1350gpm to 4018gpm. The GISALLE code provides three models for the pump characteristic curve: a regression and two other simplified models.

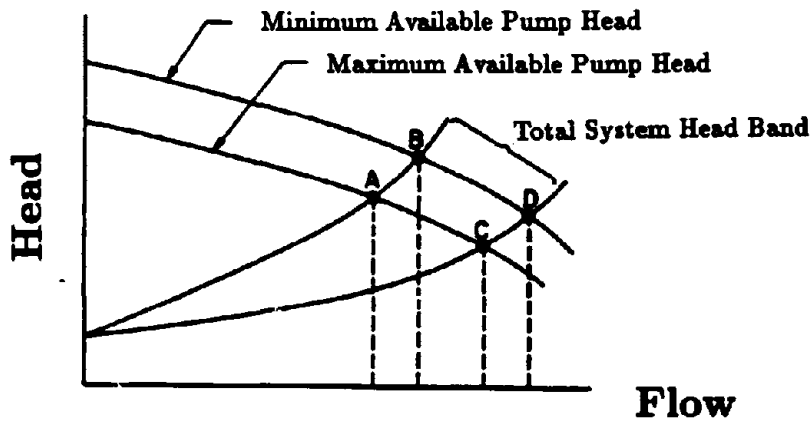
The regression model of TPHF curve is based on points $(Q_n, H_n), n = 1, \dots, 8$. For example,



a. Pump Performance Curve



b. Total System Head Curve Components



c. Interpretation of Flow Head Curves

Figure 6.5: Pump Characteristic Curve

a second degree polynomial regression is

$$H_p = -1.25 * 10^{-5} * Q_p^2 - 5.78 * 10^{-2} * Q_p + 955 \quad (6.1)$$

where H_p is pump head and Q_p is pump flow. This curve is a good approximation of the pump characteristic curve in the normal operating range of the pump which is also the most likely operating range of the AWSS pumps.

Simpler models can be useful when available test data is limited. The first of these models is based on three points as shown in Figure 6.7: (1) the cutoff head H_c corresponding to a zero flow; (2) the maximum flow Q_r in the normal operating range of the pump with the corresponding head H_r ; and (3) a flow with corresponding head (Q_p, H_p) in the normal operating range of the pump.

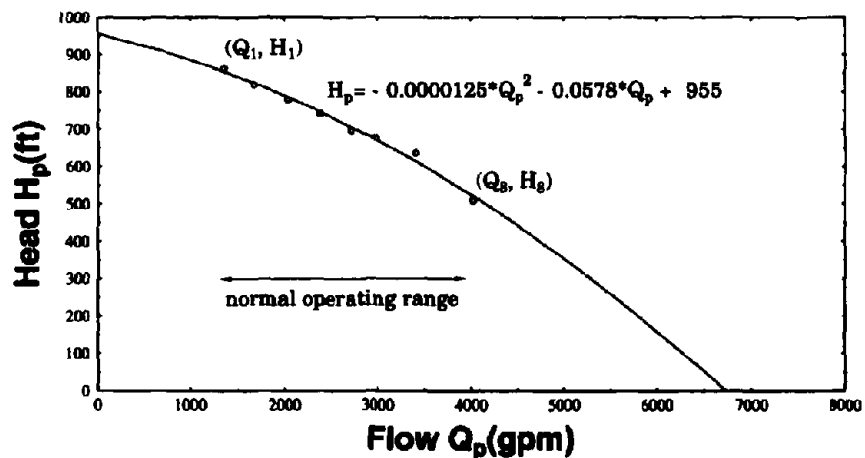


Figure 6.6: Regression Curve

The three point GISALLE pump model is

$$H_p(Q_p) = H_c - A_p * Q_p^{a_p}, \quad Q_l < Q_p < Q_r \quad (6.2)$$

where a_p and A_p are given by:

$$a_p = \frac{\log \frac{H_c - H_r}{H_c - H_m}}{\log \frac{Q_r}{Q_m}} \quad (6.3)$$

$$A_p = \frac{H_c - H_m}{Q_m^{a_p}} \quad (6.4)$$

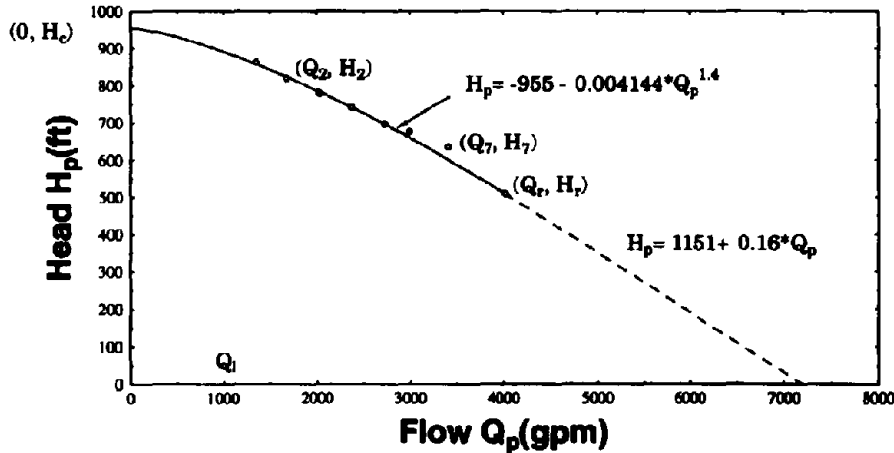


Figure 6.7: Three Point Characteristic Curve

and (Q_m, H_m) , $m = 2, \dots, 7$ are points within the normal operating range. The curve in Eq. (6.2) can be extended to flows larger than Q_r by line tangent to this curve at $Q_p = Q_r$ and shown with dotted line in Figure 6.7. The line is

$$H_p = B_p + C_p * Q_p \quad (6.5)$$

where

$$C_p = -a_p * A_p * Q_r^{a_p-1} \quad (6.6)$$

$$B_p = H_r - C_p * Q_r \quad (6.7)$$

The value of the cutoff head can be obtained from the regression as $H_c = g(0) = 955 - ft$. The minimum available flow is assumed to be $Q_l = 1000gpm$. The pump does not give any flow smaller than this flow. The experimental value of the largest flow is $Q_r = 4018gpm$ at head $H_r = 509 - ft$.

Results in Table 6.VII suggest that the prediction of the pump outflow is not sensitive to the selection of the point (Q_m, H_m) , $m = 2, \dots, 7$. These results correspond to an arbitrary supply-demand scenario for AWSS. The supply was provided by two pumps while the fire hydrants were opened at Marina and Folsom locations. Point (Q_m, H_m) , $m=2, \dots, 7$ was chosen as indicated in Figure 6.7.

Table 6.VII: Sensitivity Study for the Selection of a Middle Point

POINT 1	$Q_c = 0.0, H_c = 955 ft$					
POINT 2	(Q_2, H_2)	(Q_3, H_3)	(Q_4, H_4)	(Q_5, H_5)	(Q_6, H_6)	(Q_7, H_7)
Q_n (gpm)	3405	2988	2720	2375	2030	1670
H_n (ft)	635	676	696	742	779	820
(gpm)						
from PUMP 1	4150	4186	4223	4196	4199	4167
from PUMP 2	2885	2816	2778	2798	2808	2852
at MARINA	-1342	-1330	-1324	-1327	-1329	-1336
at FOLSOM	-5693	-5672	-5662	-5668	-5670	-5682
POINT 3	$Q_r = 4018 gpm, H_r = 509 ft$					

The simplest GISALLE pump model is based on one point description of the pump. This model can be used for preliminary analysis when experimental data are not available or for pump design. The characteristic curve can be obtained from a parametric relationship between head and flow

$$H_p(ft) = \frac{550HP(hp)}{Q_p(cfs)\gamma(slug/ft^3)} \quad (6.8)$$

in which HP is the horsepower of the pump and γ is the specific weight of water. By selecting a value for HP one can obtain an approximate pump characteristic curve. For example, the horsepower for the AWSS system corresponding to a flow of $Q = 2500gpm$ and head of $H = 315psi$ is

$$HP = \frac{H_p Q_p \gamma}{550} = 438hp \quad (6.9)$$

so that the pump characteristic curve has the form

$$H_p = \frac{1.729 * 10^6}{Q_p} \quad (6.10)$$

The curves for a variable HP are shown in Figure 6.8.

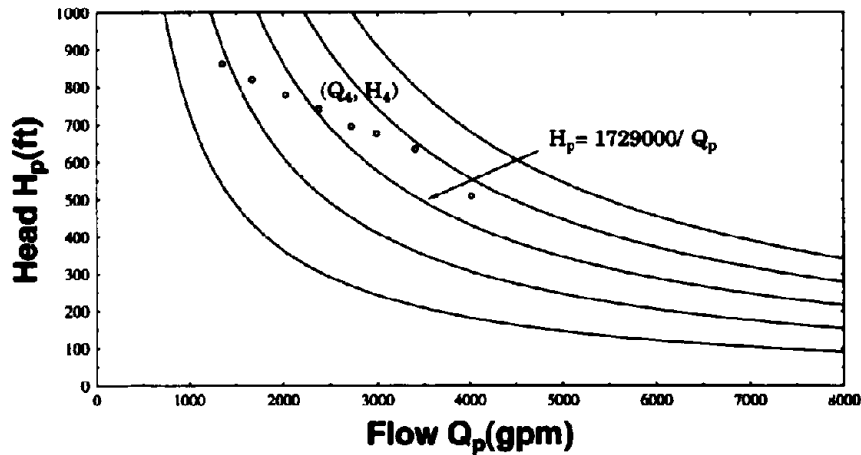


Figure 6.8: One Point Pump Characterization

6.3.3 Effect of Pump Characterization on the AWSS

Several analyses were conducted with the regression, the three point, and the one point description pump models for Loma Prieta earthquake. The results, shown in Table 6.VIII, indicate that one point and the three point curves give conservative results in the regions where they are below the regression curve and unconservative for the rest of the regions. This difference can be substantial e.g., the ratio of the flow loss from the JST for the regression and the one point pump models is 0.564 as shown in the table. The three point model gives fairly accurate results because the curve nearly coincides with the regression model in the normal operating range of the AWSS pumps.

6.4 Demand Simulation

Water demand for fire fighting can be provided only at nodes of the AWSS via open hydrants. Demand can be modeled by specifying flow or pressure at the hydrants. A flow demand is

Table 6.VIII: Sensitivity Study of Pump Curve Characterization

Pump Curve	Actual (1)	3 Point (1)/(2)	1 Point (1)/(3)
Flow at JST (gpm)	2110	0.944	0.564
Flow at Pump 1 (gpm)	4 x 4528	1.003	1.084
Head at Pump 1 (psi)	433	1.002	1.051
Flow at Pump 2 (gpm)	4 x 2897	1.011	1.072
Head at Pump 2 (psi)	682	1.010	1.066
Flow at Marina (gpm)	-5120	-1.003	-1.019
Flow at H-Break 1 (gpm)	-5981	-1.001	-1.012
Flow at H-Break 2 (gpm)	-5189	-1.001	-1.025
Flow at H-Break 3 (gpm)	-1826	-1.001	-1.012
Flow at H-Break 4 (gpm)	-4762	-1.001	-1.020
Flow at P-Break (gpm)	-8916	-1.001	-1.014
TOTAL-INFLOW (gpm)	31813	1.002	1.018
TOTAL-OUTFLOW (gpm)	-31794	-1.001	-1.017

described by constant flow at the hydrant, however, the flow may vary from hydrant to hydrant. A pressure demand can be modeled by an open hydrant at a specified pressure, for example a 20-psi pressure is required by the fire department.

Location of the nodes in the computer representation of the AWSS not necessarily correspond to site location of hydrants. It is common that more than one hydrant is open at a fire site, however, all those hydrants are very close to each other. This section verifies procedure for modeling fire demand with one or more open hydrants.

Two different fire hydrants were analyzed by GISALLE: a fire at the Marina and fire at the Folsom St. On both locations water demand was modeled with one or up to four open hydrants at 20psi pressure. The location of the hydrants is shown in Figure 6.9. It is assumed that the AWSS is under conditions occurred during Loma Prieta Earthquake. This condition are explained in Section 7.

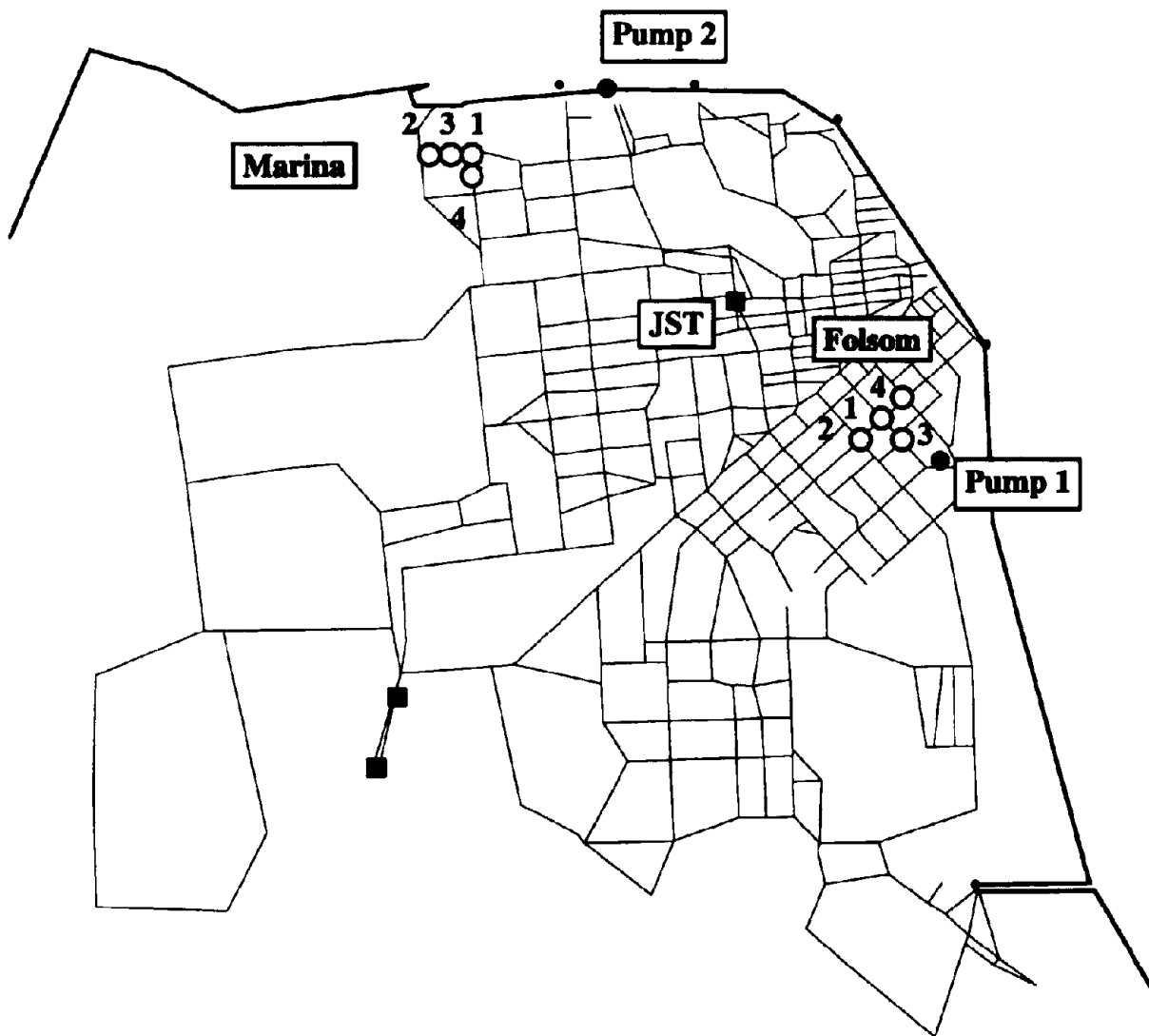


Figure 6.9: Locations of Fire Hydrants

Figures 6.10 and 6.11 show the available flows at the Marina and Folsom fires, respectively, when one, two, three, and four hydrants are open. A control flow is obtained with hydrants open to atmospheric pressure. The control flow provides an upper bound on the available flow at particular site.

Results show that the system serviceability can be increased by as much as 50% when the number of open hydrants is increased from one to four. This is true for the Folsom fire when available hydrants are not on the same flow path. For fires likely to occur in infirm area e.g., the Marina fire, where the hydrants are on the same flow path, it is sufficient to model fire demand with one open hydrant. The GISALLE code enables the user to detect the existence of alternate flow paths toward a fire location and indicates that the available flow can be increased.

6.5 Flow Tests

The San Francisco Fire Department performed several tests on the AWSS, some of which were suggested by the Cornell researchers. The tests include: three tests in the Lower Zone, five tests in the Upper Zone, and one test covering both zones. The water tanks were the only source of water in all tests. Figure 6.12 shows the location of the hydrants where pressure was monitored during the tests. Experimental measurements were compared with analytical results from GISALLE to calibrate the relationship between values of roughness coefficient and pipe diameter, and to evaluate the accuracy of the computer model.

6.5.1 Determination of Roughness Coefficients

The head loss ΔH can be calculated from Hazen-Williams equation, that in English units has the form:

$$\Delta H = \frac{4.73LQ^{1.852}}{C^{1.852}D^{4.87}} \quad (6.1)$$

in which Q = flow in (cfs), L = pipe length in (ft), D = pipe diameter in (ft), and C = roughness coefficient. It is common to assume that C has the same value for all the pipes of a system. An alternative estimate of the head loss can be based on the Darcy-Weisbach

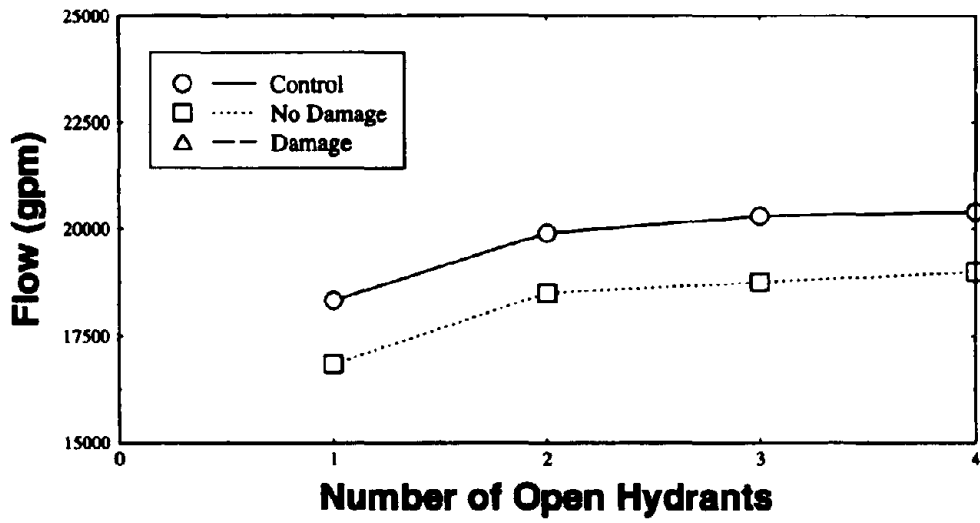


Figure 6.10: Available Flows for Alternate Water Paths

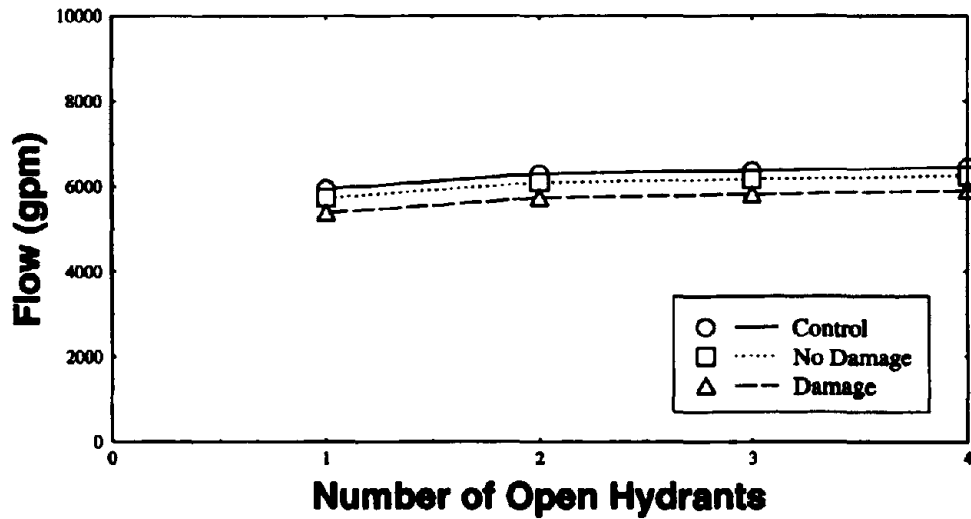


Figure 6.11: Available Flows for a Single Water Path

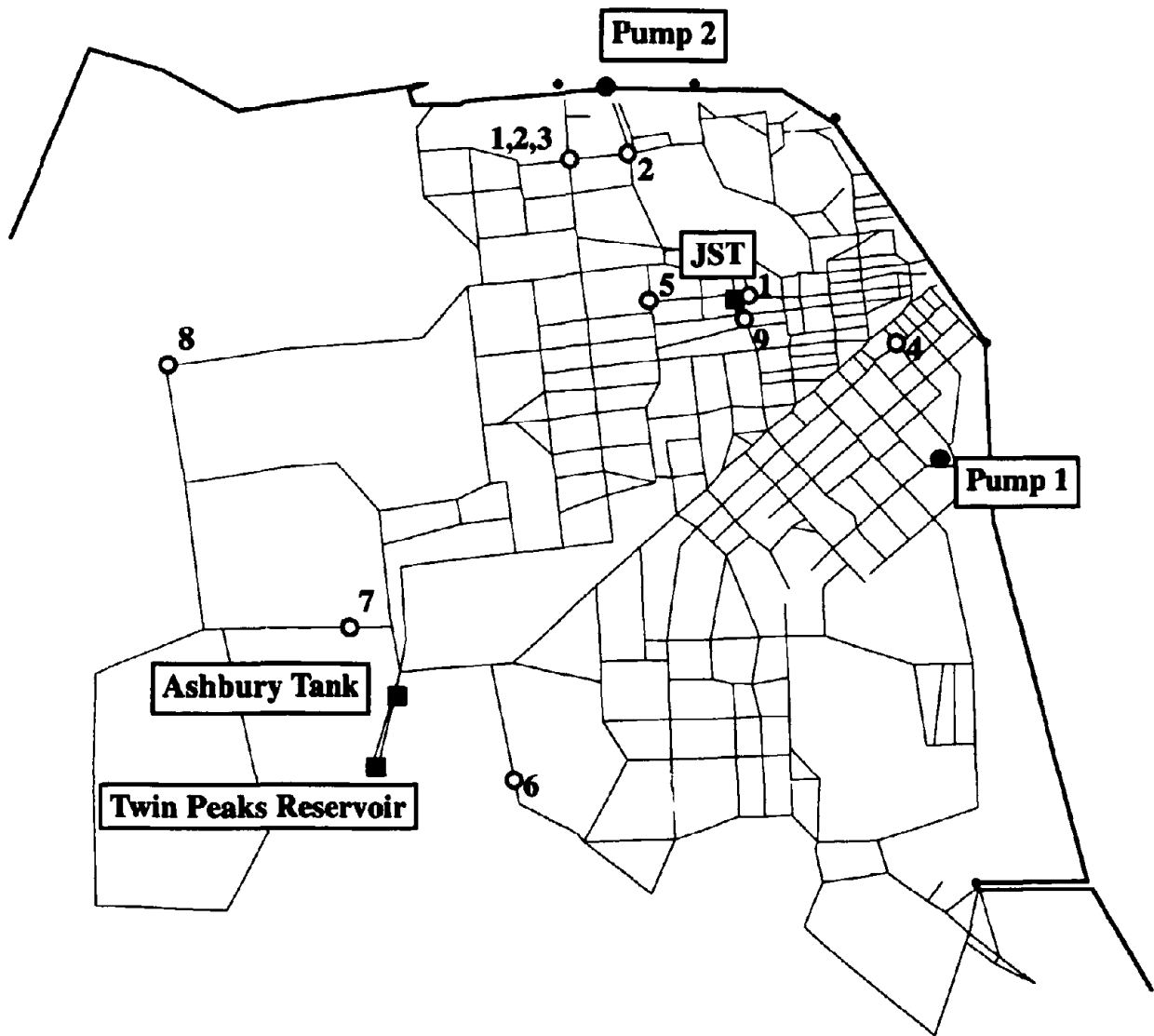


Figure 6.12: Monitored Locations for 9 Field Tests

equation

$$H = f \frac{LV^2}{2gD} \quad (6.2)$$

$$f = \frac{0.25}{\log(\epsilon/3.7D + 5.74/Re^{0.9})^2} \quad (6.3)$$

where V = average flow velocity in (ft/sec), g = gravity acceleration in (ft/sec^2), and f = dimensionless friction factor. The friction factor f depends on the relative roughness of the surface ϵ/D , where ϵ is absolute roughness in (ft), and the Reynolds number $Re = \rho VD/v$, where ρ is the density in (lb/ft^3), and v is dynamic viscosity in ($lb/ftsec$). The relationship between C and f is

$$C = \sqrt[1.852]{\frac{4.73LQ^{1.852}2g}{fD^{3.87}V^2}} \quad (6.4)$$

and can be used to calculate C from f , using results of field tests. It has been shown [44, 45,47] that C and f depend on the age of the pipe. Experimental studies indicate that the roughness coefficient of old pipes can be obtained from the roughness coefficient of new pipes times an age factor varying from 4 to 10 depending on the pipe diameter [47]. These results were used to estimate values of f for AWSS based on field tests. The corresponding values of C were determined from Eq. (6.4).

Numerical results show that the predictions of the GISALLE code are in good agreement with field measurements when the roughness coefficient C varies with pipe diameter. Optimal values of C for the Upper and Lower Zones have been obtained by minimizing the objective function

$$e_2 = \sum_{t=1}^{n_f} \left(\sum_{i=1}^r |p_{t,i} - p_{t,i}^*| \right) \quad (6.5)$$

where n_f = the number of field tests, r = the number of monitored locations in each field test, $p_{t,i}$ = the calculated pressure at monitored location i in test t , and $p_{t,i}^*$ = the measured pressure at monitored location i in test t for the upper and lower zones of the AWSS. The optimization was performed for several pipeline diameters. Figure 6.13 shows the results of the optimization algorithm. A similar dependence of the roughness coefficient with pipe diameter is reported elsewhere [7,23,31,45,48]. A difference between values of C in the Upper and Lower Zones of AWSS may be caused by the age difference between these parts of the network. Moreover, the temporary presence of salt water in the Lower Zone may also have contributed to differences in the roughness characteristics of the pipes in these zones.

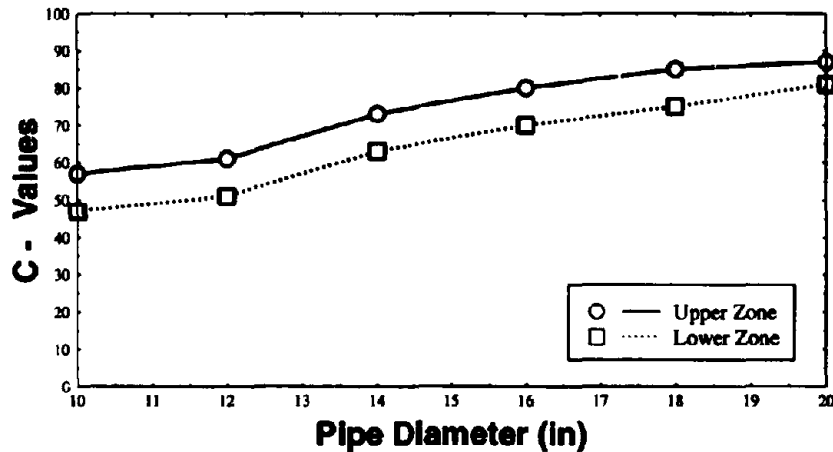


Figure 6.13: Variation of Roughness Coefficient C with Pipe Diameter

6.5.2 Computer Modeling

Table 6.IX gives results of analysis based on the GISALLE code using values of C in Figure 6.13. In Tests 1 and 2, pressures were monitored at two locations as shown in Figure 6.12. There is a very good agreement between the measured and calculated pressures for the tests in which the Upper and Lower Zones are not connected. However, some discrepancies occur when the two zones are connected. These discrepancies can be caused by differences between the values of C in the Upper and Lower Zones. Moreover, the test covering both zones was performed 20 years later than the other eight tests.

6.6 Summary

In this section the GISALLE code was validated on different ways. Test problems were design to check hydraulic analysis and procedure for elimination nodes with negative pressures as well as procedure for approximate partial flow analysis. Pump model available in the code was tested for the compliance with actual AWSS pump characteristics. Models of fire demand were examined. A single hydrant can be sufficient to provide water for a fire if there is only

Table 6.IX: Results of Field Tests and Computer Analyses

Location	Test No.	Field (psi)	Computer (psi)
Both Zones	1*	43	23.5
		7	9.6
Lower Zone	2*	45	45
		75	75
	3	13	14
	4	134	135
Upper Zone	5	78	77
	6	50	49
	7	33	26
	8	80	90
	9	43	44

pressures monitored at two locations

one water path to the fire. The code was calibrated with available field test results obtained for the AWSS. The validation of the code showed that GISALLE is capable of reproducing the actual flow and pressure distributions in AWSS.

SECTION 7

LOMA PRIETA EARTHQUAKE SCENARIO

7.1 Introduction

One main and four hydrants of AWSS broke during the the 1989 Loma Prieta earthquake. These failures were concentrated South of the Market area, a zone where hydraulic fills are underlined with a substantial depth of Holocene bay mud. Fires erupted at several locations. Jones St. Tank (JST) was the only source of water supply and remained without water in approximately 35-40 minutes. The damage and fire scenario observed during the Loma Prieta earthquake was modeled with the GISALLE code. Flows, pressures and water losses were calculated and the time required to empty the JST was determined. The GISALLE predictions were compared with the actual field observations during the earthquake. Results show that GISALLE can reproduce the field conditions adequately.

7.2 1989 Loma Prieta Earthquake

After the Loma Prieta earthquake a major fire erupted in the Marina district of San Francisco. As discussed in Section 4, the Marina was constructed from 1853 to 1912 by reclaiming land from the San Francisco Bay. Two types of fill were used in the reclamation process: loose sands from sand dunes and beach deposits, and hydraulic fill dredged and pumped from sand bars. The loose fills in combination with a thick underlying deposit of soft Recent Bay Mud contributed to liquefaction and amplification of ground waves. The strong ground shaking from locally amplified seismic waves was the main cause of damage to the timber frame structures at this location. Particularly vulnerable were timber frame apartment buildings with garages at the first floor. Strong racking caused by seismic shaking occasionally resulted in failure. The worst damage was observed in the four story apartment building where failure was followed by fire initiation.

A description of the initiation of the Marina fire can be found in [51]:

"The fire began in the four story wood framed building at 3701 Divisadero Street, at the northwest corner of Beach Street. The building is a typical corner building in the Marina

district. It was built in the 1902's and contained 21 apartments, with the ground floor primarily a parking garage. The building's lower two floors had collapsed in the earthquake, and the third and fourth floors were leaning southward several feet. The fire was in the rear of the building and was initially small which, combined with confusion following the earthquake, resulted in a delayed report such that the first SFFD unit did not arrive until approximately 5:45 PM (all times estimated). Source of ignition has not been definitely determined at this time. Wind speed was virtually zero. Arrival of SFFD Trucks 10 and 16 was closely followed by engine 41. Based on appearance of black smoke, the fire appeared to the officer in charge of E41(Lt.P.Corny) to be a wood structure fueled fire. At this time, E41 connected to the AWSS directly in front of 3701 Divisadero (the building was actually leaning over the hydrant), charged the pump but found no water pressure. Due to radiant heat E41 then withdrew across the street. At about 6:25 PM the building at the northeast corner (2080 Beach) ignited."

Figure 7.1 shows the damage sustained by the AWSS during the Loma Prieta earthquake. All breaks were concentrated in 'infirm areas'. Under normal circumstances these areas can be isolated by closing only one gate valve located on the pipe feeding water in these zones. The valve is controlled by an electric motor and can be operated by remote control. Because of the earthquake, the City had no electric power so that the valves could not be operated remotely and remained open. Hydrants were the most vulnerable components of the system with damage being concentrated at elbows that fractured at 45°. Three hydrant breaks were reported South of the Market area while one was observed at the Foot of the Market area. The most serious damage was the break at a 300-mm-diameter cast iron main on the 7th St. between the Mission and Howard Sts. In addition, two leaks were reported in the Marina district and Folsom St., as shown in the figure. Water flow through the break and leaks supplemented by losses at broken hydrants, emptied the Jones St. Tank. Its entire storage of 720,000 gallons was lost in approximately 35-40min. Loss of the reservoir led to the loss of water pressure throughout the lower zone of the AWSS where damage in the MWSS had cut off alternative source of water supply for fire fighting [40].

7.3 Computer Analysis of Loma Prieta Event

The GISALLE code, was used to predict the AWSS performance during the Loma Prieta earthquake. The damage that AWSS sustained during the earthquake is shown in Figure 7.1 and consist of one pipe break, two pipe leaks, and four hydrant breaks occurring in the lower

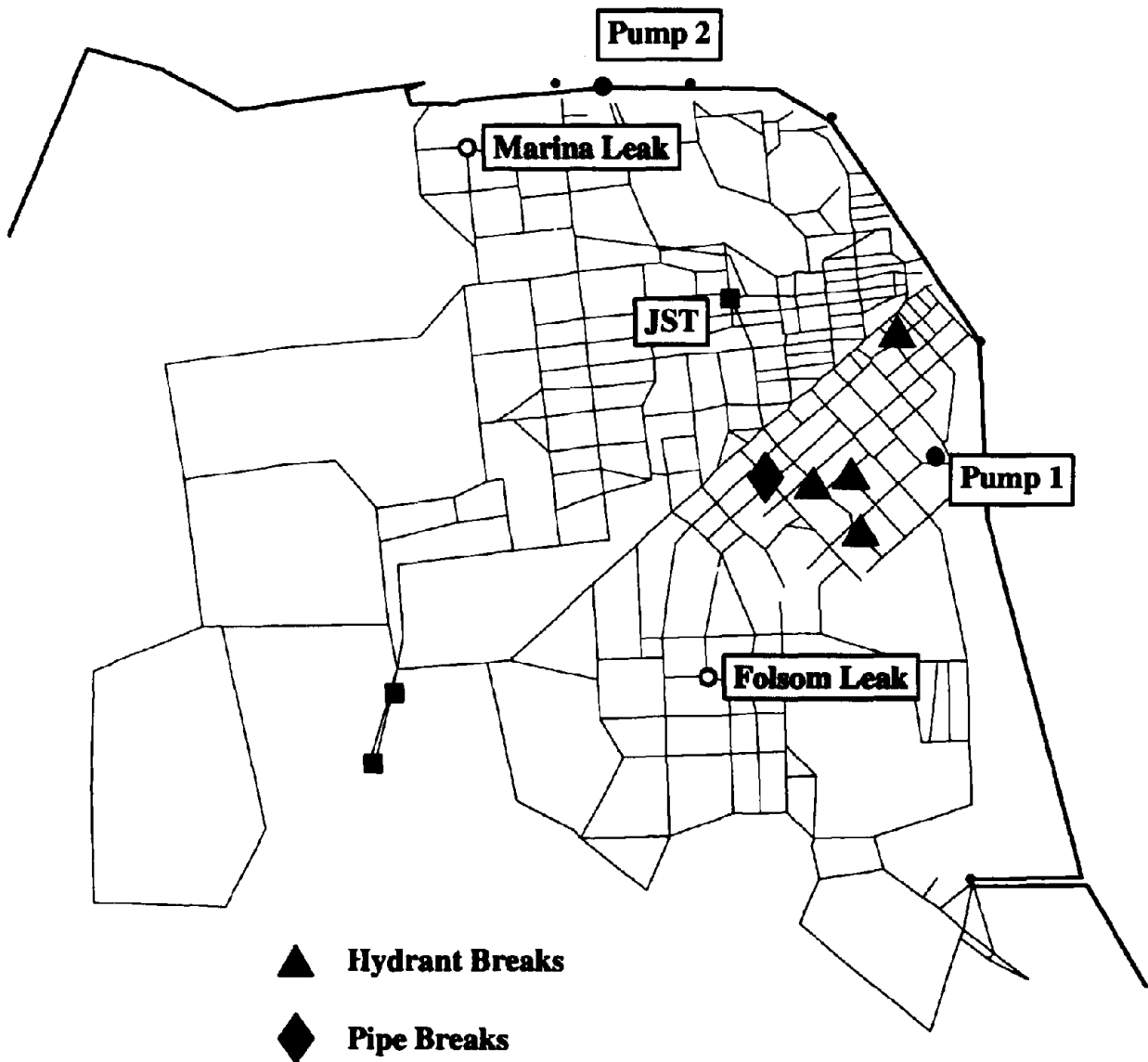


Figure 7.1: Breaks and Leaks in AWSS Caused by Loma Prieta Earthquake

zone of the system. The division gate valves between the Upper and the Lower Zones of the system were closed in the night of the earthquake. As a result, there was no interaction between the Upper and Lower Zones. Therefore, only performance of the Lower Zone was evaluated.

Two limit cases are considered. In the first case, only the breaks are modeled. In the second case, the breaks and the leaks are considered. The leaks are modeled conservatively as open hydrants with a specified pressure of 20psi. Table 7.1 gives information on the outflow at all breaks and leaks. The total water loss equals the outflow from the JST because the tank represents the only source of water. The major contribution to water loss comes from the hydrants. For example, the hydrants loss is 11,692gpm when only breaks are considered and constitutes 67% of the total water loss.

Results in Table 7.1 can be used to estimate the time to a complete loss of water supply from the system. This time can be obtained by dividing the capacity of the JST to the outflow rate from the system. It is $720,000/17,566 = 41\text{min}$ or $720,000/20009 = 36\text{min}$ for the case in which only breaks or breaks and leaks are considered, respectively.

Table 7.1: Results of the Earthquake Simulation

LOCATIONS OF WATER LOSS	Only Breaks (gpm)	Breaks + Leaks (gpm)
Hydrant 1	4254	3766
Hydrant 2	3087	2666
Hydrant 3	1299	1150
Hydrant 4	3052	2635
Marina Leak	0	2812
Folsom Leak	0	2009
Broken 12-in. Main	5874	4970
Jones St. Tank	17566	20009

7.4 Summary

The GISALLE code was used to reproduce the sequence of events occurred during the 1989 Loma Prieta earthquake. It has been shown that code is capable of reproducing the actual field conditions.

SECTION 8

SENSITIVITY STUDIES

8.1 Introduction

The seismic serviceability evaluation of the Auxiliary Water Supply System (AWSS) in San Francisco is complex because of the nonlinear nature of the hydraulic analysis and because of the enormous number of supply-demand combinations that can occur after an earthquake. The GISALLE code is applied in this section to estimate the serviceability of the AWSS following seismic events. The serviceability of the system is evaluated for numerous supply-demand scenarios and damage distribution likely to occur in San Francisco. Deterministic and stochastic studies are performed. In the deterministic studies the supply, the fire and the damage scenarios are specified. In the stochastic studies the fire scenarios and the damage states are generated by Monte-Carlo simulation consistent with a selected earthquake intensity. Pressure and flow distribution were obtained for the system. Results provide information on the potentially critical components of the system for the chosen scenarios and can be used for planning and managing of post-earthquake restoration measures.

8.2 Parameters Selection

The Lower Zone of the AWSS is more vulnerable to earthquakes induced damage than the Upper Zone because of geotechnical characteristics, as explained in Section 4. Therefore, the division gate valves between the two zones were closed and sensitivity studies were performed on the Lower Zone only for supply, fire, and damage scenarios. These scenarios are uncertain events described by deterministic and probabilistic models.

8.2.1 Supply Scenarios

The AWSS can receive water from tanks, pump stations and fire boats as shown in Figure 8.1. The city has only one fire boat, 'Phoenix' described in Section 4. The sensitivity studies include supplies from tanks and pumps only.

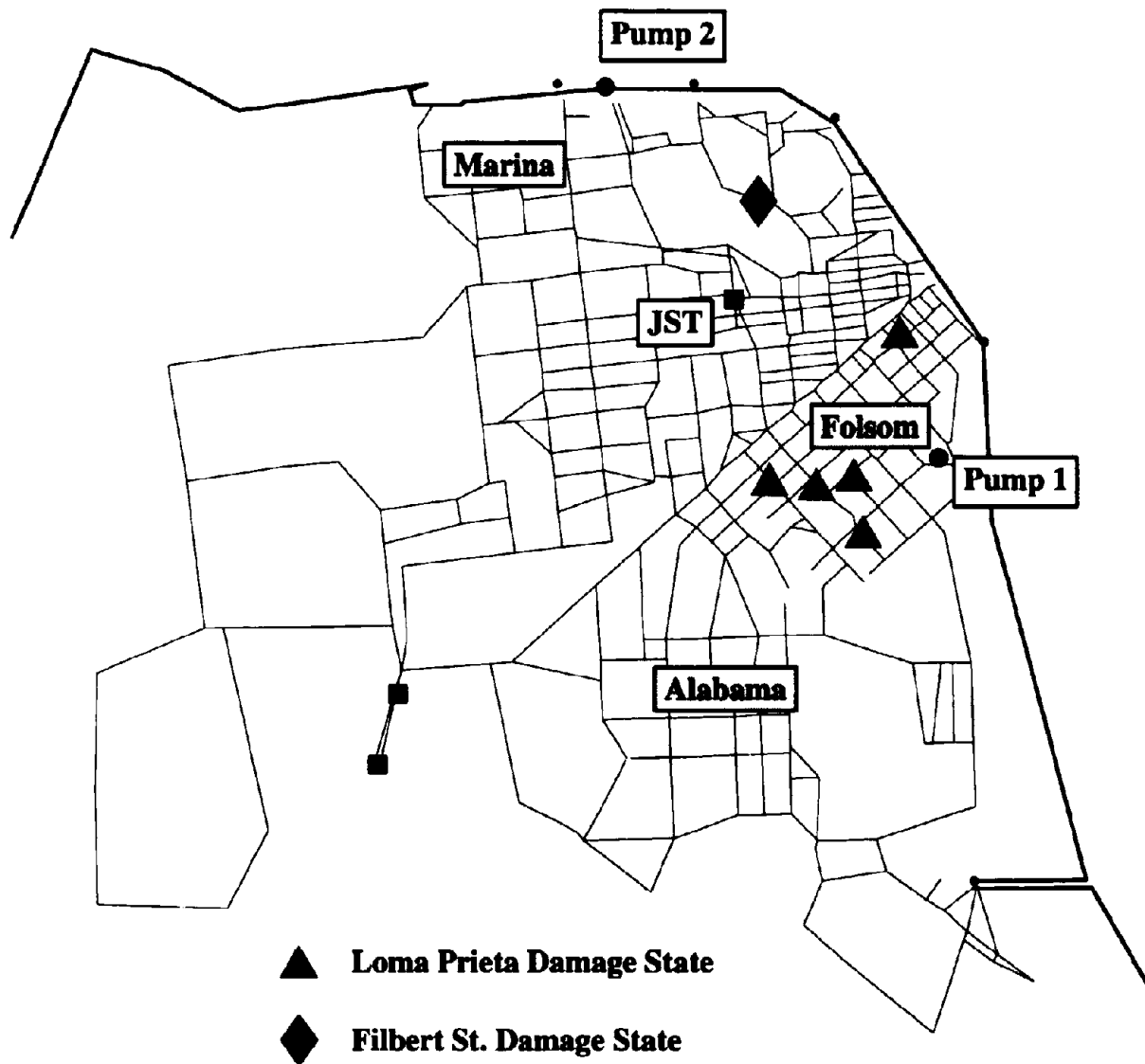


Figure 8.1: Locations of Damage States, Fires and Water supplies

The Jones St. Tank (JST) is the only tank supplying the Lower Zone when the division gate valves between the Lower and Upper Zones are closed. The tank, with capacity of 750,000 of gallons, was connected throughout most analyses. A total water loss from JST may drastically change available water supply. Therefore, the supply scenario with only two pump stations is analyzed. The stations have four engines, each providing a flow of 2,500gpm at 300psi. It has been shown in Section 6 that the pump performance can be successfully described by a curve inferred from three experimental data of the pump. This characterization was used in the sensitivity studies. A three water supply scenarios are considered:

1. Jones St. Tank only (JST)
2. Jones St. Tank and Pump station No.1 with four engines (JST+P4)
3. Jones St. Tank and Pump stations No.1 and No.2 with four engines each (JST+P44)

These scenarios were chosen to cover a range from low to high water supply conditions in the deterministic and stochastic analyses.

8.2.2 Fire Scenarios

Evidence from the past shows that some locations in the San Francisco are particularly vulnerable to fire eruptions following earthquakes [50]. In deterministic analyses three fires are considered. They are located at (1) the Marina fire at the corner of Beach St. and Scott St., (2) the Folsom at the corner of Folsom St. and 3rd St., and (3) the Alabama at the corner of Alabama St. and 18th St., as shown in Figure 8.1 Fires at the Marina and the Folsom occurred during the Loma Prieta earthquake. A potential fire at Alabama St. could spread rapidly because only one low pressure hydrant is available at this location. It is assumed that the fire occurrence follow the sequence:

- a. the Marina fire (M)
- b. the Marina + the Folsom fires (M+F)
- c. the Marina + the Folsom + the Alabama fires (M+F+A)

As discussed in Section 6, one or more hydrants can be used in the GISALLE code to supply water to a particular fire location. One hydrant was opened for the Marina fire since only

one flow path provide water to that location. One open hydrant was also conservatively used for the demand at the Folsom fire although some alternative water paths can be available. The demand for the Alabama fire can be met by opening two hydrants: a hydrant on the main water path and a hydrant on an alternative water path from infirm area No.6.

Demand for fire fighting of 5000 gallons/min at 10psi is specified at each fire location. This is a situation which assumes that fire fighters will open all hydrants in the vicinity of fire even if the available pressures are less than the required 20psi.

In stochastic analyses the same three fire locations were analysed. Each location is defined with five potential fires.

8.2.3 Damage Scenarios

Damage state of the AWSS following an earthquake can not be predicted. However, it is known that damage is most likely to occur in the infirm areas. Only one pipe break was recorded located outside of these areas in the past. Two approaches are considered for specifying the damage state: deterministic and stochastic.

Deterministic Approach

In this approach damage state is specified. Three potential damage states are considered.

- a. the Loma Prieta earthquake damage
- b. the Infirm areas damage
- c. the Filbert St. damage

The damage locations are shown in Figure 8.1. The damage of the AWSS caused by the Loma Prieta earthquake damage is described in Section 7. The damage of an infirm area is modeled as a break of the main pipe supplying that particular infirm area. The scenario provides an upper bound on the water loss in the infirm area regardless of the number of component breaks in this area. The damage at the Filbert St. consist of 18-in diameter main break.

Stochastic Approach

The statistical module of GISALLE, explained in Section 5, was used in this approach. Damage states of the AWSS were generated randomly by the Monte-Carlo simulation method. Two serviceability indices were determined for a specified range of earthquake intensities. A regression line was fitted to these indices to obtain fragility curves describing the overall seismic performance of the AWSS. These curves can be developed for various fire, water supply, and damage scenarios.

8.3 Results of Deterministic Analyses

Three damage states were considered in the deterministic analysis and described in this section.

8.3.1 Loma Prieta and Filbert St. Damage

Performance of AWSS during the Loma Prieta earthquake is described in Section 7. This section examines the serviceability of the AWSS under combined the Loma Prieta and Filbert St. damage and fire scenarios described in Section 8.2.2

An analysis is performed on the AWSS with water supplies from (i) JST, (ii) JST+P4, and (iii) JST+P44 as described in Section 8.2.1. Applied damaged states are (j) No damage, (jj) Loma Prieta Damage, and (jjj) Loma Prieta and Filbert St. damage. Available supplies at the Marina, the Folsom, and the Alabama fires are shown in Figure 8.2. The solid, shaded, and dashed bars in the figure show the available flows at these three locations for various damage states and supply scenarios. The solid bars in Figure 8.2 show the available flow at the fire locations when there is the Marina fire only. The shaded bars in the figure show the available flow at the fire locations when there are the Marina and the Folsom fires. The dashed bars in the figure show the available flow at the fire locations when there are the Marina, the Folsom and the Alabama fires.

Results for no damage state show that minimum flow of 5000gpm required by the fire department is not met at the Marina and the Alabama in many scenarios. On the other hand, a sufficient flow is available at the Folsom. The figure shows that operation of the pump stations can significantly improve the serviceability of the AWSS.

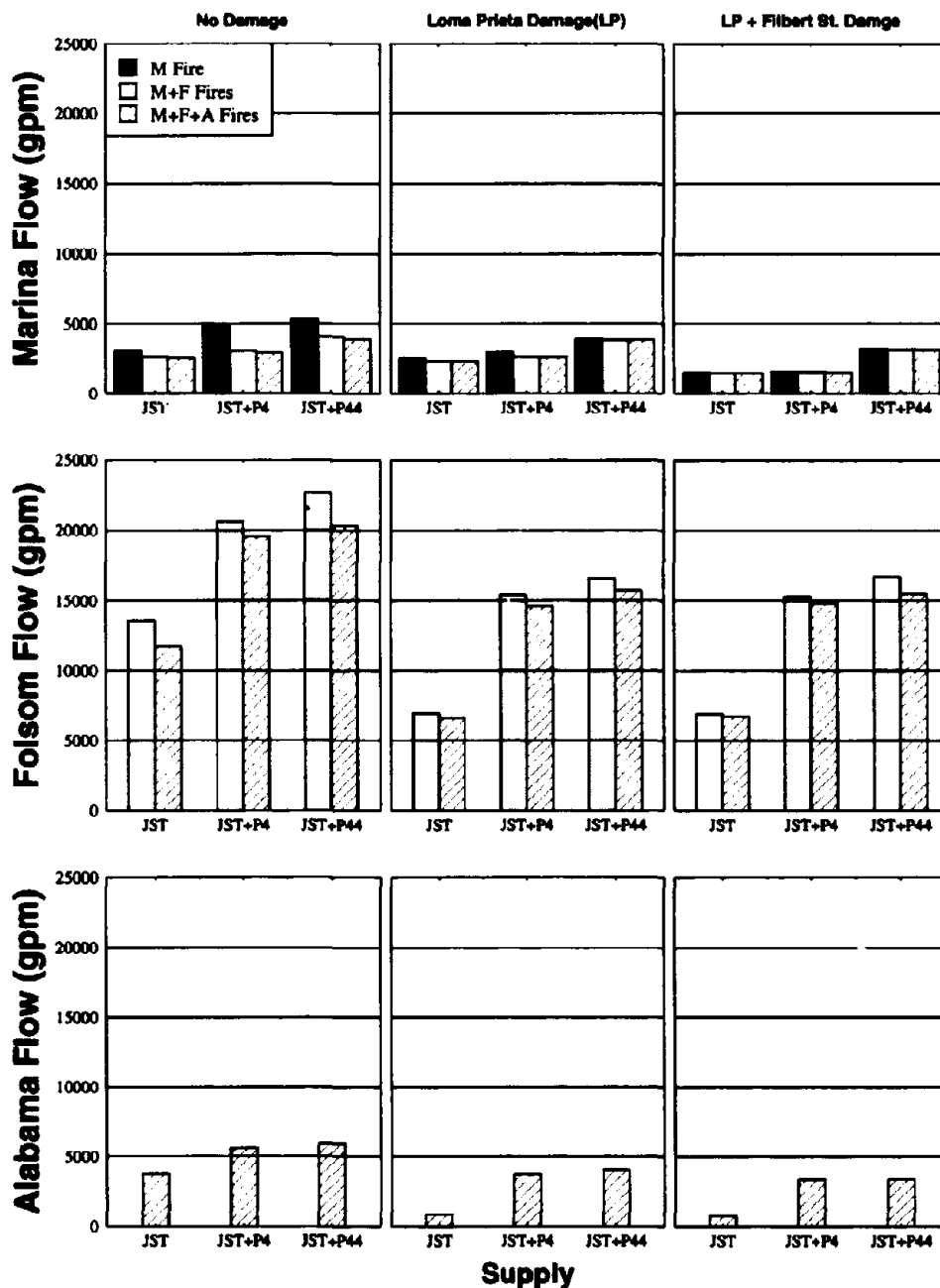


Figure 8.2: Available Flows at the Marina, the Folsom and Alabama St. for Various Damage States and Supply Scenarios

Results for the Loma Prieta earthquake damage show that the available flow is less sensitive to the fire scenario than in the previous case. The contribution of the both pumps for the Marina and the Alabama fires can not provide the minimum flow of 5000gpm. Moreover, the available flow for fire fighting relative to no-damage state decrease from 12% for the Marina location to 328% for the Alabama location. Operation of pump stations can be crucial for the Alabama fire.

Results for the Loma Prieta earthquake combined with Filbert St. damage are similar. The contribution of pump No.1 has a negligible affect on the available flow at the Marina but significant affect on the available flow at the Alabama. Available flows are slightly lower than in the previous case.

8.3.2 Infirm Area Damage States

Damage of the AWSS during an earthquake is expected to be concentrated in the infirm areas, as demonstrated by Loma Prieta and other earthquakes. The sensitivity of the seismic serviceability of the AWSS to damage location is examined in this section.

The water supply consisted of the JST only or the JST and both pumps. Figures 8.3-8.12 are obtained by the GISALE results module. They show flow paths for all damage states and water supply scenarios representing the results of twenty hydraulic analysis. The size of flow is proportional to the thickness of the line. The figures also show nodes with pressures in the range (10-20psi) marked with small stars and in the range (0-10psi) marked with large stars. These figures can be used to identify critical pipes of the AWSS. The critical pipes are pipes that in most of the scenarios have the largest flow. Breaks in these pipes would significantly effect serviceability of the system.

For example, Figure 8.3a indicate that the breaks in infirm area 1 can cutoff the main supply line to the Marina district if JST is the only source of water supply. Figure 8.5a shows that the breaks in infirm area 3 can result in a large region of low pressure if the JST is the only source of water supply. Figure8.10a shows that breaks in infirm area 8 can cutoff a large portion of the South-West part of the Lower Zone.

Figure 8.13 shows the rate of water loss for all ten damage states defined in Figures 8.3-8.12 for two cases of water supply: the JST only, and the JST and both pump stations. The bar diagrams show that the failure of the main line connecting to infirm area No.1 can be critical. The least critical failure is the break of the main line connecting to infirm area

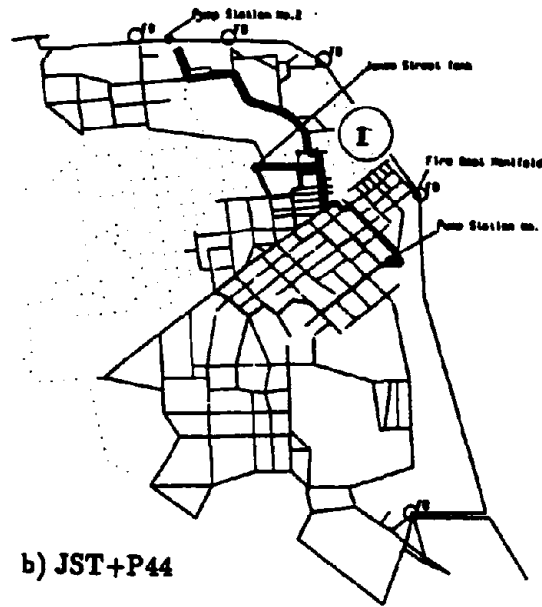
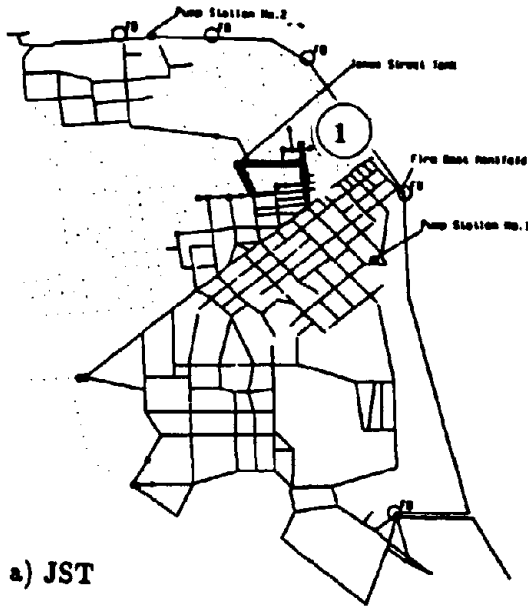


Figure 8.3: Flow Path with Damaged Infirm Area 1

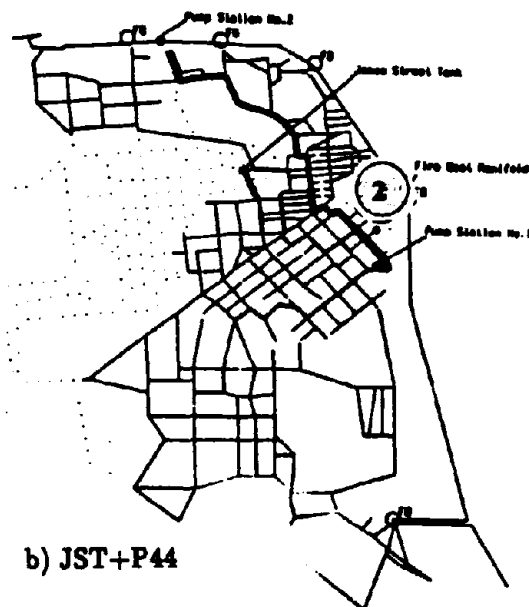
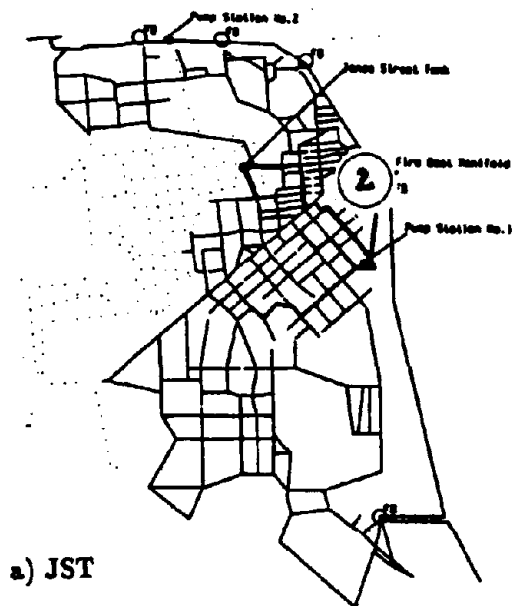


Figure 8.4: Flow Path with Damaged Infirm Area 2

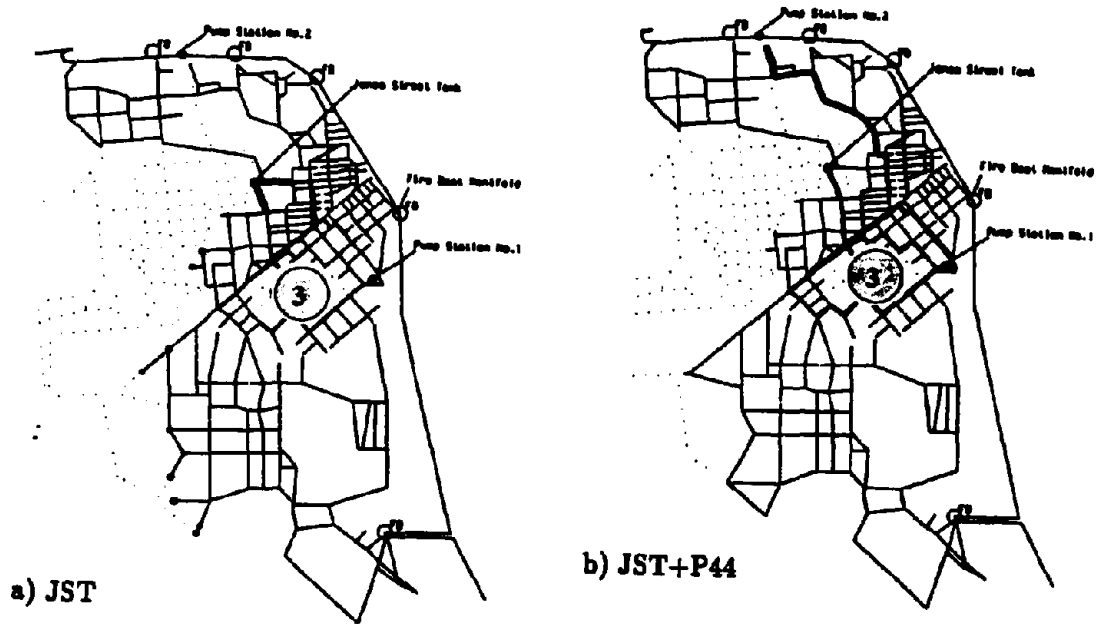


Figure 8.5: Flow Path with Damaged Infirm Area 3

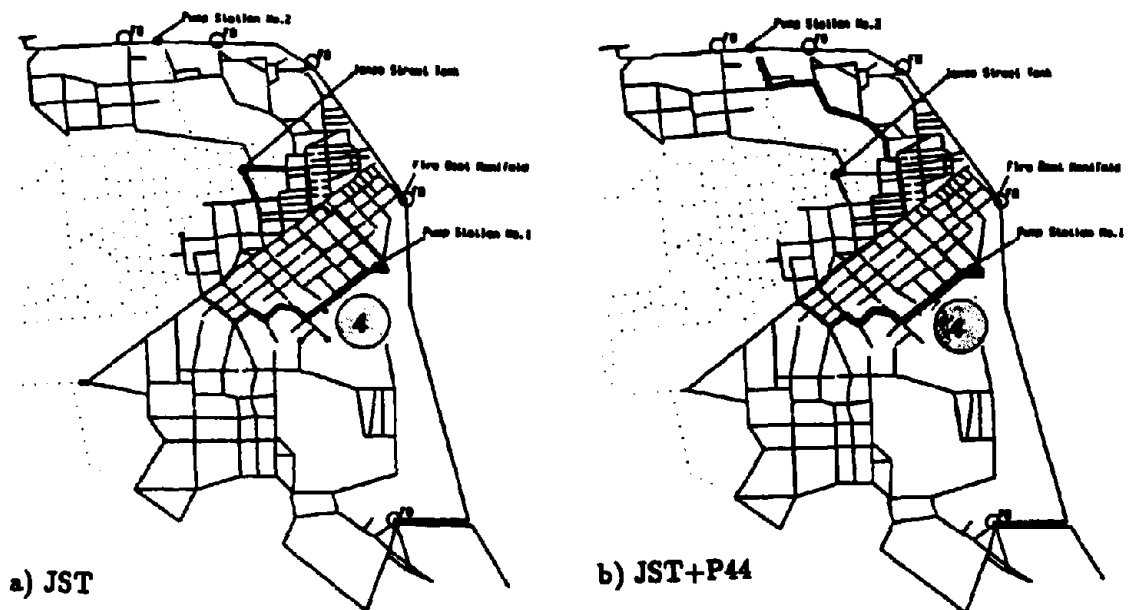


Figure 8.6: Flow Path with Damaged Infirm Area 4

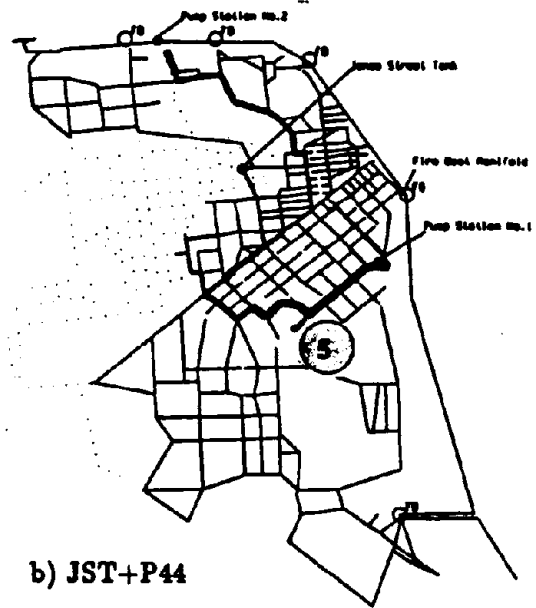
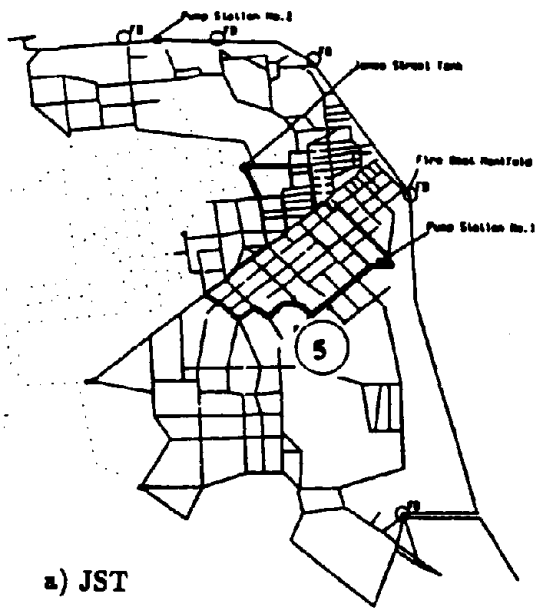


Figure 8.7: Flow Path with Damaged Infirm Area 5

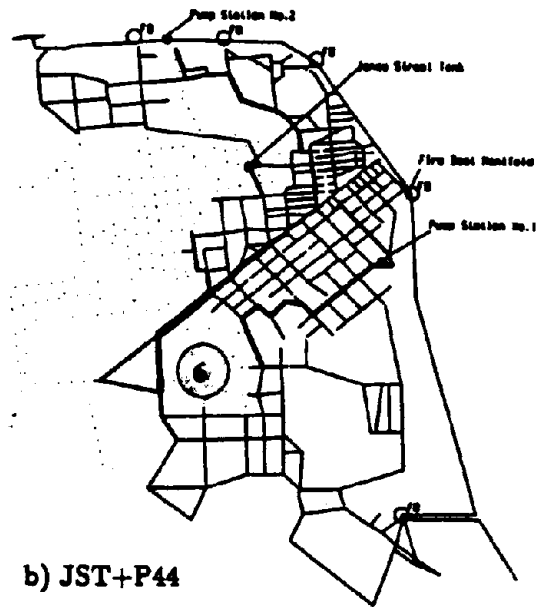
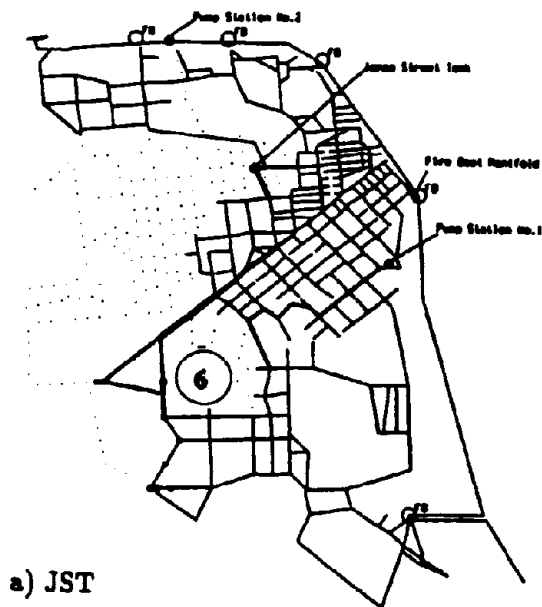


Figure 8.8: Flow Path with Damaged Infirm Area 6

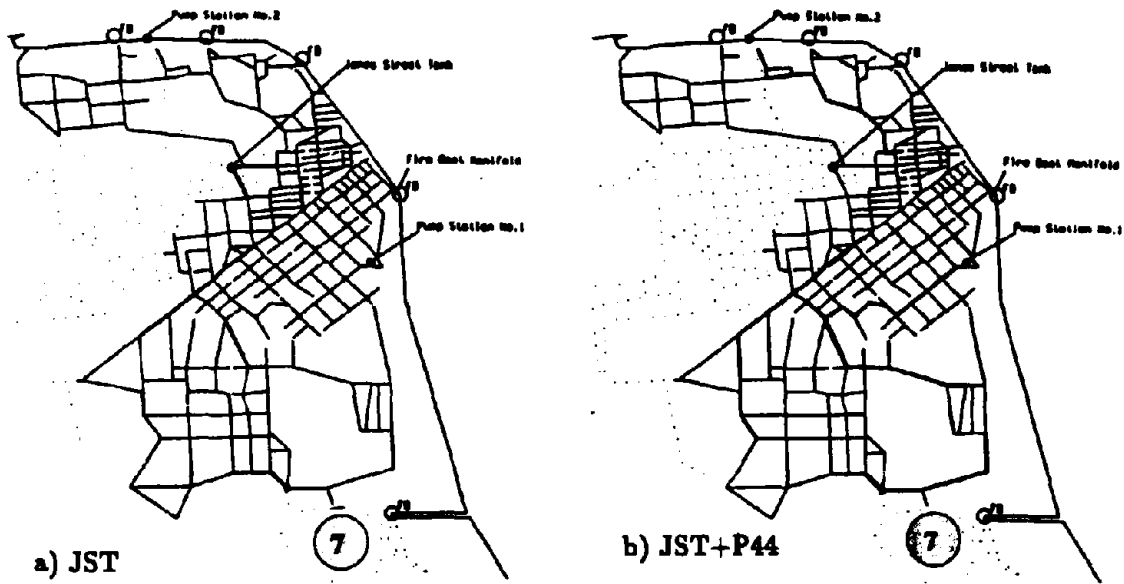


Figure 8.9: Flow Path with Damaged Infirm Area 7

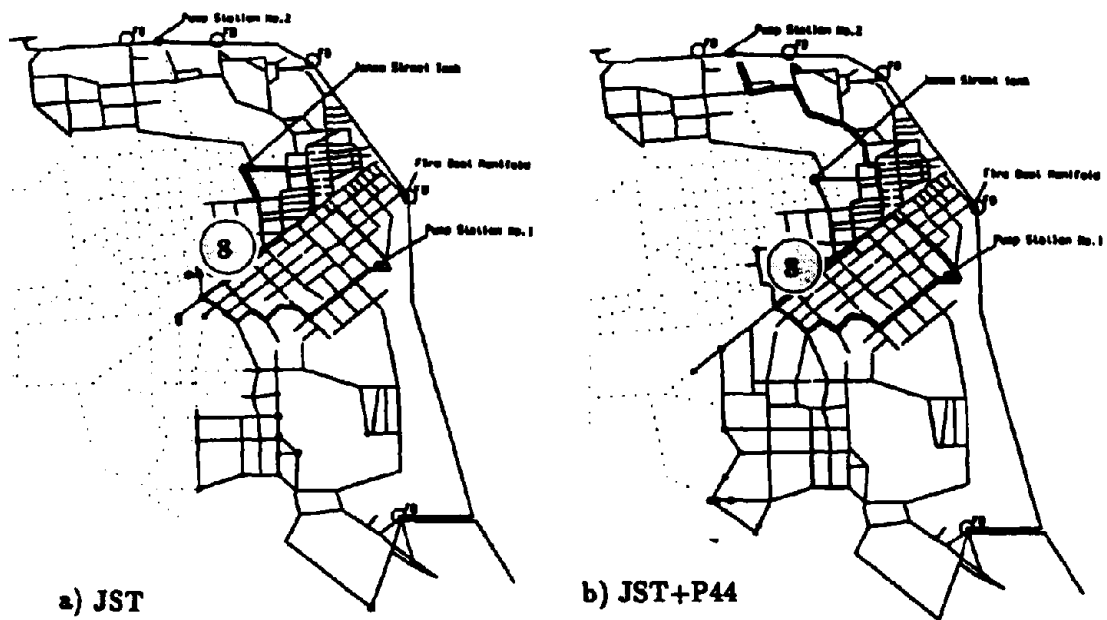


Figure 8.10: Flow Path with Damaged Infirm Area 8

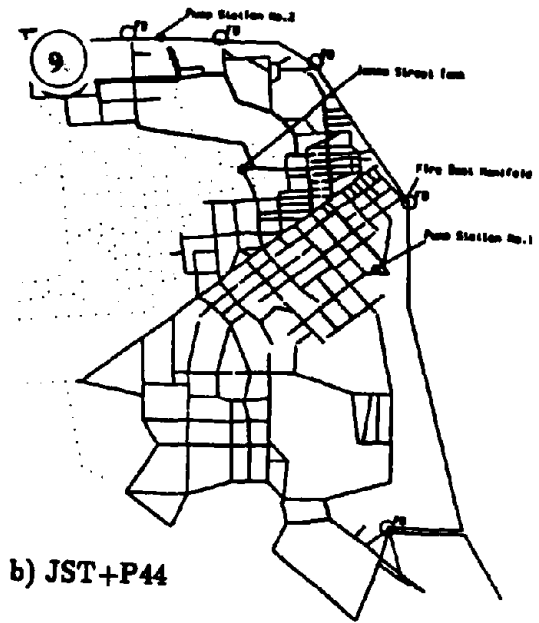
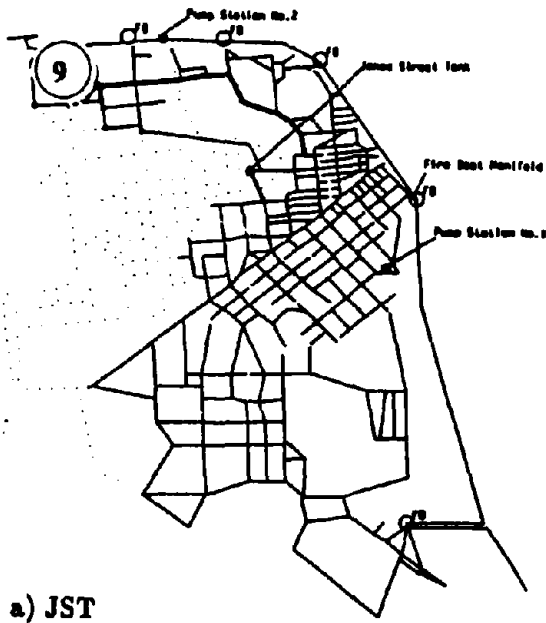


Figure 8.11: Flow Path with Damaged Infirm Area 9

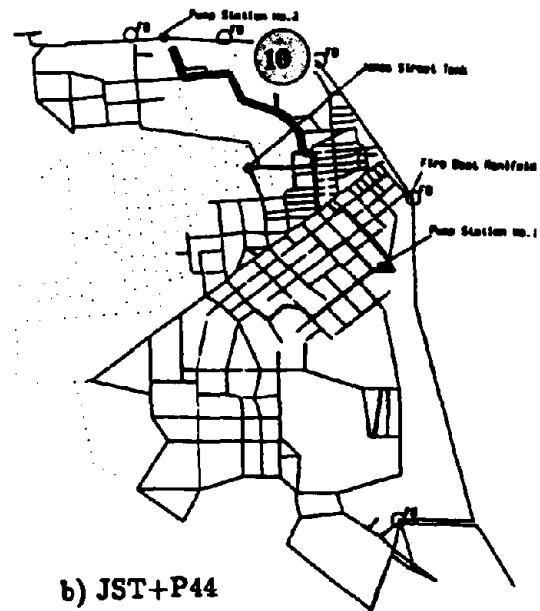
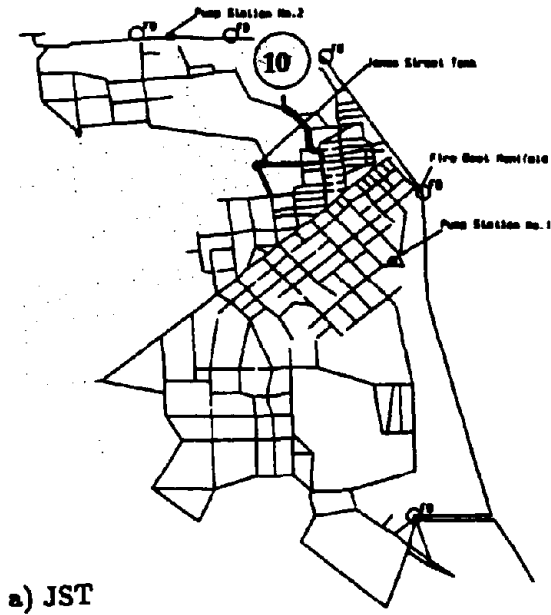


Figure 8.12: Flow Path with Damaged Infirm Area 10

No.7. Moreover, presence of both pumps running with all four engines can stop any water loss from JST providing the breaks occur in the infirm areas No. 4-10.

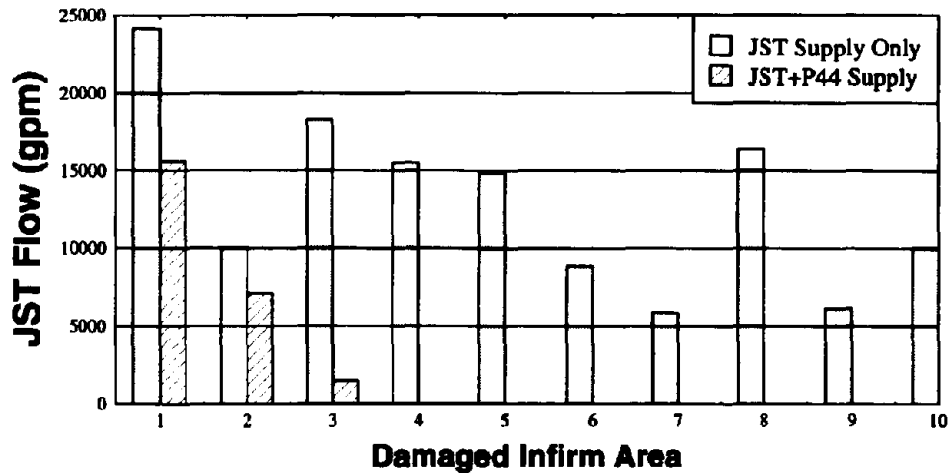


Figure 8.13: JST Water Loss vs. Break Location

Figure 8.14 shows damage index S_d and serviceability index S_s for various damage states and fire scenarios that are explained previously. The figure shows the AWSS is significantly damaged in the case of JST supply only. Operation of the pump No.1 can reduce damage potentials for the Folsom and the Alabama fire sites and operation of pump No.2 can reduce damage potentials for the Marina fire site. The serviceability index declines when damage increases. At the Marina fire site, the required serviceability is not attained in most of the scenarios.

8.4 Results of Stochastic Analyses

The stochastic model described in Section 3 and 5 is used to analyze performance of the AWSS under conditions similar to one described in deterministic approach. Sensitivity studies were performed assuming randomness in water supply condition, demand scenario and damage state.

The water supply conditions include the operation of JST and both pumps running with

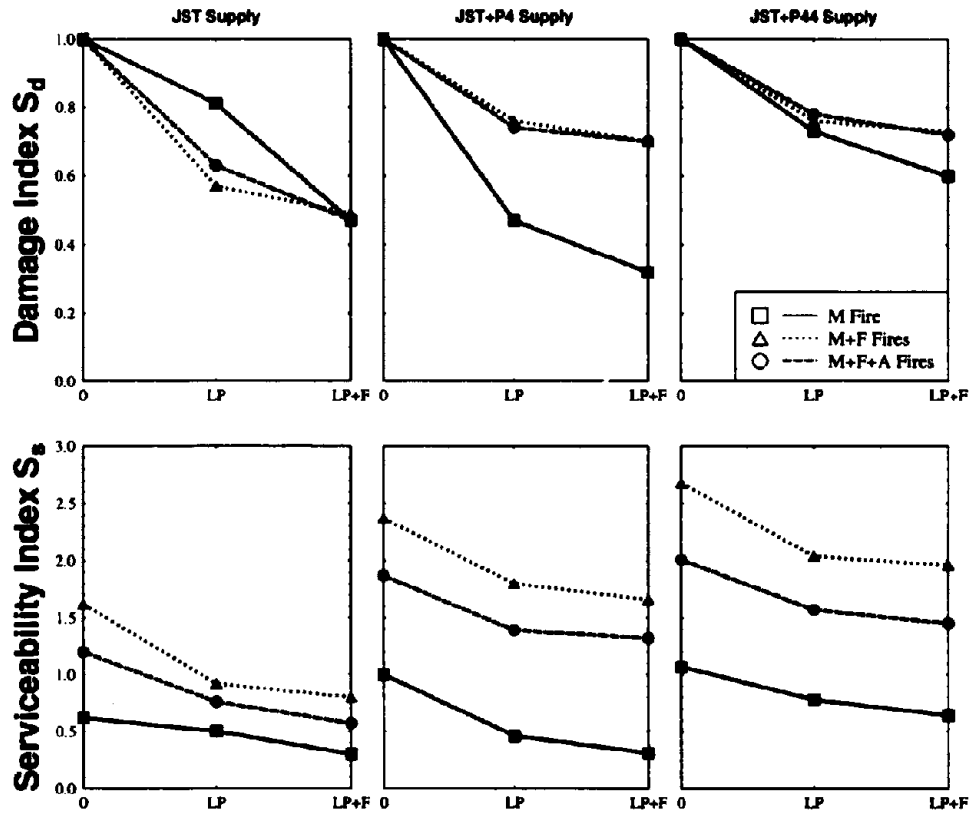


Figure 8.14: Performance indices S_d and S_s for Loma Prieta Damage (LP) and Loma Prieta and Filbert St. Damage (LP+F)

four engines each. Probability of failure of the tank and the pumps is controlled by the reliability of the pipes connecting those components to the rest of the system. For example, the failure probability of 10-ft long connection of the JST to the system is $P_p = 0.05$ for a mean break rate $\lambda = 0.01 \text{ break/km}$. This probability can be obtained by changing a seismic amplification factor to $v_p = 1682$ for the connection pipe. Stochastic analyses were performed for the λ in the range (0.01, 0.09). The range corresponds to earthquake Modified Mercalli Intensities of 6-7.

The demand scenario consists of the Marina, the Folsom, and the Alabama fires. One to four hydrants were opened for each fire to satisfy the water demand. The hydrants at each

fire site are open with a specified probability, called probability of fire ignition, because the precise location of the fire at site is uncertain. A lognormal distribution with mean 5000 gal/min and standard deviation 2500 gal/min is used to describe the water demand at each open hydrant. In the sensitivity study, the probability of a fire ignition is varied from 0.1 to 0.9.

The damage state of the AWSS includes the breaks observed during the Loma Prieta earthquake, the breaks of the 10 pipes connecting the infirm areas to the rest of the system, and the break at Filbert St. as shown in Figure 8.1. These breaks occur with specified probabilities chosen in the range (0.1, 0.9). The study is expected to provide information on the sensitivity of the system serviceability to the breaks that are likely to occur or can lead to no supply in the infirm areas. The Loma Prieta damage and damage at Filbert St have been observed in the field.

Monte-Carlo simulation method explained in Section 5 was used to determine the serviceability of the AWSS. The earthquake intensity range was discretized with eight intervals. For each interval five analyses were performed corresponding to randomly generated damage states, fire scenarios, and supply scenarios. As a result, the damage and serviceability indices are obtained. Fragility curves are developed based on statistics of these indices.

Figures 8.15 and 8.16 show the fragility curves for damage index S_d and the serviceability index S_s , respectively. The curves are obtained as third degree polynomial fitted to the available 45 points. The figures also show the 95% confidence interval. Deviation from the mean value is larger for the fragility curve based on serviceability index S_s . In this case, the confidence interval is smaller and the corresponding coefficient of determination is $R^2 = 15.67\%$. This is the result of the additional uncertainty in the required water demand on which the serviceability index is developed.

The analysis can also be used to identify critical components of the AWSS. For example, the damage state corresponding to the low serviceability indices in Figure 8.15 include consistently breaks at Filbert St., break of the pipe supplying infirm area No.1 and Loma Prieta damage state. This damage state can result in significant water shortage in the Lower Zone of the AWSS. Figure 8.17 shows the only pipes left full of water in the case of such a scenario. There was no available water supply to fight the Folsom and the Alabama fires.

The stochastic analyses captured the critical components of the AWSS for assumed scenarios which were only indicated by deterministic analysis.

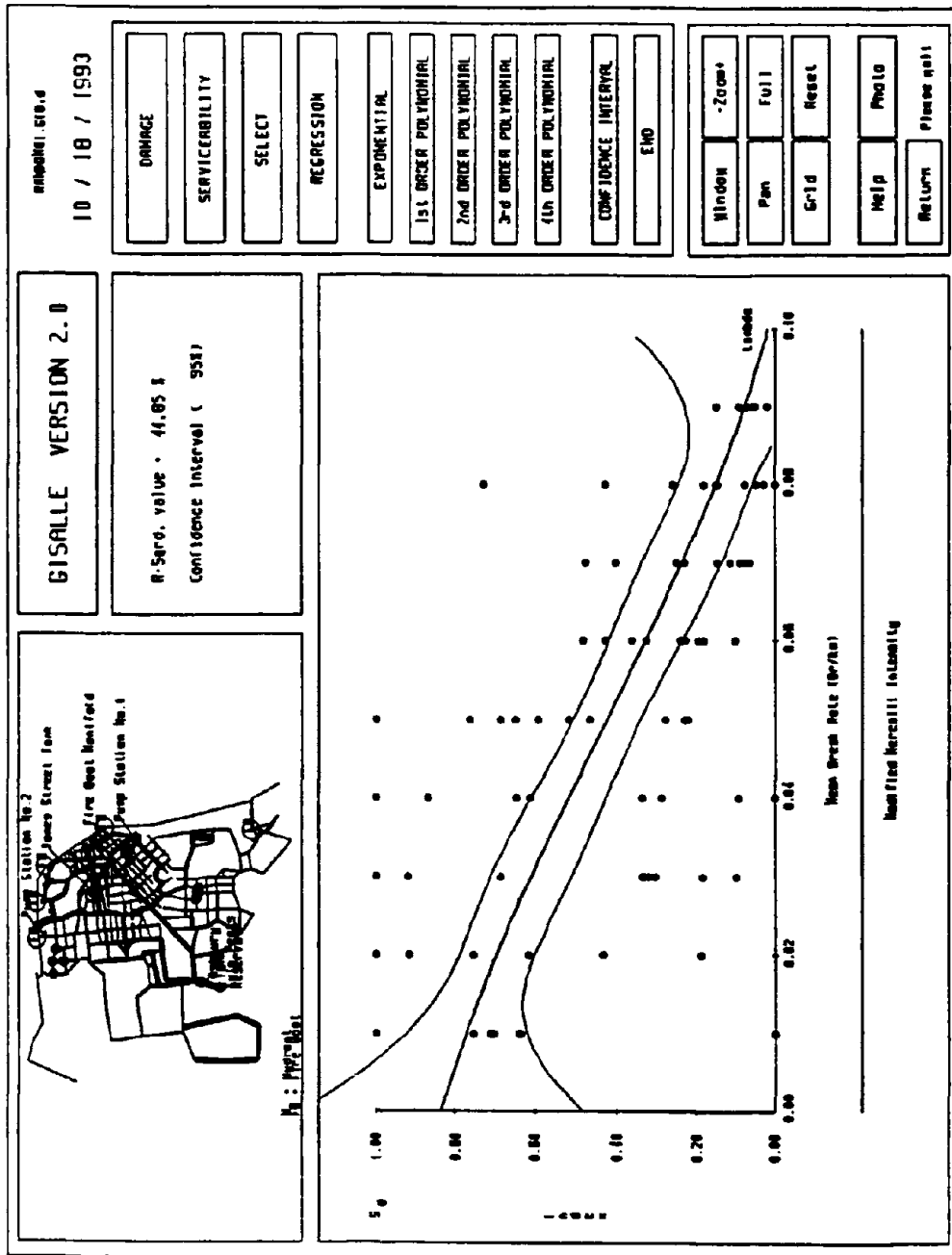


Figure 8.15: Fragility Curve for the Damage Indices

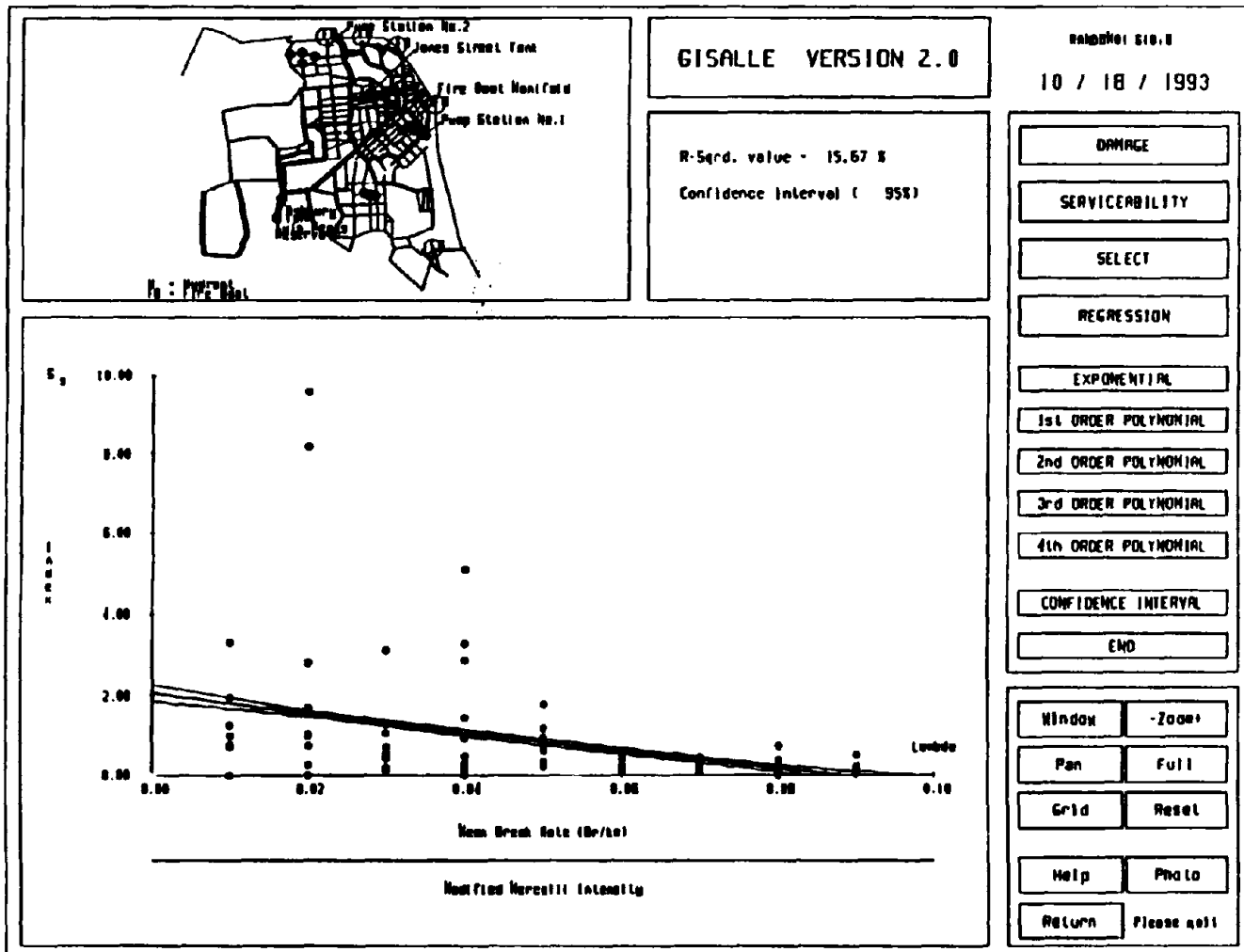


Figure 8.16: Fragility Curve for the Serviceability Indices

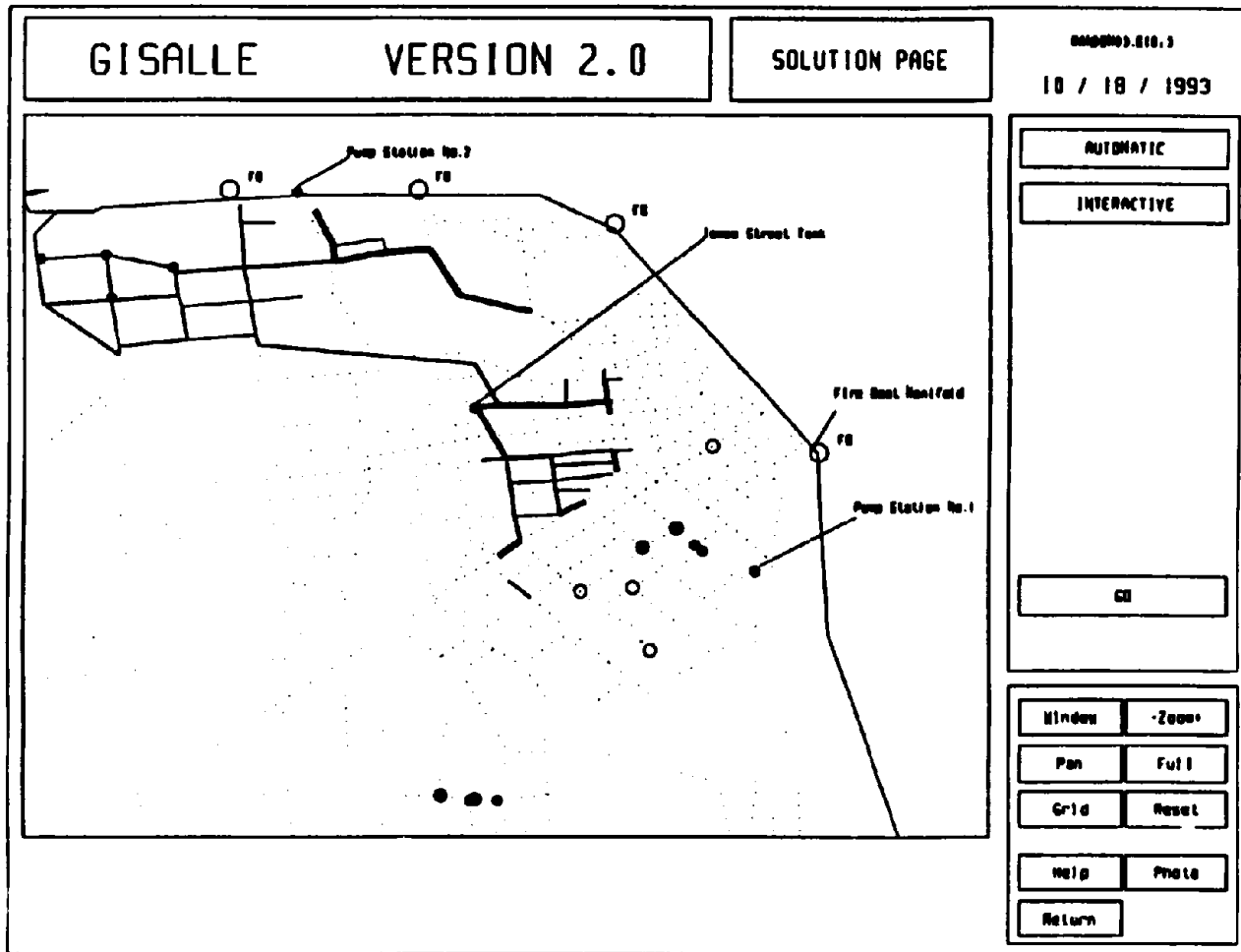


Figure 8.17: Flow Path in the AWSS with Damage at Filbert St. and Infirm Area 1

8.5 Summary

Sensitivity studies were designed to evaluate the performance of the AWSS for potential supply, fire and damage scenarios. Both deterministic and stochastic analyses were performed. The results indicate existence of critical components in the AWSS which protection is crucial for the successful performance of the system under assumed scenarios. For explored scenarios the critical components are pump No.1 and damage in infirm area No.1. The analyses also showed how deterministic analysis can be cumbersome in evaluating performance of a system. Because of enormous number of combination the stochastic analysis is the only rational way to analyze the performance of a water supply system.

SECTION 9

SUMMARY AND RECOMMENDATIONS

This report presents a new method developed to evaluate the seismic serviceability of water delivery systems. The method is general and can estimate the seismic serviceability of any water supply system regardless of its damage condition and water supply-demand scenario. Based on this new method a computer code GISALLE is developed. The code has six major modules that allow the user to (1) define and modify the system, (2) generate fire scenarios and damage states consistent with the site seismicity, (3) perform hydraulic analyses, analyze results, and calculate serviceability measures, (4) develop fragility curves and other indicators of seismic performance, and (5) provide a confidence level of the estimated seismic serviceability.

The new method is based on the Monte-Carlo simulation method and an algorithm for the hydraulic analyses of damaged water supply systems. The analysis can account for the regions with negative pressures or partial flow conditions commonly present in heavily damaged networks. The regions with negative pressures are eliminated from the system because water pipes are not air tight and cannot sustain suction. The partial flow analysis is accommodated in an approximate fashion.

The new method was validated by analytical studies as well as by field data obtained from fire flow tests performed by the San Francisco Fire Department and data obtained from the Loma Prieta earthquake. Predictions of GISALLE are consistent with the analytical studies and field data in both case studies. These results suggest that the new method is useful for assessing the seismic serviceability of a water supply system. Moreover, the method can be used to improve the seismic performance and optimize the emergency response of water supply systems.

The GISALLE code was used to perform sensitivity studies on the AWSS. Various supply, fire and damage scenarios were explored to assess the serviceability of the system after earthquake. The studies provide a better understanding of the performance of AWSS. The studies also demonstrate that the operation of pump stations in addition to the JST can be crucial for supplying an adequate flow for Marina, Folsom and Alabama fires. The seismic serviceability of AWSS can be particularly sensitive to pipe breaks in infirm area 1. Seismic protection of major pipes in this area can be crucial to assure a satisfactory performance of the AWSS.

SECTION 10

REFERENCES

- [1] Boulos, P.F. and D.J. Wood, "Explicit Calculation of Pipe-Network Parameters," *Journal of Hydraulic Engineering*, Vol.116, No.11, November 1990.
- [2] Carter, M.S., "Age Effect in Friction Factors for Coated Cast-Iron Pipes," Unpublished thesis of the Civil Engineering Department of the Massachusetts Institute of Technology, May 1936.
- [3] Chadwick, A. and J. Morfett, *Hydraulics in Civil Engineering*, Allen and Unwin, London, 1986.
- [4] Cheremisinoff, N.P., *Fluid Flow Pumps, Pipes and Channels*, Ann Arbor Science, 1981.
- [5] Colebrook, C.F. and C.M. White, "The Reduction of Carrying Capacity of the Pipes with Age," *Journal of the Institute of Civil Engineers*, Vol.10, No. 5137, 1937-1938.
- [6] Committee on Seismic Analysis of the ASCE Structural Division Committee on Nuclear Structures and Materials, *Seismic Response of Buried Pipes and Structural Components*, ASCE, 1983.
- [7] Davis, C.V., *Handbook of Applied Hydraulics*, McGraw-Hill Book Company, Inc., New York, 1942.
- [8] Dobry R., "Some Basic Aspects of Soil Liquefaction During Earthquakes," *Proceedings, Symposium on Seismic Hazards, Ground Motions, Soil-Liquefaction and engineering practice in Eastern North America*, October 20-22, 1987.
- [9] Francis, J.R.D. and P. Minton, *Civil Engineering Hydraulics*, Edward Arnold, 1984.
- [10] Genod, J.V., *Fundamentals of Pipeline Engineering*, Institut Francais du Petrole publications, Golf Publishing Company, 1984.
- [11] Goodling E., "Flexibility Analysis of Buried Pipe," *ASME/CSME Pressure Vessels and Piping Conference*, Montreal, June 25-30, 1978.
- [12] Grigoriu, M.D., T.D. O'Rourke, and M. M. Khater, "Serviceability of the San Francisco Auxiliary Water Supply System," *Proceedings, International Conference on Structural Safety and Reliability*, San Francisco, CA, Aug. 1989.
- [13] Hydraulic Institute, "Pipe Friction," *Tentative Standards of Hydraulic Institute*, Hydraulic Institute, 1948.
- [14] Hamada M., "Damage to Buried Pipes and Foundation Piles Due to Liquefaction-Induced Ground Displacement," *Earthquake Behavior of Buried Pipelines, Storage, Telecommunication, and Transportation Facilities*, *The 1989 ASME Pressure Vessels and Piping Conference*, Honolulu, Hawaii, July 23-27, 1989.

- [15] Holtz R. and W.Kovacs, *Geotechnical Engineering*, Prentice-Hall, Inc., New Jersey, 1981.
- [16] Hooper, W.B., "Calculate Head Loss Caused by Change in Pipe Size," *Chemical Engineering*, November 7, 1988.
- [17] Isenberg J., et al., "Pipeline Response to Loma Prieta Earthquake," *Journal of Structural Engineering*, Vol.117, No.7, July, 1991.
- [18] Kaizu N. "Seismic Response of Shaft for Underground Transmission Line," *Proceedings, Third Japan-U.S. Workshop on Earthquake Resistant Design of Lifeline Facilities and Countermeasures for Soil Liquefaction*, Technical Report NCEER-91-0001, Edit by T.D.O'Rourke and M.Hamada, February 1, 1991.
- [19] Kamand, F.Z., "Hydraulic Friction Factors for Pipe Flow," *Journal of Irrigation and Drainage Engineering*, Vol.114, No.2, May 1988, pp.311-323.
- [20] Kameda H. et al., "Seismic Risk and Performance of Water Lifelines," *Proceedings, Probabilistic Methods in Structural Engineering*, ASCE, Edit by Shinozuka M. and T.James, 1981
- [21] Khater, M.M., M.D. Grigoriu and T.D. O'Rourke, "Serviceability Measures and Sensitivity Factors for Estimating Seismic Performance of Water Supply Systems," *Proceedings, 9th World Conference on Earthquake Engineering*, Tokyo, Japan, Vol.VII, 1989, pp.123-128.
- [22] Khater, M.M., and M.D. Grigoriu, "Graphical Demonstration of Serviceability Analysis," *Proceedings, International Conference on Structural Safety and Reliability*, San Francisco, CA, Aug. 1989, pp.525-532.
- [23] Lea, F.C., *Hydraulics for Engineers and Engineering Students*, Longmans, Green and CO., 1930.
- [24] Lewis, F.M., "Friction Factors for Pipe Flow," *Transaction of the ASME*, Vol.66, November 1944.
- [25] Lin K. and Y.Yong, "Multiply Supported Pipeline Under Seismic Wave Excitations," *Journal of Engineering Mechanics*, ASCE, Vol. 116, No. 5, May, 1990.
- [26] Linsley, R.K. and J.B.Franzini, *Water-Resources Engineering*, McGraw-Hill Book Company, New York, 1964.
- [27] Markov J.I., M.D. Grigoriu, T.D.O'Rourke, "Seismic Serviceability of Water Supply Systems" *Proceeding, The 4th US-Japan Workshop on Earthquake Resistant Design of Lifeline Facilities and Countermeasures for Soil Liquefaction*, Honolulu, Hawaii, May, 1992.
- [28] McCaffrey M. and T.O'Rourke, "Surface Faulting and its Effect on Buried Pipelines," *NSF Report CME 8022427*, November, 1983.

- [29] Mills, H.F., *Flow of Water in Pipes*, Memories of the American Academy of Arts and Sciences, Vol.15, No.2, November 10, 1924.
- [30] Miyajima M. et al., "Study on Response of Buried Pipelines Subjected to Liquefaction-Induced Permanent Ground Displacement," *Structural Eng/Earthquake Eng.*, Vol. 6, No. 1, April 1989.
- [31] Morris, M.H. and J.M. Wiggert, *Applied Hydraulics an Engineering*, The Ronald Press Company, New York, 1963.
- [32] Roth A.R., "Liquefaction Susceptibility Mapping for San Francisco, California", *Bulletin of the Association of Engineering Geologists* Vol.XXI, N0.4, 1984.
- [33] O'Rourke T., "Risk Assessment for Pipelines Subject to Earthquake Movements," Us-Taiwan-Japan Seminar/Workshop, Taiwan, 25-27 Nov. 1985.
- [34] O'Rourke et al., "Seismic Response of Buried Pipelines," ASCE, *The Pressure Vessel and Piping Technology, A Decade of Progress*, 1985.
- [35] O'Rourke, D.T., T.E. Gowdy, H.E. Stewart, and J.W. Pease, "Lifeline and Geotechnical Aspects of the 1989 Loma Prieta Earthquake," *Proceedings*, 2nd International Conference on Recent Advances in Geotechnical Earthquake Engineering and Soil Dynamics, St.Louis, MO, Vol. II, March 1991, pp.1601-1612.
- [36] O'Rourke T. and P.Lane, "Liquefaction Hazards and Their Effects on Buried Pipelines," *Technical Report*, NCEER-89-0007, February, 1989.
- [37] O'Rourke D.T., M.M. Khater, and M.D. Grigoriu "Earthquake Performance on the San Francisco Water Supply," *Technical Report*, NCEER, 1985.
- [38] O'Rourke M. and C.Nordberg, "Analysis Procedures for Buried Pipelines Subject to Longitudinal and Transverse Permanent Ground Deformation," *Proceedings*, Third Japan-U.S. Workshop on Earthquake Resistant Design of Lifeline Facilities and Countermeasures for Soil Liquefaction," Technical Report NCEER-91-0001, Edit by T.D.O'Rourke and M.Hamada, February 1, 1991.
- [39] O'Rourke, T.D., J.W. Pease, "Large Ground Deformation and their Effects on Lifeline Facilities: 1989 Loma Prieta Earthquake," *Technical Report NCEER-92-0002*, National Center for Earthquake Engineering Research, Buffalo, NY, 1992.
- [40] O'Rourke, T.D., H.E. Stewart, F.T. Blackburn, and T.S. Dickerman, "Geotechnical and Lifeline Aspects of the October 17, 1989 Loma Prieta Earthquake in San Francisco," *Technical Report NCEER-90-001*, National Center for Earthquake Engineering Research, Buffalo, NY, Jan. 1990.
- [41] O'Rourke, T.D., H.E. Stewart, B.L. Roth, and C.H. Trautmann, "Reconnaissance Report on Geotechnical Aspects of the October 17, 1989 Loma Prieta Earthquake in San Francisco" *Report*, School of Civil and Environmental Engineering, Cornell University, Ithaca, NY, Dec. 1989.

- [42] O'Rourke T. and M.Tawfik, "Large Ground Movement Effects On High Pressure Pipelines," Cornell University, *Geotechnical Engineering Report 87-1*.
- [43] Pikul R., "Buried Pipelines Analysis/Design for Earthquakes," *PhD. Thesis*, Rensseler Polytechnic Institute, 1979.
- [44] Radford, M.D., "A Comprehensive List of Pipe Coefficients of Friction for the Hazen-Williams and Manning Formulae Derived from the Darcy-Weisbach Formula and Colebrook-White Transition Law for Roughness Values (k)," *Water SA*, Vol.16, No.4, October 1990, pp.237-256.
- [45] Report of Committee on Pipe Line Friction Coefficients, *Journal of the New England Water Association*, Vol.49, No.3, September 1935, pp.235-341.
- [46] Richter, H. *Rohrhydraulik, Ein Handbuch zur Praktischen Stromungsberechnung*, Springer-Verlag, Berlin, 1958.
- [47] Russell, G.E., *Hydraulics*, Henry Holt and Company, New York, 1934.
- [48] Russell, G.E., *Text-Book on Hydraulics*, Henry Holt and Company, New York, 1934.
- [49] Scawthorn, C., "Fire Following Earthquake," *Report*, Dames and Moore, March 1987.
- [50] Scawthorn, C. and T.D. O'Rourke, "Effects of Ground Failure on Water supply and Fire Following Earthquake: The 1906 San Francisco Earthquake," *Technical Report NCEER-89-0032*, National Center for Earthquake Engineering Research, Buffalo, NY, Dec. 1989, pp.16-35.
- [51] Scawthorn, C. and F.T. Blackburn, "Performance of the San Francisco Auxiliary and Portable Water Supply System in the 17 October, 1989 Loma Prieta Earthquake," *Proceedings*, 4th U.S. Conference on Earthquake Engineering, Palm Beach, CA, May 1990, Vol.1, pp.171-180.
- [52] Shah H. and S.Chu, "Seismic Analysis of Underground Structural Elements," *Journal of the Power Division*, ASCE, Vol. 100, No. PO1, July, 1974.
- [53] Sharp, J., *Some Considerations Regarding Cast Iron and Steel Pipes*, Longmans, Green and CO., 1914.
- [54] Shinozuka M. and T. Koike, "Estimation of Structural Strains in Underground Lifeline Pipes," *Technical Report No.NDF-PFR-78-15049-CU-4*. Dep. of Civil Engineering and Engineering Mechanics, Columbia University, NY, 1978
- [55] Suzuki N. and N.Masuda, "Idealization of Permanent Ground Movement and Strain Estimation of Buried Pipe," *Proceedings*, Third Japan-U.S. Workshop on Earthquake Resistant Design of Lifeline Facilities and Countermeasures for Soil Liquefaction," Technical Report NCEER-91-0001, Edit by T.D.O'Rourke and M.Hamada, February 1, 1991.

- [56] Takada S., et al. "Earthquake Response Simulations of T-Shaped Portion in Ductile-Iron Pipelines and Development of Earthquake Resistant Hot Branch Sleeve," Earthquake Behavior and Safety of Oil and Gas Storage Facilities, Buried Pipelines and Equipment, *1989 International Symposium on Lifeline Earthquake Engineering*, Portland, Oregon, June 19-24, 1983.
- [57] Technical Council on Lifeline Earthquake Engineering, *Guidelines for the Seismic Design of Oil and Gas Pipeline Systems* ASCE, 1984
- [58] The American Society of Mechanical Engineers, Transaction of the Hydraulic Institute of the Munich Technical University, *Bulletin 3*, 1935.
- [59] The Cast Iron Pipe Research Association, *Handbook of Cast Iron Pipe*, The Cast Iron Pipe Research Association, Chicago, 1927.
- [60] The Institution of Mechanical Engineers, *Pipe Joints-A State of the Art Review*, 1986.
- [61] Tsang, L. and L.Y. Kee, "Friction Head Losses in Pipe," *Plumbing Engineer*, Vol.15, No.3, April 1987.
- [62] Trautmann, H.C., et al., "System Model for Water Supply Following Earthquakes," *Proceedings, Lifeline Seismic Risk Analysis - Case Studies*, Seattle, WA, April 9, 1986.
- [63] Wood, D.J., "Computer Analysis of Flow in Pipe Networks Including Extended Period Simulation," *Users Manual*, Univ. of Kentucky, 1980.

**NATIONAL CENTER FOR EARTHQUAKE ENGINEERING RESEARCH
LIST OF TECHNICAL REPORTS**

The National Center for Earthquake Engineering Research (NCEER) publishes technical reports on a variety of subjects related to earthquake engineering written by authors funded through NCEER. These reports are available from both NCEER's Publications Department and the National Technical Information Service (NTIS). Requests for reports should be directed to the Publications Department, National Center for Earthquake Engineering Research, State University of New York at Buffalo, Red Jacket Quadrangle, Buffalo, New York 14261. Reports can also be requested through NTIS, 5285 Port Royal Road, Springfield, Virginia 22161. NTIS accession numbers are shown in parenthesis, if available.

- NCEER-87-0001 "First-Year Program in Research, Education and Technology Transfer," 3/5/87, (PB88-134275).
- NCEER-87-0002 "Experimental Evaluation of Instantaneous Optimal Algorithms for Structural Control," by R.C. Lin, T.T. Soong and A.M. Reinhorn, 4/20/87, (PB88-134341).
- NCEER-87-0003 "Experimentation Using the Earthquake Simulation Facilities at University at Buffalo," by A.M. Reinhorn and R.L. Ketter, to be published.
- NCEER-87-0004 "The System Characteristics and Performance of a Shaking Table," by J.S. Hwang, K.C. Chang and G.C. Lee, 6/1/87, (PB88-134259). This report is available only through NTIS (see address given above).
- NCEER-87-0005 "A Finite Element Formulation for Nonlinear Viscoplastic Material Using a Q Model," by O. Gyebe and G. Dasgupta, 11/2/87, (PB88-213764).
- NCEER-87-0006 "Symbolic Manipulation Program (SMP) - Algebraic Codes for Two and Three Dimensional Finite Element Formulations," by X. Lee and G. Dasgupta, 11/9/87, (PB88-218522).
- NCEER-87-0007 "Instantaneous Optimal Control Laws for Tall Buildings Under Seismic Excitations," by J.N. Yang, A. Akbarpour and P. Ghaemmaghami, 6/10/87, (PB88-134333). This report is only available through NTIS (see address given above).
- NCEER-87-0008 "IDARC: Inelastic Damage Analysis of Reinforced Concrete Frame - Shear-Wall Structures," by Y.J. Park, A.M. Reinhorn and S.K. Kunnath, 7/20/87, (PB88-134325).
- NCEER-87-0009 "Liquefaction Potential for New York State: A Preliminary Report on Sites in Manhattan and Buffalo," by M. Budhu, V. Vijayakumar, R.F. Giese and L. Baumgras, 8/31/87, (PB88-163704). This report is available only through NTIS (see address given above).
- NCEER-87-0010 "Vertical and Torsional Vibration of Foundations in Inhomogeneous Media," by A.S. Veletsos and K.W. Dotson, 6/1/87, (PB88-134291).
- NCEER-87-0011 "Seismic Probabilistic Risk Assessment and Seismic Margins Studies for Nuclear Power Plants," by Howard H.M. Hwang, 6/15/87, (PB88-134267).
- NCEER-87-0012 "Parametric Studies of Frequency Response of Secondary Systems Under Ground-Acceleration Excitations," by Y. Yong and Y.K. Lin, 5/10/87, (PB88-134309).
- NCEER-87-0013 "Frequency Response of Secondary Systems Under Seismic Excitation," by J.A. HoLung, J. Cai and Y.K. Lin, 7/31/87, (PB88-134317).
- NCEER-87-0014 "Modelling Earthquake Ground Motions in Seismically Active Regions Using Parametric Time Series Methods," by G.W. Ellis and A.S. Cakmak, 8/25/87, (PB88-134283).
- NCEER-87-0015 "Detection and Assessment of Seismic Structural Damage," by E. DiPasquale and A.S. Cakmak, 8/25/87, (PB88-163712).

- NCEER-87-0016 "Pipeline Experiment at Parkfield, California," by J. Isenberg and E. Richardson, 9/15/87, (PB88-163720). This report is available only through NTIS (see address given above).
- NCEER-87-0017 "Digital Simulation of Seismic Ground Motion," by M. Shinozuka, G. Deodatis and T. Harada, 8/31/87, (PB88-155197). This report is available only through NTIS (see address given above).
- NCEER-87-0018 "Practical Considerations for Structural Control: System Uncertainty, System Time Delay and Truncation of Small Control Forces," J.N. Yang and A. Akbarpour, 8/10/87, (PB88-163738).
- NCEER-87-0019 "Modal Analysis of Nonclassically Damped Structural Systems Using Canonical Transformation," by J.N. Yang, S. Sarkani and F.X. Long, 9/27/87, (PB88-187851).
- NCEER-87-0020 "A Nonstationary Solution in Random Vibration Theory," by J.R. Red-Horse and P.D. Spanos, 11/3/87, (PB88-163746).
- NCEER-87-0021 "Horizontal Impedances for Radially Inhomogeneous Viscoelastic Soil Layers," by A.S. Veletsos and K.W. Dotson, 10/15/87, (PB88-150859).
- NCEER-87-0022 "Seismic Damage Assessment of Reinforced Concrete Members," by Y.S. Chung, C. Meyer and M. Shinozuka, 10/9/87, (PB88-150867). This report is available only through NTIS (see address given above).
- NCEER-87-0023 "Active Structural Control in Civil Engineering," by T.T. Soong, 11/11/87, (PB88-187778).
- NCEER-87-0024 "Vertical and Torsional Impedances for Radially Inhomogeneous Viscoelastic Soil Layers," by K.W. Dotson and A.S. Veletsos, 12/87, (PB88-187786).
- NCEER-87-0025 "Proceedings from the Symposium on Seismic Hazards, Ground Motions, Soil-Liquefaction and Engineering Practice in Eastern North America," October 20-22, 1987, edited by K.H. Jacob, 12/87, (PB88-188115).
- NCEER-87-0026 "Report on the Whittier-Narrows, California, Earthquake of October 1, 1987," by J. Pantelic and A. Reinhorn, 11/87, (PB88-187752). This report is available only through NTIS (see address given above).
- NCEER-87-0027 "Design of a Modular Program for Transient Nonlinear Analysis of Large 3-D Building Structures," by S. Srivastav and J.F. Abel, 12/30/87, (PB88-187950).
- NCEER-87-0028 "Second-Year Program in Research, Education and Technology Transfer," 3/8/88, (PB88-219480).
- NCEER-88-0001 "Workshop on Seismic Computer Analysis and Design of Buildings With Interactive Graphics," by W. McGuire, J.F. Abel and C.H. Conley, 1/18/88, (PB88-187760).
- NCEER-88-0002 "Optimal Control of Nonlinear Flexible Structures," by J.N. Yang, F.X. Long and D. Wong, 1/22/88, (PB88-213772).
- NCEER-88-0003 "Substructuring Techniques in the Time Domain for Primary-Secondary Structural Systems," by G.D. Manolis and G. Juhn, 2/10/88, (PB88-213780).
- NCEER-88-0004 "Iterative Seismic Analysis of Primary-Secondary Systems," by A. Singhal, L.D. Lutes and P.D. Spanos, 2/23/88, (PB88-213798).
- NCEER-88-0005 "Stochastic Finite Element Expansion for Random Media," by P.D. Spanos and R. Ghanem, 3/14/88, (PB88-213806).

- NCEER-88-0006 "Combining Structural Optimization and Structural Control," by F.Y. Cheng and C.P. Pantelides, 1/10/88, (PB88-213814).
- NCEER-88-0007 "Seismic Performance Assessment of Code-Designed Structures," by H.H-M. Hwang, J-W. Jaw and H-J. Shau, 3/20/88, (PB88-219423).
- NCEER-88-0008 "Reliability Analysis of Code-Designed Structures Under Natural Hazards," by H.H-M. Hwang, H. Ushiba and M. Shinozuka, 2/29/88, (PB88-229471).
- NCEER-88-0009 "Seismic Fragility Analysis of Shear Wall Structures," by J-W Jaw and H.H-M. Hwang, 4/30/88, (PB89-102867).
- NCEER-88-0010 "Base Isolation of a Multi-Story Building Under a Harmonic Ground Motion - A Comparison of Performances of Various Systems," by F-G Fan, G. Ahmadi and I.G. Tadjbakhsh, 5/18/88, (PB89-122238).
- NCEER-88-0011 "Seismic Floor Response Spectra for a Combined System by Green's Functions," by F.M. Lavelle, L.A. Bergman and P.D. Spanos, 5/1/88, (PB89-102875).
- NCEER-88-0012 "A New Solution Technique for Randomly Excited Hysteretic Structures," by G.Q. Cai and Y.K. Lin, 5/16/88, (PB89-102883).
- NCEER-88-0013 "A Study of Radiation Damping and Soil-Structure Interaction Effects in the Centrifuge," by K. Weissman, supervised by J.H. Prevost, 5/24/88, (PB89-144703).
- NCEER-88-0014 "Parameter Identification and Implementation of a Kinematic Plasticity Model for Frictional Soils," by J.H. Prevost and D.V. Griffiths, to be published.
- NCEER-88-0015 "Two- and Three- Dimensional Dynamic Finite Element Analyses of the Long Valley Dam," by D.V. Griffiths and J.H. Prevost, 6/17/88, (PB89-144711).
- NCEER-88-0016 "Damage Assessment of Reinforced Concrete Structures in Eastern United States," by A.M. Reinhorn, M.J. Seidel, S.K. Kunnath and Y.J. Park, 6/15/88, (PB89-122220).
- NCEER-88-0017 "Dynamic Compliance of Vertically Loaded Strip Foundations in Multilayered Viscoelastic Soils," by S. Ahmad and A.S.M. Israil, 6/17/88, (PB89-102891).
- NCEER-88-0018 "An Experimental Study of Seismic Structural Response With Added Viscoelastic Dampers," by R.C. Lin, Z. Liang, T.T. Soong and R.H. Zhang, 6/30/88, (PB89-122212). This report is available only through NTIS (see address given above).
- NCEER-88-0019 "Experimental Investigation of Primary - Secondary System Interaction," by G.D. Manolis, G. Juhn and A.M. Reinhorn, 5/27/88, (PB89-122204).
- NCEER-88-0020 "A Response Spectrum Approach For Analysis of Nonclassically Damped Structures," by J.N. Yang, S. Sarkani and F.X. Long, 4/22/88, (PB89-102909).
- NCEER-88-0021 "Seismic Interaction of Structures and Soils: Stochastic Approach," by A.S. Veletsos and A.M. Prasad, 7/21/88, (PB89-122196).
- NCEER-88-0022 "Identification of the Serviceability Limit State and Detection of Seismic Structural Damage," by E. DiPasquale and A.S. Cakmak, 6/15/88, (PB89-122188). This report is available only through NTIS (see address given above).
- NCEER-88-0023 "Multi-Hazard Risk Analysis: Case of a Simple Offshore Structure," by B.K. Bhartia and E.H. Vanmarcke, 7/21/88, (PB89-145213).

- NCEER-88-0024 "Automated Seismic Design of Reinforced Concrete Buildings," by Y.S. Chung, C. Meyer and M. Shinozuka, 7/5/88, (PB89-122170). This report is available only through NTIS (see address given above).
- NCEER-88-0025 "Experimental Study of Active Control of MDOF Structures Under Seismic Excitations," by L.L. Chung, R.C. Lin, T.T. Soong and A.M. Reinhorn, 7/10/88, (PB89-122600).
- NCEER-88-0026 "Earthquake Simulation Tests of a Low-Rise Metal Structure," by J.S. Hwang, K.C. Chang, G.C. Lee and R.L. Ketter, 8/1/88, (PB89-102917).
- NCEER-88-0027 "Systems Study of Urban Response and Reconstruction Due to Catastrophic Earthquakes," by F. Kozin and H.K. Zhou, 9/22/88, (PB90-162348).
- NCEER-88-0028 "Seismic Fragility Analysis of Plane Frame Structures," by H.H-M. Hwang and Y.K. Low, 7/31/88, (PB89-131445).
- NCEER-88-0029 "Response Analysis of Stochastic Structures," by A. Kardara, C. Bucher and M. Shinozuka, 9/22/88, (PB89-174429).
- NCEER-88-0030 "Nonnormal Accelerations Due to Yielding in a Primary Structure," by D.C.K. Chen and L.D. Lutes, 9/19/88, (PB89-131437).
- NCEER-88-0031 "Design Approaches for Soil-Structure Interaction," by A.S. Veletsos, A.M. Prasad and Y. Tang, 12/30/88, (PB89-174437). This report is available only through NTIS (see address given above).
- NCEER-88-0032 "A Re-evaluation of Design Spectra for Seismic Damage Control," by C.J. Turkstra and A.G. Tallin, 11/7/88, (PB89-145221).
- NCEER-88-0033 "The Behavior and Design of Noncontact Lap Splices Subjected to Repeated Inelastic Tensile Loading," by V.E. Sagan, P. Gergely and R.N. White, 12/8/88, (PB89-163737).
- NCEER-88-0034 "Seismic Response of Pile Foundations," by S.M. Mamoon, P.K. Banerjee and S. Ahmad, 11/1/88, (PB89-145239).
- NCEER-88-0035 "Modeling of R/C Building Structures With Flexible Floor Diaphragms (IDARC2)," by A.M. Reinhorn, S.K. Kunnath and N. Panahshahi, 9/7/88, (PB89-207153).
- NCEER-88-0036 "Solution of the Dam-Reservoir Interaction Problem Using a Combination of FEM, BEM with Particular Integrals, Modal Analysis, and Substructuring," by C-S. Tsai, G.C. Lee and R.L. Ketter, 12/31/88, (PB89-207146).
- NCEER-88-0037 "Optimal Placement of Actuators for Structural Control," by F.Y. Cheng and C.P. Pantelides, 8/15/88, (PB89-162846).
- NCEER-88-0038 "Teflon Bearings in Aseismic Base Isolation: Experimental Studies and Mathematical Modeling," by A. Mokha, M.C. Constantinou and A.M. Reinhorn, 12/5/88, (PB89-218457). This report is available only through NTIS (see address given above).
- NCEER-88-0039 "Seismic Behavior of Flat Slab High-Rise Buildings in the New York City Area," by P. Weidlinger and M. Ettouney, 10/15/88, (PB90-145681).
- NCEER-88-0040 "Evaluation of the Earthquake Resistance of Existing Buildings in New York City," by P. Weidlinger and M. Ettouney, 10/15/88, to be published.
- NCEER-88-0041 "Small-Scale Modeling Techniques for Reinforced Concrete Structures Subjected to Seismic Loads," by W. Kim, A. El-Attar and R.N. White, 11/22/88, (PB89-189625).

- NCEER-88-0042 "Modeling Strong Ground Motion from Multiple Event Earthquakes," by G.W. Ellis and A.S. Cakmak, 10/15/88, (PB89-174445).
- NCEER-88-0043 "Nonstationary Models of Seismic Ground Acceleration," by M. Grigoriu, S.E. Ruiz and E. Rosenblueth, 7/15/88, (PB89-189617).
- NCEER-88-0044 "SARCF User's Guide: Seismic Analysis of Reinforced Concrete Frames," by Y.S. Chung, C. Meyer and M. Shinozuka, 11/9/88, (PB89-174452).
- NCEER-88-0045 "First Expert Panel Meeting on Disaster Research and Planning," edited by J. Pantelic and J. Stoyke, 9/15/88, (PB89-174460).
- NCEER-88-0046 "Preliminary Studies of the Effect of Degrading Infill Walls on the Nonlinear Seismic Response of Steel Frames," by C.Z. Chrysostomou, P. Gergely and J.F. Abel, 12/19/88, (PB89-208383).
- NCEER-88-0047 "Reinforced Concrete Frame Component Testing Facility - Design, Construction, Instrumentation and Operation," by S.P. Pessiki, C. Conley, T. Bond, P. Gergely and R.N. White, 12/16/88, (PB89-174478).
- NCEER-89-0001 "Effects of Protective Cushion and Soil Compliancy on the Response of Equipment Within a Seismically Excited Building," by J.A. HoLung, 2/16/89, (PB89-207179).
- NCEER-89-0002 "Statistical Evaluation of Response Modification Factors for Reinforced Concrete Structures," by H.H-M. Hwang and J-W. Jaw, 2/17/89, (PB89-207187).
- NCEER-89-0003 "Hysteretic Columns Under Random Excitation," by G-Q. Cai and Y.K. Lin, 1/9/89, (PB89-196513).
- NCEER-89-0004 "Experimental Study of 'Elephant Foot Bulge' Instability of Thin-Walled Metal Tanks," by Z-H. Jia and R.L. Ketter, 2/22/89, (PB89-207195).
- NCEER-89-0005 "Experiment on Performance of Buried Pipelines Across San Andreas Fault," by J. Isenberg, E. Richardson and T.D. O'Rourke, 3/10/89, (PB89-218440). This report is available only through NTIS (see address given above).
- NCEER-89-0006 "A Knowledge-Based Approach to Structural Design of Earthquake-Resistant Buildings," by M. Subramani, P. Gergely, C.H. Conley, J.F. Abel and A.H. Zaghaw, 1/15/89, (PB89-218465).
- NCEER-89-0007 "Liquefaction Hazards and Their Effects on Buried Pipelines," by T.D. O'Rourke and P.A. Lane, 2/1/89, (PB89-218481).
- NCEER-89-0008 "Fundamentals of System Identification in Structural Dynamics," by H. Imai, C-B. Yun, O. Maruyama and M. Shinozuka, 1/26/89, (PB89-207211).
- NCEER-89-0009 "Effects of the 1985 Michoacan Earthquake on Water Systems and Other Buried Lifelines in Mexico," by A.G. Ayala and M.J. O'Rourke, 3/8/89, (PB89-207229).
- NCEER-89-R010 "NCEER Bibliography of Earthquake Education Materials," by K.E.K. Ross, Second Revision. 9/1/89, (PB90-125352).
- NCEER-89-0011 "Inelastic Three-Dimensional Response Analysis of Reinforced Concrete Building Structures (IDARC-3D), Part I - Modeling," by S.K. Kunnath and A.M. Reinhorn, 4/17/89, (PB90-114612).
- NCEER-89-0012 "Recommended Modifications to ATC-14," by C.D. Poland and J.O. Malley, 4/12/89, (PB90-108648).

- NCEER-89-0013 "Repair and Strengthening of Beam-to-Column Connections Subjected to Earthquake Loading," by M. Corazao and A.J. Durrani, 2/28/89, (PB90-109885).
- NCEER-89-0014 "Program EXKAL2 for Identification of Structural Dynamic Systems," by O. Maruyama, C-B. Yun, M. Hoshiya and M. Shinozuka, 5/19/89, (PB90-109877).
- NCEER-89-0015 "Response of Frames With Bolted Semi-Rigid Connections, Part I - Experimental Study and Analytical Predictions," by P.J. DiCorso, A.M. Reinhorn, J.R. Dickerson, J.B. Radzimirski and W.L. Harper, 6/1/89, to be published.
- NCEER-89-0016 "ARMA Monte Carlo Simulation in Probabilistic Structural Analysis," by P.D. Spanos and M.P. Mignolet, 7/10/89, (PB90-109893).
- NCEER-89-P017 "Preliminary Proceedings from the Conference on Disaster Preparedness - The Place of Earthquake Education in Our Schools," Edited by K.E.K. Ross, 6/23/89, (PB90-108606).
- NCEER-89-0017 "Proceedings from the Conference on Disaster Preparedness - The Place of Earthquake Education in Our Schools," Edited by K.E.K. Ross, 12/31/89, (PB90-207895). This report is available only through NTIS (see address given above).
- NCEER-89-0018 "Multidimensional Models of Hysteretic Material Behavior for Vibration Analysis of Shape Memory Energy Absorbing Devices, by E.J. Graesser and F.A. Cozzarelli, 6/7/89, (PB90-164146).
- NCEER-89-0019 "Nonlinear Dynamic Analysis of Three-Dimensional Base Isolated Structures (3D-BASIS)," by S. Nagarajaiah, A.M. Reinhorn and M.C. Constantinou, 8/3/89, (PB90-161936). This report is available only through NTIS (see address given above).
- NCEER-89-0020 "Structural Control Considering Time-Rate of Control Forces and Control Rate Constraints," by F.Y. Cheng and C.P. Pantelides, 8/3/89, (PB90-120445).
- NCEER-89-0021 "Subsurface Conditions of Memphis and Shelby County," by K.W. Ng, T-S. Chang and H-H.M. Hwang, 7/26/89, (PB90-120437).
- NCEER-89-0022 "Seismic Wave Propagation Effects on Straight Jointed Buried Pipelines," by K. Elhadi and M.J. O'Rourke, 8/24/89. (PB90-162322).
- NCEER-89-0023 "Workshop on Serviceability Analysis of Water Delivery Systems," edited by M. Grigoriu, 3/6/89, (PB90-127424).
- NCEER-89-0024 "Shaking Table Study of a 1/5 Scale Steel Frame Composed of Tapered Members," by K.C. Chang, J.S. Hwang and G.C. Lee, 9/18/89, (PB90-160169).
- NCEER-89-0025 "DYNAID: A Computer Program for Nonlinear Seismic Site Response Analysis - Technical Documentation," by Jean H. Prevost, 9/14/89, (PB90-161944). This report is available only through NTIS (see address given above).
- NCEER-89-0026 "1:4 Scale Model Studies of Active Tendon Systems and Active Mass Dampers for Aseismic Protection," by A.M. Reinhorn, T.T. Soong, R.C. Lin, Y.P. Yang, Y. Fukao, H. Abe and M. Nakai, 9/15/89, (PB90-173246).
- NCEER-89-0027 "Scattering of Waves by Inclusions in a Nonhomogeneous Elastic Half Space Solved by Boundary Element Methods," by P.K. Hadley, A. Askar and A.S. Cakmak, 6/15/89, (PB90-145699).
- NCEER-89-0028 "Statistical Evaluation of Deflection Amplification Factors for Reinforced Concrete Structures," by H.H.M. Hwang, J-W. Jaw and A.L. Ch'ng, 8/31/89, (PB90-164633).

- NCEER-89-0029 "Bedrock Accelerations in Memphis Area Due to Large New Madrid Earthquakes," by H.H.M. Hwang, C.H.S. Chen and G. Yu, 11/7/89, (PB90-162330).
- NCEER-89-0030 "Seismic Behavior and Response Sensitivity of Secondary Structural Systems," by Y.Q. Chen and T.T. Soong, 10/23/89, (PB90-164658).
- NCEER-89-0031 "Random Vibration and Reliability Analysis of Primary-Secondary Structural Systems," by Y. Ibrahim, M. Grigoriu and T.T. Soong, 11/10/89, (PB90-161951).
- NCEER-89-0032 "Proceedings from the Second U.S. - Japan Workshop on Liquefaction, Large Ground Deformation and Their Effects on Lifelines, September 26-29, 1989," Edited by T.D. O'Rourke and M. Hamada, 12/1/89, (PB90-209388).
- NCEER-89-0033 "Deterministic Model for Seismic Damage Evaluation of Reinforced Concrete Structures," by J.M. Bracci, A.M. Reinhorn, J.B. Mander and S.K. Kunnath, 9/27/89.
- NCEER-89-0034 "On the Relation Between Local and Global Damage Indices," by E. DiPasquale and A.S. Cakmak, 8/15/89, (PB90-173865).
- NCEER-89-0035 "Cyclic Undrained Behavior of Nonplastic and Low Plasticity Silts," by A.J. Walker and H.E. Stewart, 7/26/89, (PB90-183518).
- NCEER-89-0036 "Liquefaction Potential of Surficial Deposits in the City of Buffalo, New York," by M. Budhu, R. Giese and L. Baumgrass, 1/17/89, (PB90-208455).
- NCEER-89-0037 "A Deterministic Assessment of Effects of Ground Motion Incoherence," by A.S. Veletsos and Y. Tang, 7/15/89, (PB90-164294).
- NCEER-89-0038 "Workshop on Ground Motion Parameters for Seismic Hazard Mapping," July 17-18, 1989, edited by R.V. Whitman, 12/1/89, (PB90-173923).
- NCEER-89-0039 "Seismic Effects on Elevated Transit Lines of the New York City Transit Authority," by C.J. Costantino, C.A. Miller and E. Heymsfield, 12/26/89, (PB90-207887).
- NCEER-89-0040 "Centrifugal Modeling of Dynamic Soil-Structure Interaction," by K. Weissman, Supervised by J.H. Prevost, 5/10/89, (PB90-207879).
- NCEER-89-0041 "Linearized Identification of Buildings With Cores for Seismic Vulnerability Assessment," by I-K. Ho and A.E. Aktan, 11/1/89, (PB90-251943).
- NCEER-90-0001 "Geotechnical and Lifeline Aspects of the October 17, 1989 Loma Prieta Earthquake in San Francisco," by T.D. O'Rourke, H.E. Stewart, F.T. Blackburn and T.S. Dickerman, 1/90, (PB90-208596).
- NCEER-90-0002 "Nonnormal Secondary Response Due to Yielding in a Primary Structure," by D.C.K. Chen and L.D. Lutes, 2/28/90, (PB90-251976).
- NCEER-90-0003 "Earthquake Education Materials for Grades K-12," by K.E.K. Ross, 4/16/90, (PB91-251984).
- NCEER-90-0004 "Catalog of Strong Motion Stations in Eastern North America," by R.W. Busby, 4/3/90, (PB90-251984).
- NCEER-90-0005 "NCEER Strong-Motion Data Base: A User Manual for the GeoBase Release (Version 1.0 for the Sun3)," by P. Friberg and K. Jacob, 3/31/90 (PB90-258062).
- NCEER-90-0006 "Seismic Hazard Along a Crude Oil Pipeline in the Event of an 1811-1812 Type New Madrid Earthquake," by H.H.M. Hwang and C.H.S. Chen, 4/16/90(PB90-258054).

- NCEER-90-0007 "Site-Specific Response Spectra for Memphis Sheahan Pumping Station," by H.H.M. Hwang and C.S. Lee, 5/15/90, (PB91-108811).
- NCEER-90-0008 "Pilot Study on Seismic Vulnerability of Crude Oil Transmission Systems," by T. Ariman, R. Dobry, M. Grigoriu, F. Kozin, M. O'Rourke, T. O'Rourke and M. Shinozuka, 5/25/90, (PB91-108837).
- NCEER-90-0009 "A Program to Generate Site Dependent Time Histories: EQGEN," by G.W. Ellis, M. Srinivasan and A.S. Cakmak, 1/30/90, (PB91-108829).
- NCEER-90-0010 "Active Isolation for Seismic Protection of Operating Rooms," by M.E. Talbot, Supervised by M. Shinozuka, 6/8/9, (PB91-110205).
- NCEER-90-0011 "Program LINEARID for Identification of Linear Structural Dynamic Systems," by C-B. Yun and M. Shinozuka, 6/25/90, (PB91-110312).
- NCEER-90-0012 "Two-Dimensional Two-Phase Elasto-Plastic Seismic Response of Earth Dams," by A.N. Yiagous, Supervised by J.H. Prevost, 6/20/90, (PB91-110197).
- NCEER-90-0013 "Secondary Systems in Base-Isolated Structures: Experimental Investigation, Stochastic Response and Stochastic Sensitivity," by G.D. Manolis, G. Juhn, M.C. Constantinou and A.M. Reinhorn, 7/1/90, (PB91-110320).
- NCEER-90-0014 "Seismic Behavior of Lightly-Reinforced Concrete Column and Beam-Column Joint Details," by S.P. Pessiki, C.H. Conley, P. Gergely and R.N. White, 8/22/90, (PB91-108795).
- NCEER-90-0015 "Two Hybrid Control Systems for Building Structures Under Strong Earthquakes," by J.N. Yang and A. Daniellians, 6/29/90, (PB91-125393).
- NCEER-90-0016 "Instantaneous Optimal Control with Acceleration and Velocity Feedback," by J.N. Yang and Z. Li, 6/29/90, (PB91-125401).
- NCEER-90-0017 "Reconnaissance Report on the Northern Iran Earthquake of June 21, 1990," by M. Mehraein, 10/4/90, (PB91-125377).
- NCEER-90-0018 "Evaluation of Liquefaction Potential in Memphis and Shelby County," by T.S. Chang, P.S. Tang, C.S. Lee and H. Hwang, 8/10/90, (PB91-125427).
- NCEER-90-0019 "Experimental and Analytical Study of a Combined Sliding Disc Bearing and Helical Steel Spring Isolation System," by M.C. Constantinou, A.S. Mokha and A.M. Reinhorn, 10/4/90, (PB91-125385).
- NCEER-90-0020 "Experimental Study and Analytical Prediction of Earthquake Response of a Sliding Isolation System with a Spherical Surface," by A.S. Mokha, M.C. Constantinou and A.M. Reinhorn, 10/11/90, (PB91-125419).
- NCEER-90-0021 "Dynamic Interaction Factors for Floating Pile Groups," by G. Gazetas, K. Fan, A. Kaynia and E. Kausel, 9/10/90, (PB91-170381).
- NCEER-90-0022 "Evaluation of Seismic Damage Indices for Reinforced Concrete Structures," by S. Rodriguez-Gomez and A.S. Cakmak, 9/30/90, PB91-171322).
- NCEER-90-0023 "Study of Site Response at a Selected Memphis Site," by H. Desai, S. Ahmad, E.S. Gazetas and M.R. Oh, 10/11/90, (PB91-196857).
- NCEER-90-0024 "A User's Guide to Strongmo: Version 1.0 of NCEER's Strong-Motion Data Access Tool for PCs and Terminals," by P.A. Friberg and C.A.T. Susch, 11/15/90, (PB91-171272).

- NCEER-90-0025 "A Three-Dimensional Analytical Study of Spatial Variability of Seismic Ground Motions," by L-L. Hong and A.H.-S. Ang, 10/30/90, (PB91-170399).
- NCEER-90-0026 "MUMOID User's Guide - A Program for the Identification of Modal Parameters," by S. Rodriguez-Gomez and E. DiPasquale, 9/30/90, (PB91-171298).
- NCEER-90-0027 "SARCF-II User's Guide - Seismic Analysis of Reinforced Concrete Frames," by S. Rodriguez-Gomez, Y.S. Chung and C. Meyer, 9/30/90, (PB91-171280).
- NCEER-90-0028 "Viscous Dampers: Testing, Modeling and Application in Vibration and Seismic Isolation," by N. Makris and M.C. Constantinou, 12/20/90 (PB91-190561).
- NCEER-90-0029 "Soil Effects on Earthquake Ground Motions in the Memphis Area," by H. Hwang, C.S. Lee, K.W. Ng and T.S. Chang, 8/2/90, (PB91-190751).
- NCEER-91-0001 "Proceedings from the Third Japan-U.S. Workshop on Earthquake Resistant Design of Lifeline Facilities and Countermeasures for Soil Liquefaction, December 17-19, 1990," edited by T.D. O'Rourke and M. Hamada, 2/1/91, (PB91-179259).
- NCEER-91-0002 "Physical Space Solutions of Non-Proportionally Damped Systems," by M. Tong, Z. Liang and G.C. Lee, 1/15/91, (PB91-179242).
- NCEER-91-0003 "Seismic Response of Single Piles and Pile Groups," by K. Fan and G. Gazetas, 1/10/91, (PB92-174994).
- NCEER-91-0004 "Damping of Structures: Part I - Theory of Complex Damping," by Z. Liang and G. Lee, 10/10/91, (PB92-197235).
- NCEER-91-0005 "3D-BASIS - Nonlinear Dynamic Analysis of Three Dimensional Base Isolated Structures: Part II," by S. Nagarajah, A.M. Reinhorn and M.C. Constantinou, 2/28/91, (PB91-190553).
- NCEER-91-0006 "A Multidimensional Hysteretic Model for Plasticity Deforming Metals in Energy Absorbing Devices," by E.J. Graesser and F.A. Cozzarelli, 4/9/91, (PB92-108364).
- NCEER-91-0007 "A Framework for Customizable Knowledge-Based Expert Systems with an Application to a KBES for Evaluating the Seismic Resistance of Existing Buildings," by E.G. Ibarra-Anaya and S.J. Fennes, 4/9/91, (PB91-210930).
- NCEER-91-0008 "Nonlinear Analysis of Steel Frames with Semi-Rigid Connections Using the Capacity Spectrum Method," by G.G. Deierlein, S-H. Hsieh, Y-J. Shen and J.F. Abel, 7/2/91, (PB92-113828).
- NCEER-91-0009 "Earthquake Education Materials for Grades K-12," by K.E.K. Ross, 4/30/91, (PB91-212142).
- NCEER-91-0010 "Phase Wave Velocities and Displacement Phase Differences in a Harmonically Oscillating Pile," by N. Makris and G. Gazetas, 7/8/91, (PB92-108356).
- NCEER-91-0011 "Dynamic Characteristics of a Full-Size Five-Story Steel Structure and a 2/5 Scale Model," by K.C. Chang, G.C. Yao, G.C. Lee, D.S. Hao and Y.C. Yeh, 7/2/91, (PB93-116648).
- NCEER-91-0012 "Seismic Response of a 2/5 Scale Steel Structure with Added Viscoelastic Dampers," by K.C. Chang, T.T. Soong, S-T. Oh and M.L. Lai, 5/17/91, (PB92-110816).
- NCEER-91-0013 "Earthquake Response of Retaining Walls; Full-Scale Testing and Computational Modeling," by S. Alampalli and A-W.M. Elgamal, 6/20/91, to be published.

- NCEER-91-0014 "3D-BASIS-M: Nonlinear Dynamic Analysis of Multiple Building Base Isolated Structures," by P.C. Tsopelas, S. Nagarajaiah, M.C. Constantinou and A.M. Reinhorn, 5/28/91, (PB92-113885).
- NCEER-91-0015 "Evaluation of SEAOC Design Requirements for Sliding Isolated Structures," by D. Theodossiou and M.C. Constantinou, 6/10/91, (PB92-114602).
- NCEER-91-0016 "Closed-Loop Modal Testing of a 27-Story Reinforced Concrete Flat Plate-Core Building," by H.R. Somprasad, T. Toksoy, H. Yoshiyuki and A.E. Aktan, 7/15/91, (PB92-129980).
- NCEER-91-0017 "Shake Table Test of a 1/6 Scale Two-Story Lightly Reinforced Concrete Building," by A.G. El-Attar, R.N. White and P. Gergely, 2/28/91, (PB92-222447).
- NCEER-91-0018 "Shake Table Test of a 1/8 Scale Three-Story Lightly Reinforced Concrete Building," by A.G. El-Attar, R.N. White and P. Gergely, 2/28/91, (PB93-116630).
- NCEER-91-0019 "Transfer Functions for Rigid Rectangular Foundations," by A.S. Veletsos, A.M. Prasad and W.H. Wu, 7/31/91.
- NCEER-91-0020 "Hybrid Control of Seismic-Excited Nonlinear and Inelastic Structural Systems," by J.N. Yang, Z. Li and A. Daniellians, 8/1/91, (PB92-143171).
- NCEER-91-0021 "The NCEER-91 Earthquake Catalog: Improved Intensity-Based Magnitudes and Recurrence Relations for U.S. Earthquakes East of New Madrid," by L. Seeber and J.G. Armbruster, 8/28/91, (PB92-176742).
- NCEER-91-0022 "Proceedings from the Implementation of Earthquake Planning and Education in Schools: The Need for Change - The Roles of the Changemakers," by K.E.K. Ross and F. Winslow, 7/23/91, (PB92-129998).
- NCEER-91-0023 "A Study of Reliability-Based Criteria for Seismic Design of Reinforced Concrete Frame Buildings," by H.H.M. Hwang and H-M. Hsu, 8/10/91, (PB92-140235).
- NCEER-91-0024 "Experimental Verification of a Number of Structural System Identification Algorithms," by R.G. Ghanem, H. Gavin and M. Shinozuka, 9/18/91, (PB92-176577).
- NCEER-91-0025 "Probabilistic Evaluation of Liquefaction Potential," by H.H.M. Hwang and C.S. Lee, 11/25/91, (PB92-143429).
- NCEER-91-0026 "Instantaneous Optimal Control for Linear, Nonlinear and Hysteretic Structures - Stable Controllers," by J.N. Yang and Z. Li, 11/15/91, (PB92-163807).
- NCEER-91-0027 "Experimental and Theoretical Study of a Sliding Isolation System for Bridges," by M.C. Constantinou, A. Kartoun, A.M. Reinhorn and P. Bradford, 11/15/91, (PB92-176973).
- NCEER-92-0001 "Case Studies of Liquefaction and Lifeline Performance During Past Earthquakes, Volume 1: Japanese Case Studies," Edited by M. Hamada and T. O'Rourke, 2/17/92, (PB92-197243).
- NCEER-92-0002 "Case Studies of Liquefaction and Lifeline Performance During Past Earthquakes, Volume 2: United States Case Studies," Edited by T. O'Rourke and M. Hamada, 2/17/92, (PB92-197250).
- NCEER-92-0003 "Issues in Earthquake Education," Edited by K. Ross, 2/3/92, (PB92-222389).
- NCEER-92-0004 "Proceedings from the First U.S. - Japan Workshop on Earthquake Protective Systems for Bridges," Edited by I.G. Buckle, 2/4/92, (PB94-142239, A99, MF-A06).
- NCEER-92-0005 "Seismic Ground Motion from a Haskell-Type Source in a Multiple-Layered Half-Space," A.P. Theoharis, G. Deodatis and M. Shinozuka, 1/2/92, to be published.

- NCEER-92-0006 "Proceedings from the Site Effects Workshop," Edited by R. Whitman, 2/29/92, (PB92-197201).
- NCEER-92-0007 "Engineering Evaluation of Permanent Ground Deformations Due to Seismically-Induced Liquefaction," by M.H. Baziar, R. Dobry and A-W.M. Elgamal, 3/24/92, (PB92-222421).
- NCEER-92-0008 "A Procedure for the Seismic Evaluation of Buildings in the Central and Eastern United States," by C.D. Poland and J.O. Malley, 4/2/92, (PB92-222439).
- NCEER-92-0009 "Experimental and Analytical Study of a Hybrid Isolation System Using Friction Controllable Sliding Bearings," by M.Q. Feng, S. Fujii and M. Shinozuka, 5/15/92, (PB93-150282).
- NCEER-92-0010 "Seismic Resistance of Slab-Column Connections in Existing Non-Ductile Flat-Plate Buildings," by A.J. Durrani and Y. Du, 5/18/92.
- NCEER-92-0011 "The Hysteretic and Dynamic Behavior of Brick Masonry Walls Upgraded by Ferrocement Coatings Under Cyclic Loading and Strong Simulated Ground Motion," by H. Lee and S.P. Prawl, 5/11/92, to be published.
- NCEER-92-0012 "Study of Wire Rope Systems for Seismic Protection of Equipment in Buildings," by G.F. Demetriades, M.C. Constantinou and A.M. Reinhorn, 5/20/92.
- NCEER-92-0013 "Shape Memory Structural Dampers: Material Properties, Design and Seismic Testing," by P.R. Witting and F.A. Cozzarelli, 5/26/92.
- NCEER-92-0014 "Longitudinal Permanent Ground Deformation Effects on Buried Continuous Pipelines," by M.J. O'Rourke, and C. Nordberg, 6/15/92.
- NCEER-92-0015 "A Simulation Method for Stationary Gaussian Random Functions Based on the Sampling Theorem," by M. Grigoriu and S. Balopoulou, 6/11/92, (PB93-127496).
- NCEER-92-0016 "Gravity-Load-Designed Reinforced Concrete Buildings: Seismic Evaluation of Existing Construction and Detailing Strategies for Improved Seismic Resistance," by G.W. Hoffmann, S.K. Kunnath, A.M. Reinhorn and J.B. Mander, 7/15/92, (PB94-142007, A08, MF-A02).
- NCEER-92-0017 "Observations on Water System and Pipeline Performance in the Limón Area of Costa Rica Due to the April 22, 1991 Earthquake," by M. O'Rourke and D. Ballantyne, 6/30/92, (PB93-126811).
- NCEER-92-0018 "Fourth Edition of Earthquake Education Materials for Grades K-12," Edited by K.E.K. Ross, 8/10/92.
- NCEER-92-0019 "Proceedings from the Fourth Japan-U.S. Workshop on Earthquake Resistant Design of Lifeline Facilities and Countermeasures for Soil Liquefaction," Edited by M. Hamada and T.D. O'Rourke, 8/12/92, (PB93-163939).
- NCEER-92-0020 "Active Bracing System: A Full Scale Implementation of Active Control," by A.M. Reinhorn, T.T. Soong, R.C. Lin, M.A. Riley, Y.P. Wang, S. Aizawa and M. Higashino, 8/14/92, (PB93-127512).
- NCEER-92-0021 "Empirical Analysis of Horizontal Ground Displacement Generated by Liquefaction-Induced Lateral Spreads," by S.F. Bartlett and T.L. Youd, 8/17/92, (PB93-188241).
- NCEER-92-0022 "IDARC Version 3.0: Inelastic Damage Analysis of Reinforced Concrete Structures," by S.K. Kunnath, A.M. Reinhorn and R.F. Lobo, 8/31/92, (PB93-227502, A07, MF-A02).
- NCEER-92-0023 "A Semi-Empirical Analysis of Strong-Motion Peaks in Terms of Seismic Source, Propagation Path and Local Site Conditions," by M. Kamiyama, M.J. O'Rourke and R. Flores-Berrones, 9/9/92, (PB93-150266).
- NCEER-92-0024 "Seismic Behavior of Reinforced Concrete Frame Structures with Nonductile Details, Part I: Summary of Experimental Findings of Full Scale Beam-Column Joint Tests," by A. Beres, R.N. White and P. Gergely, 9/30/92, (PB93-227783, A05, MF-A01).

- NCEER-92-0025 "Experimental Results of Repaired and Retrofitted Beam-Column Joint Tests in Lightly Reinforced Concrete Frame Buildings," by A. Beres, S. El-Borgi, R.N. White and P. Gergely, 10/29/92, (PB93-227791, A05, MF-A01).
- NCEER-92-0026 "A Generalization of Optimal Control Theory: Linear and Nonlinear Structures," by J.N. Yang, Z. Li and S. Vongchavalitkul, 11/2/92, (PB93-188621).
- NCEER-92-0027 "Seismic Resistance of Reinforced Concrete Frame Structures Designed Only for Gravity Loads: Part I - Design and Properties of a One-Third Scale Model Structure," by J.M. Bracci, A.M. Reinhorn and J.B. Mander, 12/1/92, (PB94-104502, A08, MF-A02).
- NCEER-92-0028 "Seismic Resistance of Reinforced Concrete Frame Structures Designed Only for Gravity Loads: Part II - Experimental Performance of Subassemblages," by L.E. Aycardi, J.B. Mander and A.M. Reinhorn, 12/1/92, (PB94-104510, A08, MF-A02).
- NCEER-92-0029 "Seismic Resistance of Reinforced Concrete Frame Structures Designed Only for Gravity Loads: Part III - Experimental Performance and Analytical Study of a Structural Model," by J.M. Bracci, A.M. Reinhorn and J.B. Mander, 12/1/92, (PB93-227528, A09, MF-A01).
- NCEER-92-0030 "Evaluation of Seismic Retrofit of Reinforced Concrete Frame Structures: Part I - Experimental Performance of Retrofitted Subassemblages," by D. Choudhuri, J.B. Mander and A.M. Reinhorn, 12/8/92, (PB93-198307, A07, MF-A02).
- NCEER-92-0031 "Evaluation of Seismic Retrofit of Reinforced Concrete Frame Structures: Part II - Experimental Performance and Analytical Study of a Retrofitted Structural Model," by J.M. Bracci, A.M. Reinhorn and J.B. Mander, 12/8/92, (PB93-198315, A09, MF-A03).
- NCEER-92-0032 "Experimental and Analytical Investigation of Seismic Response of Structures with Supplemental Fluid Viscous Dampers," by M.C. Constantinou and M.D. Symans, 12/21/92, (PB93-191435).
- NCEER-92-0033 "Reconnaissance Report on the Cairo, Egypt Earthquake of October 12, 1992," by M. Khater, 12/23/92, (PB93-188621).
- NCEER-92-0034 "Low-Level Dynamic Characteristics of Four Tall Flat-Plate Buildings in New York City," by H. Gavin, S. Yuan, J. Grossman, E. Pekelis and K. Jacob, 12/28/92, (PB93-188217).
- NCEER-93-0001 "An Experimental Study on the Seismic Performance of Brick-Infilled Steel Frames With and Without Retrofit," by J.B. Mander, B. Nair, K. Wojtkowski and J. Ma, 1/29/93, (PB93-227510, A07, MF-A02).
- NCEER-93-0002 "Social Accounting for Disaster Preparedness and Recovery Planning," by S. Cole, E. Pantoja and V. Razak, 2/22/93, (PB94-142114, A12, MF-A03).
- NCEER-93-0003 "Assessment of 1991 NEHRP Provisions for Nonstructural Components and Recommended Revisions," by T.T. Soong, G. Chen, Z. Wu, K-H. Zhang and M. Giugliu, 3/1/93, (PB93-188621).
- NCEER-93-0004 "Evaluation of Static and Response Spectrum Analysis Procedures of SEAOC/UBC for Seismic Isolated Structures," by C.W. Winters and M.C. Constantinou, 3/23/93, (PB93-198299).
- NCEER-93-0005 "Earthquakes in the Northeast - Are We Ignoring the Hazard? A Workshop on Earthquake Science and Safety for Educators," edited by K.E.K. Ross, 4/2/93, (PB94-103066, A09, MF-A02).
- NCEER-93-0006 "Inelastic Response of Reinforced Concrete Structures with Viscoelastic Braces," by R.F. Lobo, J.M. Bracci, K.L. Shen, A.M. Reinhorn and T.T. Soong, 4/5/93, (PB93-227486, A05, MF-A02).

- NCEER-93-0007 "Seismic Testing of Installation Methods for Computers and Data Processing Equipment," by K. Kosar, T.T. Soong, K.L. Shen, J.A. HoLung and Y.K. Lin, 4/12/93, (PB93-198299).
- NCEER-93-0008 "Retrofit of Reinforced Concrete Frames Using Added Dampers," by A. Reinhorn, M. Constantinou and C. Li, to be published.
- NCEER-93-0009 "Seismic Behavior and Design Guidelines for Steel Frame Structures with Added Viscoelastic Dampers," by K.C. Chang, M.L. Lai, T.T. Soong, D.S. Hao and Y.C. Yeh, 5/1/93, (PB94-141959, A07, MF-A02).
- NCEER-93-0010 "Seismic Performance of Shear-Critical Reinforced Concrete Bridge Piers," by J.B. Mander, S.M. Waheed, M.T.A. Chaudhary and S.S. Chen, 5/12/93, (PB93-227494, A08, MF-A02).
- NCEER-93-0011 "3D-BASIS-TABS: Computer Program for Nonlinear Dynamic Analysis of Three Dimensional Base Isolated Structures," by S. Nagarajaiah, C. Li, A.M. Reinhorn and M.C. Constantinou, 8/2/93, (PB94-141819, A09, MF-A02).
- NCEER-93-0012 "Effects of Hydrocarbon Spills from an Oil Pipeline Break on Ground Water," by O.J. Helweg and H.H.M. Hwang, 8/3/93, (PB94-141942, A06, MF-A02).
- NCEER-93-0013 "Simplified Procedures for Seismic Design of Nonstructural Components and Assessment of Current Code Provisions," by M.P. Singh, L.E. Suarez, E.E. Matheu and G.O. Maldonado, 8/4/93, (PB94-141827, A09, MF-A02).
- NCEER-93-0014 "An Energy Approach to Seismic Analysis and Design of Secondary Systems," by G. Chen and T.T. Soong, 8/6/93, (PB94-142767, A11, MF-A03).
- NCEER-93-0015 "Proceedings from School Sites: Becoming Prepared for Earthquakes - Commemorating the Third Anniversary of the Loma Prieta Earthquake," Edited by F.E. Winslow and K.E.K. Ross, 8/16/93.
- NCEER-93-0016 "Reconnaissance Report of Damage to Historic Monuments in Cairo, Egypt Following the October 12, 1992 Dahshur Earthquake," by D. Sykora, D. Look, G. Croci, E. Karaesmen and E. Karaesmen, 8/19/93, (PB94-142221, A08, MF-A02).
- NCEER-93-0017 "The Island of Guam Earthquake of August 8, 1993," by S.W. Swan and S.K. Harris, 9/30/93, (PB94-141843, A04, MF-A01).
- NCEER-93-0018 "Engineering Aspects of the October 12, 1992 Egyptian Earthquake," by A.W. Elgamal, M. Amer, K. Adalier and A. Abul-Fadl, 10/7/93, (PB94-141983, A05, MF-A01).
- NCEER-93-0019 "Development of an Earthquake Motion Simulator and its Application in Dynamic Centrifuge Testing," by I. Krstelj, Supervised by J.H. Prevost, 10/23/93.
- NCEER-93-0020 "NCEER-Taisei Corporation Research Program on Sliding Seismic Isolation Systems for Bridges: Experimental and Analytical Study of a Friction Pendulum System (FPS)," by M.C. Constantinou, P. Tsopelas, Y-S. Kim and S. Okamoto, 11/1/93, (PB94-142775, A08, MF-A02).
- NCEER-93-0021 "Finite Element Modeling of Elastomeric Seismic Isolation Bearings," by L.J. Billings, Supervised by R. Shepherd, 11/8/93, to be published.
- NCEER-93-0022 "Seismic Vulnerability of Equipment in Critical Facilities: Life-Safety and Operational Consequences," by K. Porter, G.S. Johnson, M.M. Zadeh, C. Scawthorn and S. Eder, 11/24/93.
- NCEER-93-0023 "Hokkaido Nansei-oki, Japan Earthquake of July 12, 1993, by P.I. Yanev and C.R. Scawthorn, 12/23/93.
- NCEER-94-0001 "An Evaluation of Seismic Serviceability of Water Supply Networks with Application to San Francisco Auxiliary Water Supply System," by I. Markov, Supervised by M. Grigoriu and T. O'Rourke, 1/21/94.